

University of Nebraska - Lincoln

DigitalCommons@University of Nebraska - Lincoln

---

Theses, Dissertations, & Student Research in  
Computer Electronics & Engineering

Electrical & Computer Engineering, Department of

---

Summer 5-2015

# ENERGY HARVESTING AND STORAGE: THE CATALYST TO THE POWER CONSTRAINT FOR LEVERAGING INTERNET OF THINGS (IoT) ON TRAINS

Kelechi Nwogu

University of Nebraska-Lincoln, kcnwogu@gmail.com

Follow this and additional works at: <http://digitalcommons.unl.edu/ceendiss>



Part of the [Computer and Systems Architecture Commons](#), [Power and Energy Commons](#), [Signal Processing Commons](#), [Systems and Communications Commons](#), and the [Systems Engineering Commons](#)

---

Nwogu, Kelechi, "ENERGY HARVESTING AND STORAGE: THE CATALYST TO THE POWER CONSTRAINT FOR LEVERAGING INTERNET OF THINGS (IoT) ON TRAINS" (2015). *Theses, Dissertations, & Student Research in Computer Electronics & Engineering*. 33.

<http://digitalcommons.unl.edu/ceendiss/33>

This Article is brought to you for free and open access by the Electrical & Computer Engineering, Department of at DigitalCommons@University of Nebraska - Lincoln. It has been accepted for inclusion in Theses, Dissertations, & Student Research in Computer Electronics & Engineering by an authorized administrator of DigitalCommons@University of Nebraska - Lincoln.

**ENERGY HARVESTING AND STORAGE: THE CATALYST TO THE POWER  
CONSTRAINT FOR LEVERAGING INTERNET OF THINGS (IoT) ON TRAINS**

By

Kelechi Obiajulu Nwogu

A THESIS

Presented to the Faculty of

The Graduate College at the University of Nebraska

In Partial Fulfilment of Requirements

For the Degree of Master of Science

Major: Telecommunication Engineering

Under the Supervision of Professor Hamid Sharif

Lincoln, Nebraska

May, 2015

# ENERGY HARVESTING AND STORAGE: THE CATALYST TO THE POWER CONSTRAINT FOR LEVERAGING THE INTERNET OF THINGS (IOT) ON TRAINS

Kelechi Obiajulu Nwogu, MS.

University of Nebraska, 2015

Adviser: Hamid Sharif

The success of Wireless Sensor Networks is heavily constrained by its reliance on storage technology like batteries, which are a finite resource. Whilst the number of transistors in an IC doubles every 18 months, the energy density of batteries is relatively flat during the same time period. This is a key challenge in leveraging the Internet of Things on trains.

The gravity of this problem is increased by an order of magnitude when the network is to be scaled up to hundreds or thousands of nodes. Comprehensive research and development efforts have been devoted to building ultra-low power sensors. These ultra-low power sensors are configured to have very low duty cycle and are practically asleep most of the time. Short duty cycle might extend the battery life, but the energy will inevitably run out.

Energy harvesting has emerged as a viable solution to the energy loss issue by ensuring sensors never run out of energy. Though, there could be a significant upfront cost in employing energy harvesting; several studies have shown it takes 24 months or less to break even. Energy harvesters, unlike batteries, are not commonly a one size fits all; some customization is required based on the environment.

Mechanical harvesting sources are ideal for the rail environment because this environment has an abundant amount of vibration energy.

This thesis focuses on how Energy Harvesting and Storage can be used as the sole power source for the Wireless Sensor Networks that make up the Internet of Things in the railroad industry. It synthesizes the various works carried out in the energy harvesting techniques like solar and piezo, and storage technology like Lithium-ion batteries and Supercapacitors.

After introducing the general concept of Internet of Things, Energy Harvesting, and Storage, this document provides an in-depth analysis of the data gathered during this research. The data was used to determine sensor node power consumption when arranged in a linear topology like the train, available ambient energy on the train, and optimal energy harvesting sources for the railroad.

## COPYRIGHT NOTICE AND DISCLAIMER

THE CONTENT OF THIS DOCUMENT IS NOT ENDORSED OR REFLECTS THE  
OPINION OF ANY RAILROAD. IT IS A REFLECTION OF THE AUTHOR'S VIEWS  
AND INTERPRETATION OF THE CITED PUBLICATIONS.

Copyright © 2015

Kelechi Obiajulu Nwogu

All Rights Reserved

## Acknowledgements

*First of all, I would like to give thanks to the almighty for giving me the strength to complete this thesis. Philippians 4:13 resonated with me during this journey.*

*Special thanks to Carolyn Wilson for your ever-enthusiastic and wise pep talk. She took it upon herself that I was on schedule. The several times I hit a road block you had the perfect advice. I am very grateful.*

*To Dan Rubin, I thank you for the support and mentorship. Without it this process would have been difficult.*

*I would like to express my sincere gratitude to my advisor, Dr. Sharif. Your wisdom, guidance and encouraging words made this a reality. This thesis was possible because of you. You talked me into it and believed in me.*

*My sincere gratitude goes to the other committee members Dr. Qian and Dr. Subramaniam. I appreciate you taking out time to be a part of the committee and your valuable feedback.*

*Lastly to my family, friends and the people that proofread this document (Charleen Buswell to name a few), I appreciate you guys for tolerating me speak of Energy harvesting and wireless sensors ad nauseam for months. Thanks for your patience, love and support.*

# Table of Contents

<b>COPYRIGHT NOTICE AND DISCLAIMER .....</b>	<b>ii</b>
<b>List of Figures.....</b>	<b>vii</b>
<b>List of Tables .....</b>	<b>x</b>
<b>Acronyms .....</b>	<b>1</b>
<b>Chapter 1: Introduction .....</b>	<b>2</b>
1.1 History of “Internet of Things” .....	2
1.2 Technologies to Realize the IoT.....	4
1.2.1 IPv6.....	4
1.2.2 Automated Identification .....	6
1.2.3 Motes .....	12
1.2.4 Energy Harvesting .....	13
1.3 Thesis Organization.....	14
<b>Chapter 2: Problem Statement.....</b>	<b>15</b>
2.1 Motivations.....	16
2.2 Significance of Proposed Approach .....	19
2.3 Research Challenges .....	21
2.4 Proposed Research Objectives .....	22

2.5	Related work .....	23
<b>Chapter 3:</b>	<b>Literature Review.....</b>	<b>25</b>
3.1	Energy Harvesting Overview .....	25
3.1.1	What is <i>Energy</i> ?.....	26
3.1.2	What is <i>harvesting</i> ? .....	26
3.2	Energy Harvesting Sources .....	28
3.2.1	Solar Energy .....	31
3.2.2	Vibration Energy .....	33
3.3	Energy Storage .....	36
3.3.1	Battery .....	36
3.3.2	Supercapacitors.....	40
<b>Chapter 4:</b>	<b>Results and Analysis .....</b>	<b>42</b>
4.1	Power Consumption by Sensors.....	42
4.1.1	Experimental Setup.....	42
4.1.2	Experimental Procedure .....	44
4.1.3	Observation.....	45
4.1.4	Error Analysis.....	52
4.1.5	Section summary .....	60
4.2	How much vibration does the Railcar generate?.....	61
4.2.1	Experimental Setup.....	61



4.2.2	Experimental Procedure .....	66
4.2.3	Analysis of Data from Loaded Car.....	68
4.2.4	Analysis of Data from Empty car .....	76
4.3	Section Summary .....	86
4.3.1	Converting the Vibration to Power.....	87
<b>Chapter 5:</b>	<b>Conclusion.....</b>	<b>90</b>
5.1	Summary .....	90
<b>Chapter 6:</b>	<b>Bibliography .....</b>	<b>92</b>
<b>Appendix A:</b>	<b>Source Code .....</b>	<b>98</b>
<b>Appendix B:</b>	<b>Vulture Datasheet .....</b>	<b>108</b>
<b>Appendix C:</b>	<b>Vibration Data Logger Specification.....</b>	<b>122</b>
<b>Appendix D:</b>	<b>Electrical Circuit Schematic .....</b>	<b>125</b>

## List of Figures

Figure 1–1: IPv6 Adoption [13].....	6
Figure 1–2: Bar code representation of 12 Alphanumeric Characters.....	8
Figure 1–3: QR code representation of 12 Alphanumeric Characters in 200x200.....	8
Figure 1–4: Bar code representation of 61 Alphanumeric Characters.....	9
Figure 1–5: QR code representation of 61 Alphanumeric Characters in 200x200.....	9
Figure 1–6: Bar code representation of 366 Alphanumeric Characters.....	10
Figure 1–7: QR code representation of 366 Alphanumeric Characters in 200x200.....	10
Figure 3–1: Ambient Energy Power Source before conversion [35].....	29
Figure 3–2: Freight car graffiti .....	30
Figure 3–3: Energy Harvesting System Block Diagram [36] .....	31
Figure 3–4: Mechanical-to-Electrical converters [35] .....	36
Figure 3–5: Cross section of a Li battery with Lithium salt as electrolyte [40] .....	37
Figure 3–6: Ragone plot [40].....	38
Figure 3–7: Source: TIAX .....	39
Figure 3–8: Lithium vs. Supercapacitors historical cost (Source IDTechEx) .....	41
Figure 4–1: Motes placement.....	43
Figure 4–2: Current representation .....	46
Figure 4–3: Zoomed into 5/27 .....	47
Figure 4–4: Zoomed in 5/28 .....	48

Figure 4–5: Current use by the nodes placed at beginning, center and end of the path for 5/28 .....	49
Figure 4–6: Current use by the nodes placed at beginning, center and end of the path for 5/29 .....	50
Figure 4–7: Trend of the current used by the nodes placed at beginning, center and end of the path for 05/28.....	51
Figure 4–8: Motes Link count.....	53
Figure 4–9: Sum of Total TX and RX (for 5/27).....	54
Figure 4–10: Transmissions and Receptions for Node 33 .....	57
Figure 4–11: Failed Tx vs. Total Transmissions for Node 33 .....	58
Figure 4–12: Sum of Total TX and RX (5/28) .....	59
Figure 4–13: Slam Stick Data Logger Mount orientation .....	61
Figure 4–14: Railcar 1 (Flat car).....	62
Figure 4–15: Vibration Data logger Mount location on Car 1.....	63
Figure 4–16: Railcar 2 (loaded Covered Hopper Car).....	63
Figure 4–17: Vibration Data logger Mount Location on Car 2 .....	64
Figure 4–18: Railcar 3 (Empty coal car).....	64
Figure 4–19: Vibration Data logger Mount Location on Car 3 .....	65
Figure 4–20: Railcar 4 (Loaded Tank car).....	65
Figure 4–21: Vibration Data logger Mount location for Car 4.....	66
Figure 4–22: Time Domain (Loaded Railcar) .....	68
Figure 4–23: X – Axis Frequency.....	70

Figure 4–24: Y – Axis Frequency .....	71
Figure 4–25: Vibration Data Logger mount location for Loaded Car .....	72
Figure 4–26: Z – Axis Frequency .....	73
Figure 4–27: X Channel Frequency (2-D) .....	74
Figure 4–28: Y Channel Frequency (2-D) .....	75
Figure 4–29: Z Channel Frequency (2-D) .....	76
Figure 4–30: Time Domain.....	77
Figure 4–31: Y Channel Frequency (2-D Experiment Attempt 1) .....	79
Figure 4–32: Y Channel Frequency (2-D Experiment Attempt 2) .....	80
Figure 4–33: X – Axis Frequency.....	81
Figure 4–34: Y – Axis Frequency.....	82
Figure 4–35: Z – Axis Frequency .....	83
Figure 4–36: X Channel Frequency (2-D Experiment Attempt 3) .....	84
Figure 4–37: Y Channel Frequency (2-D Experiment Attempt 3) .....	85
Figure 4–38: Maximum vibration of railcar .....	86

## List of Tables

Table 0–1 Acronym Definitions	1
Table 2: Node 33 Neighbor List	56
Table 4–3: Statistics of data from Empty car (Experiment 1)	77
Table 4–4: Statistics of data from Empty car (Experiment 2)	80
Table 4–5: Statistics of data from Empty car (Experiment 3)	81

## Acronyms

The following table defines acronyms used in this document.

Table 0–1 Acronym Definitions

Acronym	Description
<b>dBi</b>	Decibels relative to an isotropic antenna. The measurement of the antenna gain.
<b>EH</b>	Energy Harvesting
<b>IoT</b>	Internet Of Things
<b>RSSI</b>	Received Signal Strength
<b>g</b>	Acceleration of gravity ( $\text{m/s}^2$ )
<b>WSN</b>	Wireless Sensor Networks.
<b>PTC</b>	Positive Train Control
<b>IPv4</b>	Internet Protocol version 4
<b>IPv6</b>	Internet Protocol version 6
<b>RFID</b>	Radio Frequency Identification

## Chapter 1: Introduction

### 1.1 History of “Internet of Things”

It is the dawn of the 21<sup>st</sup> century and the vision of Mark Weiser [1] can be felt.

Ubiquitous computing is no longer a theory. Although computers are not yet as Weiser imagined as “a walk in the park”, they are definitely more context-aware [2] and can make “smart” decisions. There has been a lot of buzz about making everything smart.

Smart cars, smart TV, smart watch, smart railroad [3]...etc.

What makes an object “smart”? An object is said to be smart if it has network connectivity and is able to sense and respond intelligently and intuitively to analog input forming a pervasive system. Such systems can be found in the automotive industry, where perception of the environment and the user’s behavior are intrinsic components of safety. The coalescence of smart physical objects to form an interactive network is the Internet of Things (IoT).

The first documented use of the phrase “Internet of Things” was by Kevin Ashton in 1999 during a presentation at Procter & Gamble (P&G) [4, 5, 6]. In the presentation, Ashton correlated the new concept of RFID used in P&G’s supply chain to the exploding topic of the internet. This was in an effort to get the executive’s attention [6]. Ashton would later go on to invent the MIT Auto-ID Center.

Smart physical objects are the “things” in IoT. Smart objects are made up of several sensors like GPS for positioning, proximity sensors, network connectivity for data transfer and more.

To achieve visibility of the entire train system, the locomotive(s) and freight cars that make the train must have network connectivity.

With the government mandate of Positive Train Control (PTC [7]), the railroad is set to build one of the largest interoperable networks. In it, locomotives communicate with the wayside radios, the base station and the back office as needed to make safety critical decisions about whether to self-stop the train or proceed.

In 2012, Bibel wrote about the causes of train wrecks [8]. There are two forms of cataclysmic accidents that can occur on moving trains: collision and derailment. PTC addresses train to train collision [9]. Derailment sometimes are the aftermath of a collision. Other times it as a result of a mechanical failure. The railroad recognizes the benefits of leverage the Internet of Things on the train [10]. One of the setbacks of this initiative is power, which is the focus of this thesis and is further discussed in the following chapters.



## 1.2 Technologies to Realize the IoT

The realization of the Internet of Things is predicated on the objects of concern being instrumented with identification. The identification must be wirelessly accessible. Some of the object identification technologies are Auto-IDs, RFID, and Wireless Sensors Network (WSN).

The migration to IPv6 is critical in the realization of IoT, which will be discussed in the next section.

Energy harvesting, the process of gathering ambient energy from the surrounding, another key piece of realizing the Internet of Things on trains, gets the sensors a step closer to battery independence by alleviating the cost of maintenance. Batteries will be one less thing to worry about.

### 1.2.1 IPv6

The vision of IoT is to have all physical objects connect. These objects will need some sort of unique identification to differentiate them. RFID is one popular method of assigning identification to objects, but it requires near field communication.

For long range communication similar to Wi-Fi or Bluetooth, the internet protocol (IP) method of addressing is required. The issue with having everything connected is that there are a finite amount of unique addresses to assign to objects. The addresses can be

reused, but it becomes difficult to reuse addresses if the objects are expected to be active for a majority of the time. Sensor's sleep time is not long enough for the address to be reused.

The internet was launched in 1983 with IPv4. This protocol has 32-bit ( $2^{32}$ ) address or 4.3 billion address space, which according to [11] has exhausted its capacity.

IPv6 offers 128-bit ( $2^{128}$ ) address [12] given 340 trillion-trillion-trillion addresses (340 Undecillionth). This growth allows  $\sim 7.9 \times 10^{28}$  more addresses. This is more than enough for every individual on earth. If distributed evenly, each person on earth will have over an Octillion address spaces ( $10^{27}$ ). This is great news for the growth for smart things.

IPv6 launched on June 6<sup>th</sup> 2012, but is adopted by less than 7% of internet users as shown in Figure 1–1.

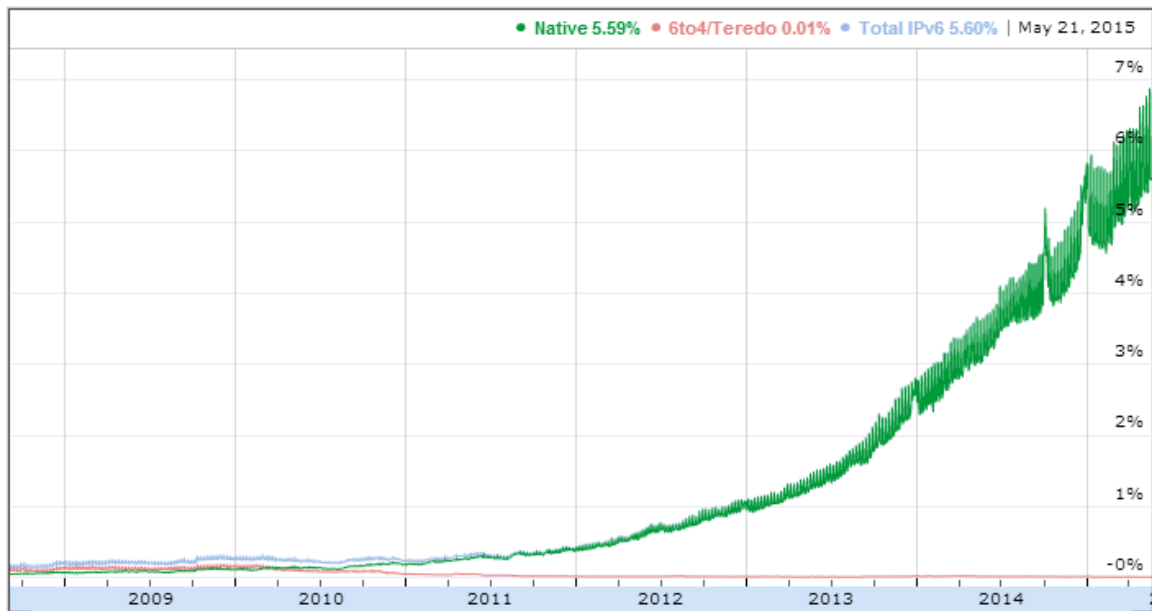


Figure 1–1: IPv6 Adoption [13]

### 1.2.2 Automated Identification

“Auto-ID” as the name implies is an automated identification process, which encompasses the identification technologies used to streamline the processes of asset management. The railroad’s rendition of the Auto ID is called the Automatic Equipment Identification (AEI) [14]. The Auto-ID refers to a broad class of identification technologies used in industry to automate, reduce errors, and increase efficiency [5]. These technologies are still in use today. Examples include the bar/QR codes (optical ID), smart cards, sensors, voice recognition and biometrics [5]. Some of these technologies are limited in their range and abilities.

### 1.2.2.1 Bar / QR Code

Automated identification (Auto-ID) has made great impact on product distribution and lead to the standard Universal Product Code (UPC) otherwise known as barcode symbols. UPC is used by logistics / Courier companies for package tracking, grocery stores for inventory...etc. The success of the Auto-ID cannot be overstated. Almost every item in stores have some form of Auto-ID. Why is it so popular? It is a cheap, versatile, and an effective way of tracking of inventory.

Barcodes can be printed on practically any surface. In addition, Auto-ID requires a unique character printed on one-dimensional (or two-dimensional) objects, as well as machine to scan the object for information. With this level of popularity, is there a possibility that Auto-ID might have shortcomings? Absolutely.

One of the major deficiencies of this method is that it requires the sensing device to be near the tag, and to have a clear *line of sight* [14]. One can quickly identify the severity of this deficiency – it can be consider as high maintenance.

If any form of dirt, paint, graffiti, or opaque object hinders the view of the bar code reader by obscuring required information, this will affect the accuracy of reading.

Another deficiency is that bar codes are susceptible to physical damage. Since the bar code can be printed on virtually anything, reliability (or readability) is influenced by the durability, integrity, and resistance to environmental factors of the printed surface. Minor

changes to a label that alter the image, degrade readability. The third deficiency when using a barcode is scalability, in terms of adding information to a label. More information can be added by increasing the barcode surface area, shrinking the image size, and/or using a finer marker to accommodate additional information in the printing surface, hence affecting readability. To put in perspective, the following figures show the barcode and QR code representation of my first and last name – Kelechi Nwogu:



Figure 1–2: Bar code representation of 12 Alphanumeric Characters



Figure 1–3: QR code representation of 12 Alphanumeric Characters in 200x200

The bar and QR code representation of the characters of my first and last name shown in **Figure 1–2** and **Figure 1–3** above is easily readable using a smart phone with a QR code scanner installed. Now, let's add more information to the code of my first and last name by including my student ID and Department. The results are shown in **Figure 1–4** and **Figure 1–5**:



Figure 1–4: Bar code representation of 61 Alphanumeric Characters



Figure 1–5: QR code representation of 61 Alphanumeric Characters in 200x200

The labels shown in shown in **Figure 1–4** and **Figure 1–5** are still readable, but the region is getting filled. Now, let's increase the data to 366<sup>1</sup> characters. The bar code runs out of space for this. The label doesn't represent the recorded identification.



Figure 1–6: Bar code representation of 366 Alphanumeric Characters

The tag information represented in Figure 1–6 is incomplete because the printing ran out of real estate. Figure 1–7 below shows that the areas on the label are saturated.



Figure 1–7: QR code representation of 366 Alphanumeric Characters in 200x200

---

<sup>1</sup> This was done by creating 6 copies of the 61 character identification from **Figure 1–4** and **Figure 1–5**.

Passive Auto-IDs can store a limited amount of information before becoming unreadable. The data stored in these labels cannot be modified after printing. Granted, these methods of optical object identification are inexpensive and versatile, it is obvious an alternative robust method is needed.

#### 1.2.2.2 Radio Frequency Identification (RFID)

One technique that remedies the deficiencies of optical ID is the Radio Frequency Identification (RFID). This method uses radio frequency to identify physical objects. RFID technology has existed for more than a century [14]. It shares a similarity with the QR and barcodes in that they are not battery powered; however, RFID has more circuitry. They are powered wirelessly by the RF transmission from the reader.

Some can argue that the Auto ID was the first attempt to implement the Internet of Things. The goal was to assign identities to things that a computer can understand, so that the information could be transmitted over the existing internet.

#### 1.2.2.3 Machine Learning (Pervasive Computing)

Computers have evolved over the centuries. Nineteenth century computers *learned to do* things but required a lengthy sequence of actions from the user. In the twentieth century computers, *learned to think* and make decisions based on the provided input. Twenty-first



century computers are learning to *perceive* events and patterns – the machine learning paradigm [5].

The ability of machines to perceive and act intelligently and intuitively is the catalyst for the Internet of Things. An application of this is the Nest thermostat [15], which learns the behavior of the owner and automatically adjusts the temperature to conserve energy.

The Internet of Things is the idea that the objects/items we utilize in our everyday life are connected, intelligent, aware, and interactive. A famous video [16] put together by Cisco depicted a world where all things in the home were intelligent and interactive with the owner.

### 1.2.3 Motes

What is a mote? The Wikipedia defines mote as a *sensor node*. As Henry Ford once said, “*Every object tells a story if you know how to read it...*” [17] motes are the virtual eyes and ears for reading and translating these stories to human readable format and getting the stories heard via a network like IoT. These “stories” can be the physical object’s status. An example is a sensor that monitors the bearing temperature of a railcar or locomotive and alerts the user when the temperature exceeds a certain threshold. The physical object in this case is the bearing and the “story” being told is “temperature exceed threshold.”

Mote is a major step up from NFC and Barcode type technology. There is a vast list of underlying network options for motes. The popular ones are Wi-Fi, Cellular, Bluetooth, ZigBee, 802.15.4...etc. Each of these have their pros and cons, which is outside of the scope of this research.

#### 1.2.4 Energy Harvesting

Energy harvesting technology has been around for years. Piezoelectricity is an example of energy harvesting technology and was invented in 1880 by the Curie brothers [18].

Why is this significant today?

First, we can thank Moore's law for predicting that transistors in integrated circuits (IC) would double every 18 months. More transistors mean more processing power and smaller ICs. Smaller integrated circuits have led to smaller devices that are more power efficient.

Secondly, advancements have been made in battery technology and sensors are less power hungry. Though the small amounts of power generated by Piezoelectricity are not sufficient enough to power an entire home, they are sufficient enough to power small sensors or devices like wearable electronics.

In places where it is difficult to have wiring or maintain a battery or where it will be expensive, like the freight car, then energy harvesting can be used. One the benefits of

energy harvesting is that wherever light, vibration, or temperature differential exist, any device can potentially operate battery-free for long periods of time.

Mechanical energy harvesting is ideal for the railroad environment. It can be found in very old devices, such as mechanical watches or in new devices like piezo equipped shoes. The train environment has an abundant amount of vibration.

### 1.3 Thesis Organization

In this thesis, Energy Harvesting is researched as a way of powering the motes planned to go on rail cars. Piezoelectric and solar energy sources were studied as possible energy harvesting solutions for the railroad environment.


Chapter 2 presents the problem statement and gives evidence to support the severity of the problem as well as provides an overview of related work.

Chapter 3 covers the fundamental of energy and an intensive literature review of the physics behind the energy, harvester and storage mechanism was done.

Chapter 4 presents data gathered from research, analysis and results.

The thesis is concluded in Chapter 5 with summary of the findings and suggestions on future work based on results.

## Chapter 2: Problem Statement



I THINK NOW THAT THE GREAT THING IS NOT SO MUCH THE FORMULATION OF  
AN ANSWER FOR MYSELF...RATHER THE MOST ACCURATE POSSIBLE  
STATEMENT OF THE PROBLEM [29].

Arthur Miller

One of the biggest constraints in Wireless Sensor Network Technology is energy consumption. Several wireless sensors utilize different approaches to conserve energy, but the energy stored is eventually exhausted and a new power source (battery) is needed. Majority of the batteries have less than a year lifespan in moderate use. Some advances have been made in the battery technology. One such advancement includes using batteries made with Lithium Thionyl Chloride, which is advertised to have a ten year shelf life in certain circumstances. However, it is inconvenient to replace and dispose of dead batteries, which can be toxic to the environment. For many WSN applications, energy harvesting is more attractive.

This project sets forth a research plan for analyzing existing and emerging Energy Harvesting solutions for wireless sensor network technologies used in an industrial environment like the Railroad.

## 2.1 Motivations

Since the industrial revolution of 1800, the railroad has continued to play a vital role in America's economy. The impact of the railroad in American lives is enormous. From the cars we drive, the food we eat and our entertainment. The railroad has evolved from the steam engine locomotives used back in the 1900 to more efficient ones. The significance of energy harvesting in train application cannot be understood without first declaring the significance of the application – Internet of Things (IoT).

The adoption of IoT in the railroad is a potential advancement in railroad safety. There will be greater visibility on asset tracking; knowing about a problem before it occurs – kind of like a 6th sense. Visualize the wheelset of the railcar having the ability to inform users when the bearing is too hot or uneven. Theoretically, most of the failure trends leading to derailment can be detected early and prevented [10].

As mentioned in Introduction section of Chapter 1, there are two forms of cataclysmic accidents that can occur on moving trains: collision and derailment. Some of the root causes of these accidents can be prevented with technology. PTC is the solution to train

collision [19] [20] [9]. Derailments are sometimes the aftermath of a collision and other times the result of mechanical failure. Imagine if mechanical failures could be detected early? Early detection can be achieved using sensors, data analytics and IoT.

What part does Energy Harvesting play in the adoption of IoT? Conventional wisdom suggests that safety attributes of a system must be available 24/7 since no one can predict when safety attributes will be needed. Imagine if airbags in a vehicle were defective and did not inflate during an accident. Or if the fire/carbon monoxide detector fails to alert the occupants of a room when a certain amount of carbon monoxide or smoke is sensed in the air. The effect will be devastating. Similarly, the accident prevention system on the train must always be available.

Other than the normal wear and tear of mechanical systems, one threat to the availability of the safety sensor system is its reliance on battery for power. This is where energy harvesting comes into play.

Many times, wireless sensors are installed on devices located in remote locations. The need for these sensors to function without interruption is very imperative. Some nodes are installed on safety critical equipment; for example, sensors used to detect defects on a railcar or airplane, fire/carbon monoxide detector in homes...etc.

In the *InfomationWeek* article [10], Murphy wrote that the vision of the railroad *is to install sensors in wheels, bearings, door locks...and those sensors would need to last on a railcar for five to seven years without replacement*. To achieve the desired longevity of

5+ years without replacement means that the system has to be self-sustaining. This was the motivation of thesis.

First let's determine approximately the number of sensors that will be required to achieve this vision. A typical railcar has 8 wheels, a bearing per wheel, and two door locks. This equates to ~18 sensors if each item needed a sensors. It is possible that one sensor can be used to monitor the bearing and wheel simultaneously. If that is the case then approximately 10 sensors maybe needed.

It would be a very expensive and an exhaustive process if batteries in these sensors needed to be replaced. Imagine the amount of toxins introduced into the environment by disposing of these batteries.

To put things in perspective, according to the Association of American Railroads (AAR), there are 1,516,593 freight cars in service [21, 22]. The vision is to get to a point where all the cars are equipped with approximately 10 sensors. Assuming one battery per sensor, which is a long stretch from reality, if we multiply this by the number of sensors per freight car, and the number of freight cars equates to over 10.5 million sensors. Imagine the amount of batteries required to keep this vision alive. In reality, each sensor can have multiple batteries to increase capacitance.

According to [23], a typical mote consumes 8 milliamps when active. The power consumption depends on the duty cycle of the mote. Assuming that the mote was

constantly active, that is 100% duty cycle, and was required to last for a year (8765.81 hours), the desired battery capacity is computed as follows:

$$8765.81 \text{ hours} \times 8\text{mA} = 70126.48 \text{ milliamp} - \text{hour} = 70.126\text{Ah} \quad (1)$$

A typical mote require 3.3Volts. A pair of D-size Lithium Thionyl Chloride Battery (Li-SOCl<sub>2</sub>) part [SBD02](#) is rated for 19Ah. To achieve the desired 70.126Ah battery capacity the following number of D-size batteries are required:

$$\left\lceil \frac{70.126\text{Ah}}{19\text{Ah}} \right\rceil = 4 \text{ pair batteries} \quad (2)$$

Going with the results in equation (2), we can quickly determine that over 40 million batteries will be required per annum. One can argue that this is smaller than the fuel consumption of Class 1 railroads over the same period of time [24]; however, it is not a compelling reason. Using batteries alone would be a nightmare to maintain.

## 2.2 Significance of Proposed Approach

It was worthwhile studying the topic of energy harvesting. The significance of this research is high, considering the increasing growth of sensors in the railroad. Wireless sensors are adopted in so many areas. They provide a tremendous benefit for a number of use cases. The ability to install sensors in remote locations to monitor assets, without the cost of running wires, will result in numerous benefits including labor savings, increased



productivity, decreased accidents due to working in a hazardous environment, and improved processes and efficiency.

The growth for wireless sensors has been seen in:

1. Industrial control and monitoring
2. Home automation and consumer electronics
3. Security and military sensing
4. Asset tracking and supply chain management
5. Intelligent agriculture and environmental sensing
6. Health monitoring

Despite the rapid growth and potential of wireless sensors, power is still a hindrance to progression. This limitation is apparent in most (if not all) wireless devices and can be seen in common devices like cell phones, where the user has to recharge the battery quite often. Imagine if all a person had to do to charge a phone was to stick it out a window for sunlight or just walk with the phone in their pocket and the displacement from walking was enough to charge the phone. The significance of this research cannot be overstated. Theoretically, an infinite amount of ambient energy exists in the environment. The challenge is to discover new ways to harness these ambient energies and convert them into electricity.

## 2.3 Research Challenges

Energy harvesting and storage provides several benefits but not without strings attached. There are numerous challenges with the study/implementation of energy harvesting. One challenge is the upfront cost to implement the process. Another challenge is when the ambient energy is not available to harvest. For example, solar energy doesn't work in a dark environment, and piezo energy requires dynamics at a certain frequency and it has to be tuned to match the natural frequency of the vibrating body. If the train is not moving, then there will be little to no energy to harvest.

Challenges also extend to storage devices as well. Batteries or super capacitors are not exempt from the world of imperfection; storage technology has limitations as well. The following are some of these limitations:

- Gets hot during charging.
- Overcharge issues.
- Catch on fire.
- Environmental pollutant.
- Expensive to manufacture.

These challenges are compounded in industrial environments such as the railroad. The railroad environment is hazardous and not as elegant when compared to consumer electronics. Thus, harvesters are more susceptible to failure.

One of the goals of this study was to determine how much vibration was available for the different types of freight cars, such as empty versus loaded. The biggest challenge of this research was locating the right railcar to use for the experiment. Another challenge was finding an affordable vibration data logger that could withstand the extreme vibrating frequency of the freight car.

## 2.4 Proposed Research Objectives

The objective of this research was to survey different solutions for energy harvesting. The research focused on the railroad environment to determine how much ambient energy is available in the train environment and make recommendations based on the outcome of the study. The expected outcome of the research was investigating the feasibility of using an energy harvester as the sole power source for the ubiquitous sensors that make up the IoT on the train, as well as gain an understanding of the processes involved in the production of materials used to harvest ambient energy and manage storage devices. The following chapters contain details of the work done to determine how much energy is consumed by motes and how an energy harvester can be used.

## 2.5 Related work

In 2013, Hart et al. developed a vibration harvester that work for low frequency  $< 20\text{Hz}$  [25]. The largest output was in response to the train vibrations which produced a peak power of  $18.5\text{ mW}$ . The recorded a natural frequency of the train at  $11\text{Hz}$ , which is 2 degrees of magnitude smaller than what was observed in this study.

Ung et al. conducted a similar study [26]. In their experiment, they recorded vibration from railcar and was able to recreate it in the lab. They were able to produce a peak power of  $1.71\text{ mW}$  and a longer term RMS power of  $874\text{ }\mu\text{W}$ .

Nelson et al researched in [27] a method of harvesting energy from the track when a railcar passes by piezoelectric.

Similar to Nelson's et al. research in [27], in 2011, Pourghodrat investigated different approaches for harvesting vibration energy from passing trains to power the rail crossing LEDs [28].

In 2014, Lin et al. developed an electromagnetic energy harvester which is stated to be capable of powering most of the trackside equipment when the train passes by. The device is advertised provide 71% mechanical efficiency and can provide up to  $50\text{W}$  [29].

The works described in the prior paragraphs, focused on harvesting vibration energy from passing railcars (train) to power track side devices. The scope of this thesis is to use energy harvesting for the wireless sensors installed on the railcar.

The contribution of this study is to determine how energy harvesting can be used in the safety sensors. First, determine the power usage of the sensor in different configurations using empirical data, survey the rail environment to determine which energy harvester(s) is/are the best fit, and find out how much power can be generated from that harvester.

## Chapter 3: Literature Review

---

*Even in literature and art, no man who bothers about originality will ever be original: whereas if you simply try to tell the truth (without caring two pence how often it has been told before) you will, nine times out of ten, become original without ever having noticed it [30].*

*- C. S. Lewis*

---

### 3.1 Energy Harvesting Overview

First let's define the meaning of Energy Harvesting. According to [30], *Energy Harvesting (also known as power harvesting or energy scavenging) is the process by which energy is derived from external sources, captured, and stored for small, wireless autonomous devices, like those used in wearable electronics and wireless sensor networks.* This definition is very specific. Let's use the method of divide and conquer to formulate a less constrained definition.

### 3.1.1 What is *Energy*?

Energy is the fundamental premise of Physics. The term *energy* is used to describe the scalar quantity that is associate with an object or a system of objects [31]. It is scalar in the sense that it has magnitude without direction. The law of conservation of energy assures that the universe will not run out of energy. It exhibits this sort of Chameleon phenomenon by changing its state based on the environment. It is also transferable between two objects (this process is called *Work*<sup>2</sup>); meaning the energy of object A can be influenced by object B, even without making contact. This is the capacity to do work [32]. This capacity exist in different variations. Some of the variations are more abundant relative to the environment. There are two forms of energy, potential and kinetic. Potential energy is important in understanding *Energy Storage*, discussed further in the Energy Density section.

### 3.1.2 What is *harvesting*?

The denotation of harvesting is “*to gather...*” [33].

---

<sup>2</sup> “Work” in this reference should not to be misunderstood as physical labor. The Work of concern is the product of force and displacement;  $W = Fd \cos \theta = \vec{F} \cdot \vec{d}$

If the two descriptions from above are combined, the resulting definition of Energy Harvesting is the process of gathering and repurposing the abundant ambient energy in the environment to a useable power source for electronics.

Another important term when speaking about energy is energy *density*. The term is used mostly in fluid and magnetic field subjects. Density is the rate of change of the magnitude of a scalar quantity with respect to the change in volume. Given by the formula:

$$\rho = \frac{\Delta(\text{magnitude of scalar})}{\Delta v} \quad (3)$$

The scalar quantity can be mass (unit is kg/m<sup>3</sup>) [34], charge (unit is C/m<sup>3</sup>) or work (unit is Joules/m<sup>3</sup>) in the case of electricity. With this equation, the formula for energy density  $E_p$  (also denoted by  $u$ ) can be determined. Energy density is the potential energy per unit volume. The potential energy is the work required to charge the capacitor [31]. This is given by the square of charge multiplied by the capacitance and divided by two. Show below:

$$\text{Potential energy (U)} = \frac{q^2}{2C} = \frac{1}{2} CV^2 \quad (4)$$

Where  $q$  = charge,  $C$  = capacitance, and  $V$  is potential difference.

With this, the energy density can be determined as:



$$u = \frac{1}{2} \epsilon_0 E^2 \quad (5)$$

E is the magnitude of the electrical field and  $\epsilon_0$  is the electric constant ( $8.85 \times 10^{-12} \frac{C^2}{Nm^2}$ ) [31]. Energy density is an important metric for determining how much energy is available. Another metric used is power density. These two metrics are needed to quantify how much ambient energy is available.

## 3.2 Energy Harvesting Sources

The popular ambient energy source available in our environment is as follows:

- Mechanical (vibration, pressure...etc.)
- Thermal energy (energy from heat)
- Radiated energy (solar, infrared RF)
- Chemical energy
- Nuclear...etc.

Each of these sources is characterized by different power densities. **Figure 3–1** below shows a breakdown of the energy density before conversion:

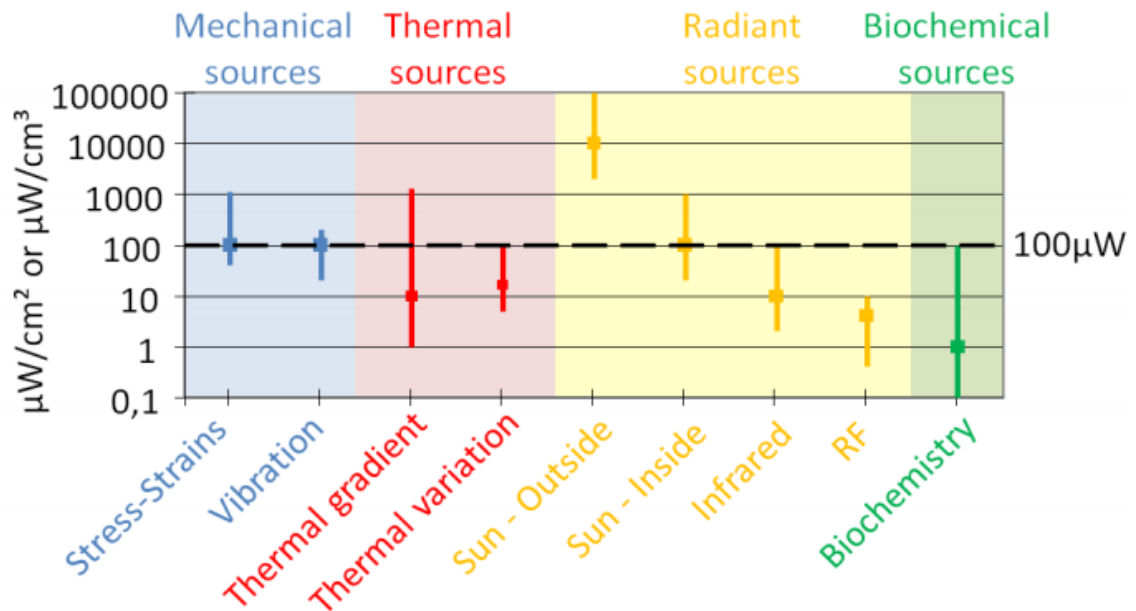


Figure 3-1: Ambient Energy Power Source before conversion [35]

As expected, radiant sources perform better outdoor than indoor. The ambient energy must be selected based on the sensor's environment. Radiated sources in the rail environment pose a problem due to assuring the surface of the harvester will be clear of opaque objects. Freight cars are notorious for graffiti as shown in **Figure 3-2**. Spray paint over the solar panel causes significant performance degradation.



Figure 3–2: Freight car graffiti

Mechanical sources are ideal solutions for the freight car environment. **Figure 3–1** shows a power density of  $100\mu\text{W}/\text{cm}^3$ . A hybrid option (combining two or more of the ambient energy sources) would ultimately be more efficient. The circuit in Appendix D supports multiple energy harvesting sources. A concise energy harvesting block diagram is shown in **Figure 3–3**.

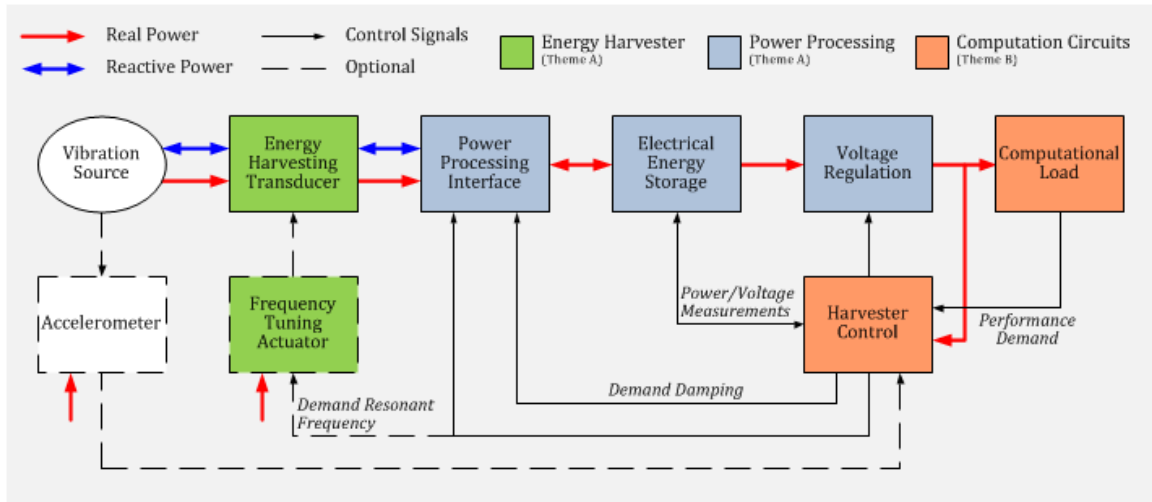


Figure 3-3: Energy Harvesting System Block Diagram [36]

### 3.2.1 Solar Energy

Solar energy, a type of radiant source, is one of the most abundant energy sources. A solar cell is a photovoltaic cell – a specialized semiconductor diode that converts visible light into (DC) electricity [37]. The unit for measured light (Illuminance) is lux (lumens/m<sup>2</sup>). Lux is represented by the symbol  $lx$ .

Solar cell output power depends on lux (lumens/m<sup>2</sup>). Lux varies greatly from indoor to outdoor. The power  $P$  in watts (W) obtained from using solar can be calculated as luminous flux  $\Phi_v$  in lumens (lm), divided by the luminous efficacy  $\eta$  in lumens per watt (lm/W):

$$P_{(W)} = \left( \frac{\phi_{V(lm)}}{\eta_{(\frac{lm}{W})}} \right) \quad (6)$$

The following are different types of solar cells [38]:

- Non-Si Thin film
  - These have a 5 – 12% efficiency
  - Can be made flexible.
  - Low cost.
  - High intrinsic losses.
- Amorphous Si Thin Film
  - 5 – 10% efficiency.
  - Similar to the non-Si thin films, can be made flexible as well.
  - Cheaper than the Non-Si Thin film.
  - Cons: High intrinsic loss.
- Polycrystalline silicon
  - More efficient than Non-Si Thin film and Amorphous Si Thin film.
  - Not as high intrinsic as thin film.
- Monocrystalline Silicon
  - Type of solar cell that is the most efficient and exhibit an efficiency of 15 – 20%.

- They are very efficient in low light environments like in doors.
- These type of solar panels have the lowest intrinsic losses
- Cons: This type of solar cell is very expensive.

Solar energy harvesters are not be the most efficient for the railroad because of the harsh environment. There is major performance degradation when the panels get dirty as shown in **Figure 3–2**.

### 3.2.2 Vibration Energy

The train environment has an abundant amount of vibration. Unlike solar, the performance of vibration harvesters is not affected by dirt. Piezoelectric material produces mechanical strain under the influence of an externally applied electrical field, and conversely produces electrical potential in response to applied mechanical strain [39].

The three main devices designed to convert mechanical energy to electricity are: piezoelectric, electromagnetic and electrostatic devices.

#### 3.2.2.1 Piezoelectric devices

Piezoelectric materials are able to harness pressure caused by stress or strain and convert it into electricity. This type of charging mechanism is very slow and it will take a while to fully charge up a battery. The pros and cons from [35] are as follows:

- Pros:

- High output voltage
  - High capacitances
  - No need to control any air gap between electrodes.
- Disadvantages
  - Materials are expensive
  - Coupling coefficient linked to material properties

#### 3.2.2.2 Electromagnetic devices

The engineering behind these devices is based on electromagnetic induction using Lenz's law. The devices transfer energy between two objects wirelessly. This is achieved by using inductive coupling coil, which forms a transformer, to create an alternating electromagnetic field from within a charging base station and second inductive coil is attached to the device that need to be charged. The charging device takes power from electromagnetic field and converts it back into electrical current to charge the battery.

The pros and cons from [35] are as follows:

- Pros:
  - High output currents
  - Long lifetime proven
  - Robustness
- Cons:

- Low output voltages
- Hard to develop MEMs devices
- May be expensive (material)
- Low efficiency in low frequencies and small sizes

This method is how the RFID (or AEI) is powered. It will not be effective for motes since these devices will be moving and is needed to operate while in motion.

### 3.2.2.3 Electrostatic devices

Electrostatic devices harvest electrostatic discharge generated by using two metals plate separated by a vacuum in a capacitor structured form. The pros and cons from [35] are as follows:

- Pros:
  - High output voltages
  - Possibility to build low cost systems
  - Coupling coefficient easy to adjust
  - High coupling coefficients reachable
  - Size reduction increases capacitances
- Cons:
  - Low capacitance. Discharges quickly
  - High impact of parasitic capacitances



- No direct mechanical-to-electrical conversion for electrets-free converters.

A diagram illustrating these methods is as follows:

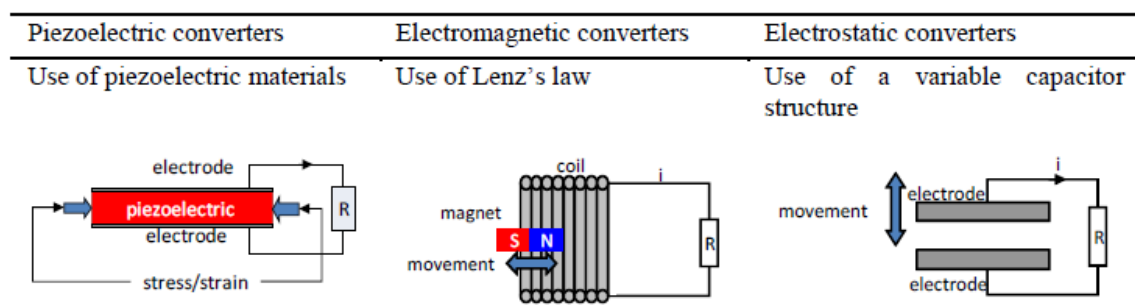


Figure 3–4: Mechanical-to-Electrical converters [35]

### 3.3 Energy Storage

When energy is harvested it makes sense to store this energy for future use, in case if the energy source is no longer available. The energy harvested must be stored to improve efficiency. This also help with quick starting of the device. Since a reservoir of energy is available, a device doesn't need to harvest energy first for it begins operation.

#### 3.3.1 Battery

Batteries are electrochemical energy storage cells. Batteries convert chemical energy to electrical through oxidation-reduction reactions. There are two categories of batteries –

rechargeable and non-rechargeable. The storage mechanism must be recharge to use energy harvesting. The battery of interest in this thesis is Lithium.

### 3.3.1.1 Lithium – Ion

Electrical current is generated when lithium ions migrate from the negative electrode (anode) to the positive electrode (cathode) through electrolyte during discharge [40]. A reverse of this process will result in the lithium ions going back into the anode and their removal from the cathode to produce a charging state.

The following diagram illustrates this process:

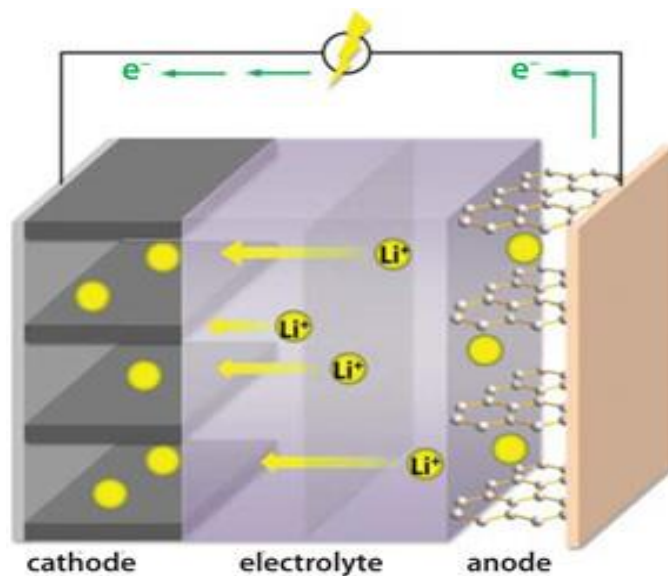


Figure 3–5: Cross section of a Li battery with Lithium salt as electrolyte [40]

Lithium batteries are exceptionally efficient compared to other battery type such as Nickel-metal hydrides (Ni-MH). Figure 3–6 shows a Ragone plot of different battery types.

Relative Performance of Various Electrochemical Energy-Storage Devices:

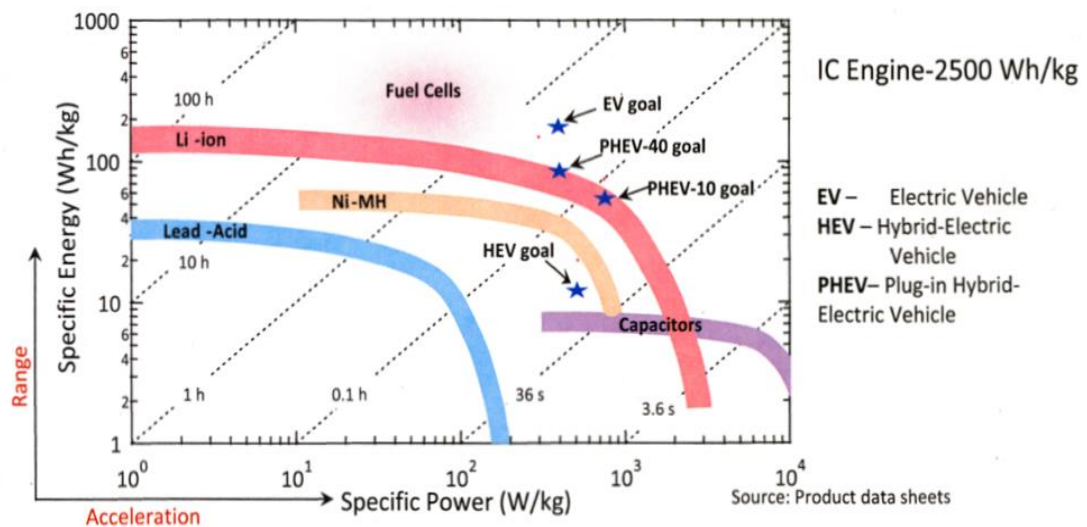


Figure 3–6: Ragone plot [40]

Li-ion batteries have the best energy density. The battery last longer than its counterparts as can be seen on the Ragone plot and charges very quickly. It is the next runner up after Super capacitors.

### 3.3.1.2 Problems with Li-Ion batteries

One of the known problems with lithium is the fact that it gets very hot during charging, and has been known to catch on fire on some occasions. There have been several recalls

of defective Lithium batteries and an incidence of the Tesla Model S catching fire. The reason for this is caused by the anode or cathode puncturing the separator, which will cause a short circuit. The aftermath of this short circuit could be as mild as a little spark or a rapid rise in temperature which will lead to fire.

This problem can be prevented by using a reinforcing material for as a separator.

### 3.3.1.3 Stagnant energy density for batteries

Energy density has been stagnant for battery technology. Moore's law clearly doesn't apply for batteries. The following graph shows the growth of batteries:

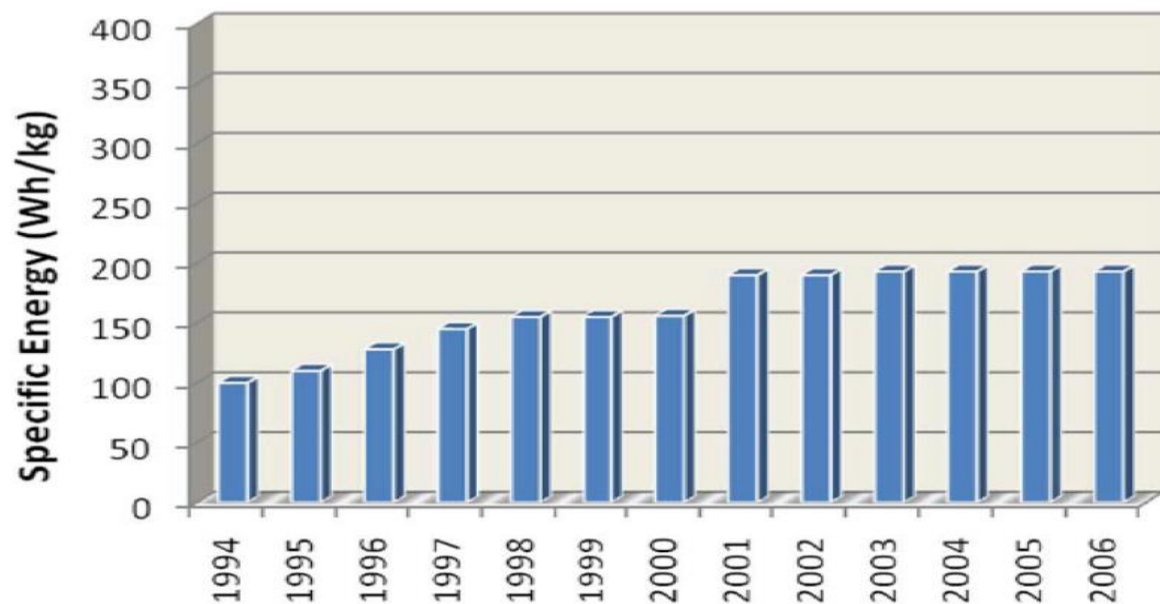


Figure 3–7: Source: TIAX

### 3.3.2 Supercapacitors

Supercapacitors are basically fast charging and discharging storage devices. The charging rate is significantly faster than batteries. Supercapacitors are used in several applications because of its capabilities. The process is analogous to a spring; It can shoot out energy fast as with a pop gun (feature is used in flash for camera) [38], and smooth out bumps as with shock absorbers in a vehicle which is why it is used to as noise/interference filter in wireless sensors networks.

Supercapacitors cross sectional structure look like two traditional capacitors combined together with an electromagnetic and separator in between them. Electrolyte is used to create a double layer.

Energy and Power principles for super capacitors show that energy and power is directly proportional to the square of the voltage. This principle sheds a light on why super capacitors charge very fast when compared to batteries. Supercapacitors also eliminate additional steps like heterogeneous charge-transfer and chemical phase changes that is in battery.

Super capacitors use to be very expensive but current report by IDTechEx in Figure 3–8 shows that the cost has significantly dropped and is getting close to Lithium-ion.

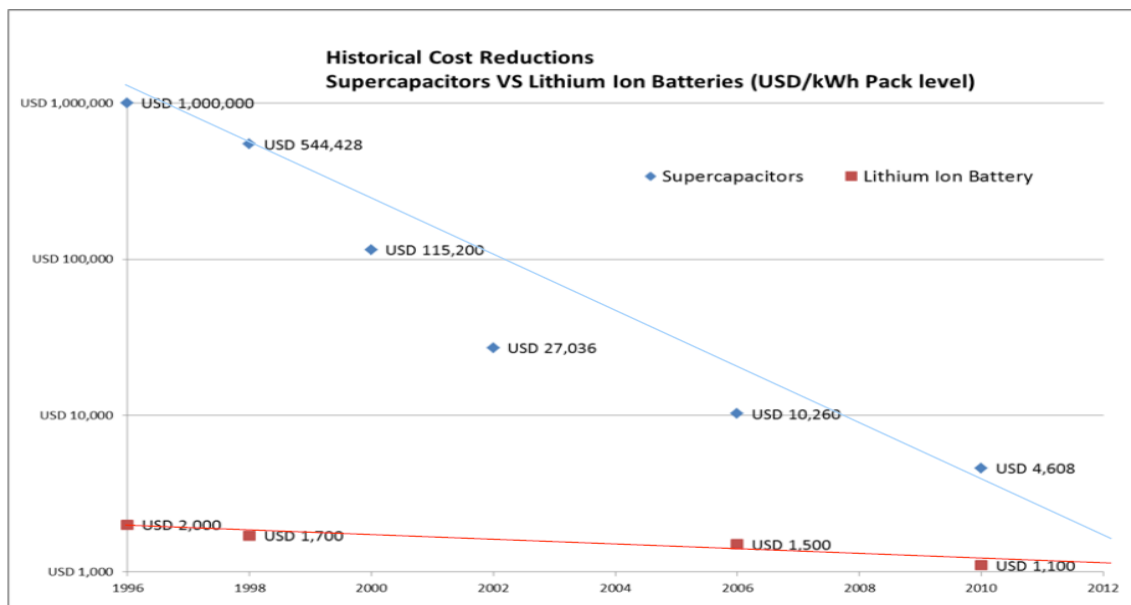


Figure 3–8: Lithium vs. Supercapacitors historical cost (Source IDTechEx)

Supercapacitors are making their way to the mainstream. Some vehicles have reported to be solely powered Supercapacitors. This technology has great potential in solving some of the slow charging rate problems. Supercapacitors, unlike batteries are not toxic to the environment. That makes them an ideal option for environmental cautious application.

## Chapter 4: Results and Analysis

This chapter covers the research that was done to determine the power requirement for the motes, and the results of evaluating each of the energy harvesting approaches and storage.

### 4.1 Power Consumption by Sensors

This section describes how the sensor power consumption was calculated using 100 motes.

#### 4.1.1 Experimental Setup

The nodes were placed in a linear topology as shown in Figure 4–1 with 25 yards between each node to simulate a 100 railcar train. 10 of the 100 nodes were placed on another set of track to evaluate the long range capability. The distance between the two tracks was 138 meters. The length of a railcar varies by type. The average length is 65 feet [41]. The experiment was performed with sensors placed 25 yards (75 feet) apart.

The setup simulated one sensor node per railcar. The main reason for this is to verify the RF range and test for the worst case scenario. Worst case in the sense where majority of

nodes are out of service. The experiment validated the self-healing feature of the network to ensure the entire network doesn't complete come to a halt.

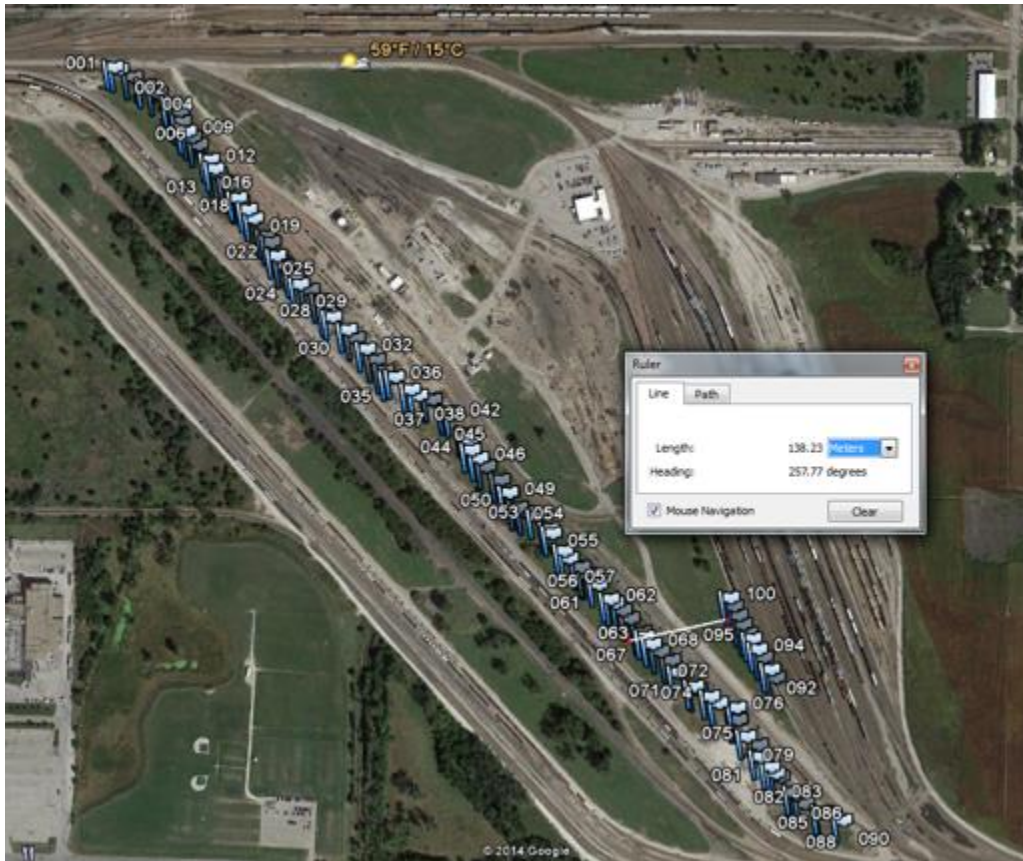


Figure 4-1: Motes placement

The nodes on the second track (nodes 91 - 100) were used to get some insight on how node to node proximity could impact the network performance. Node 91 was placed 0.76 miles away from the gateway. Items examined in this experiment:

- Maximum power usage



- Correlation of power usage vs node distance from gateway
- Impact of node to node proximity on network performance
- Will the nodes on the second track use more or less power than the rest?
- Will the last nodes on the first track use more or less power?

The gateway was placed 25 yards from node in position P001 at the northwest corner of Figure 4–8. Two antennas were used (not simultaneously) for the experiments. A directional 14.5 dBi Radome Enclosed High Gain Yagi antenna and an Omni-directional 4dBi antenna. The antenna was mounted 16 feet high to simulate the height of a locomotive.

#### 4.1.2 Experimental Procedure

1. The sensors were configured to report the charge used every 15 minutes. The charge information did not represent the cumulative charge used by the entire system including GPS and cellular. The number only included the charge used by the mesh network radio. After exporting charge data to excel, the charge and event date deltas were determined. The event date was the time the event was generated. The time was approximately 15 minutes.
2. Divided the delta of the charge by the delta of the event date to calculate the charge.

### 4.1.3 Observation

The motes had a battery pack with capacity of 76 Ah. The current was determined by using coulombs law:

$$i = \frac{dq}{dt} \quad (7)$$

The maximum current<sup>3</sup> used by the node for the time period 5/27 through 6/6 was 0.96mA as shown in Figure 4–2.

---

<sup>3</sup> This is the current used by the mesh network. Does not represent the current used by the entire system.

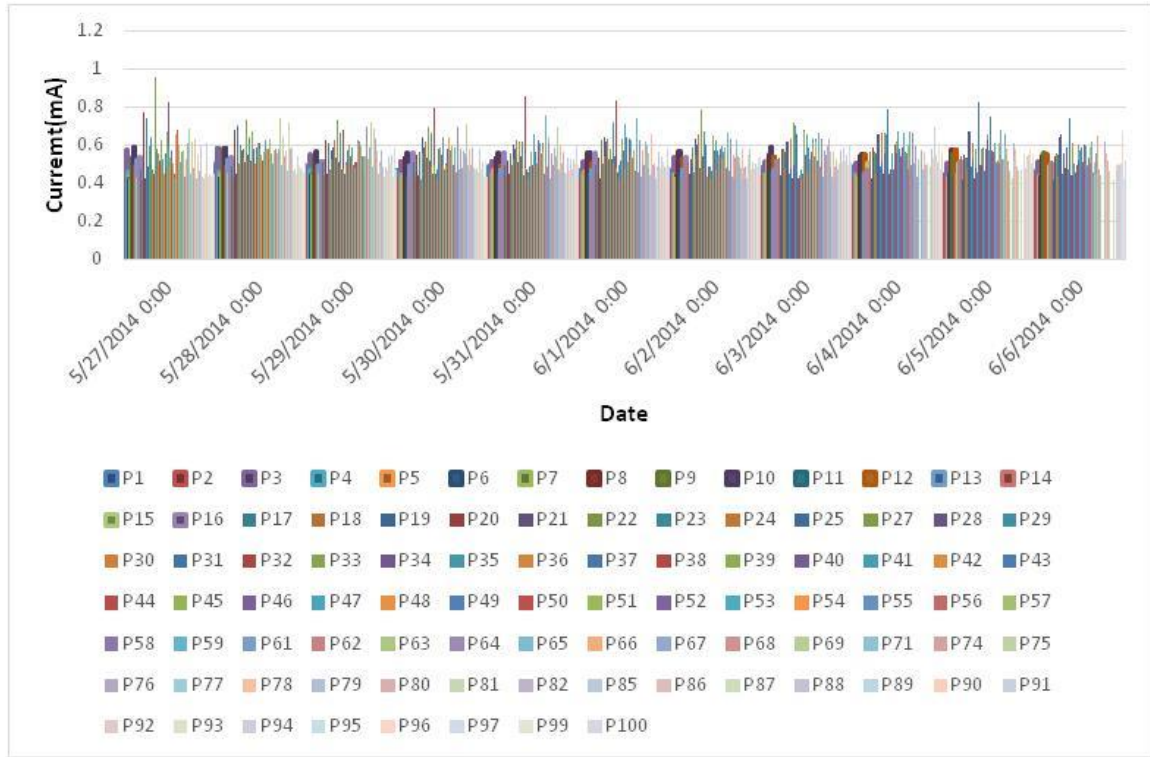


Figure 4–2: Current representation

The sensors required 3.3VDC. The total power draw is:

$$Power = Current \times Voltage \quad (8)$$

$$Power = 0.96mA \times 3.3V = 3.168mW$$

The battery duration if GPS and cell are disabled can be estimated from the current used by the mesh network.

$$\frac{Electric\ Charge(Ah)}{Current(A)} = Duration \quad (9)$$

$$\frac{76Ah}{0.96mA} = 79166.67hours = 3298.6 days = 9 years$$

Surprisingly, the node using the most power was in location 33. Figure 4–3 and Figure 4–4 show a closer look of the column graph for 5/27 and 5/28 respectively. The bars appear in the order of where the node was placed. In other words, the first bar corresponds to position 1 (P1) and the second to position 2 (P2)...and so on.

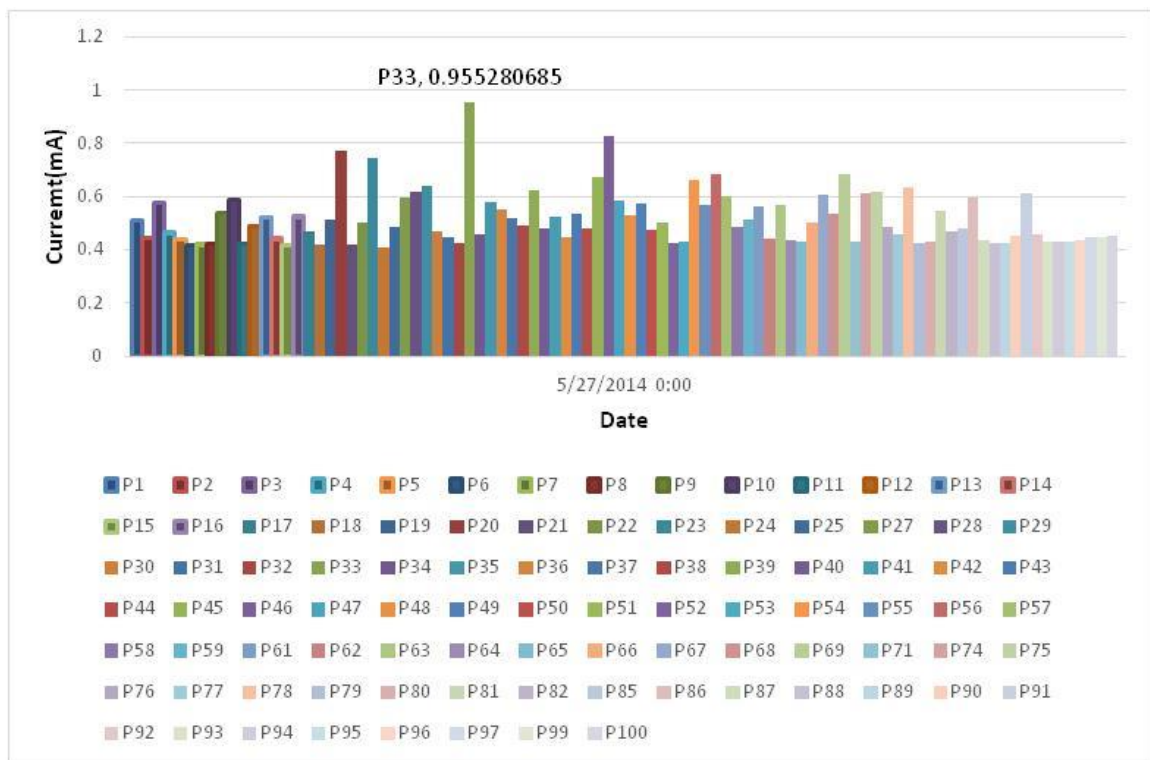


Figure 4–3: Zoomed into 5/27

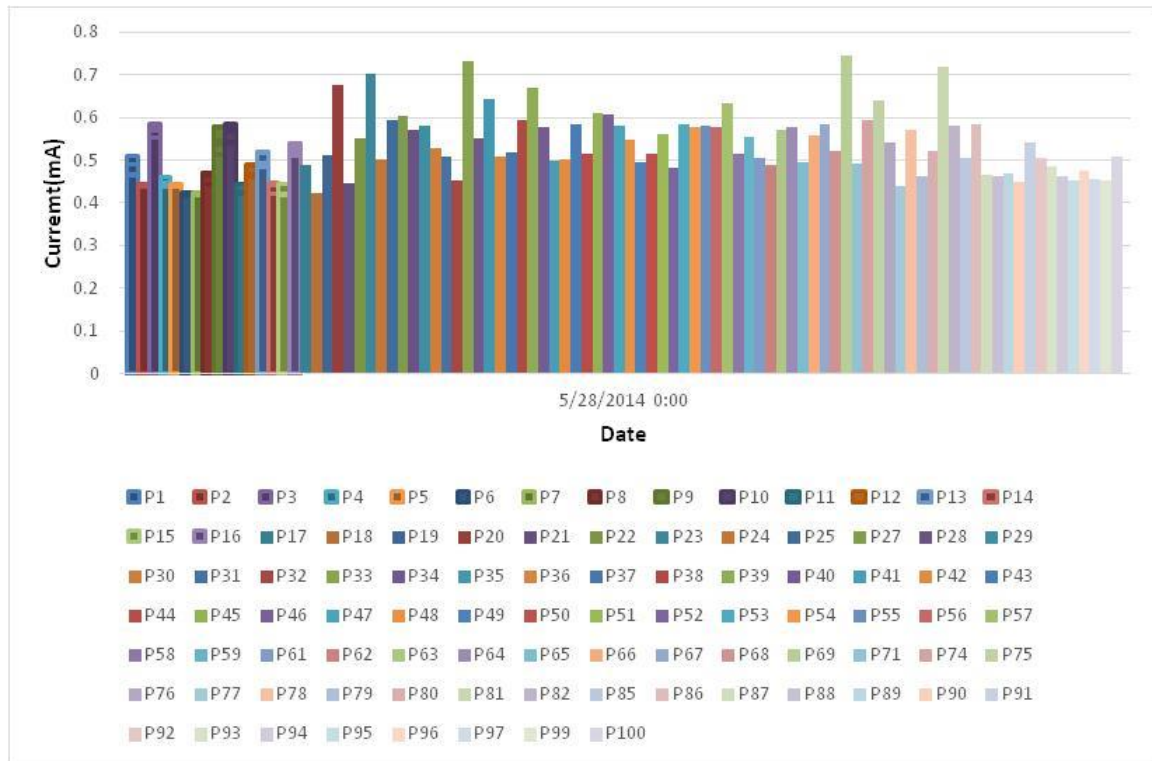


Figure 4-4: Zoomed in 5/28

A closer look at nodes placed - close to the gateway (P1 - P10), in the middle of the linear path (nodes 51 - 61), at the end of the path (nodes 81 - 90), and at the second path (nodes 91 - 100) are shown in Figure 4-5, Figure 4-6 and Figure 4-7.

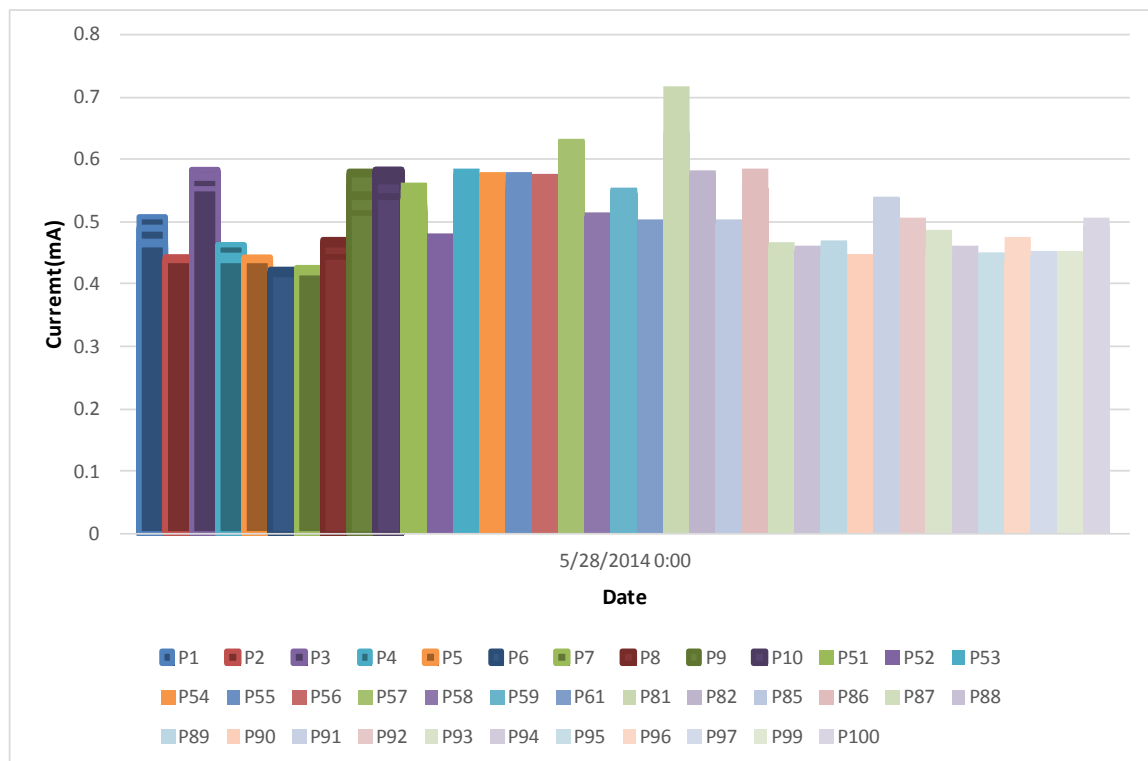


Figure 4-5: Current use by the nodes placed at beginning, center and end of the path for

5/28

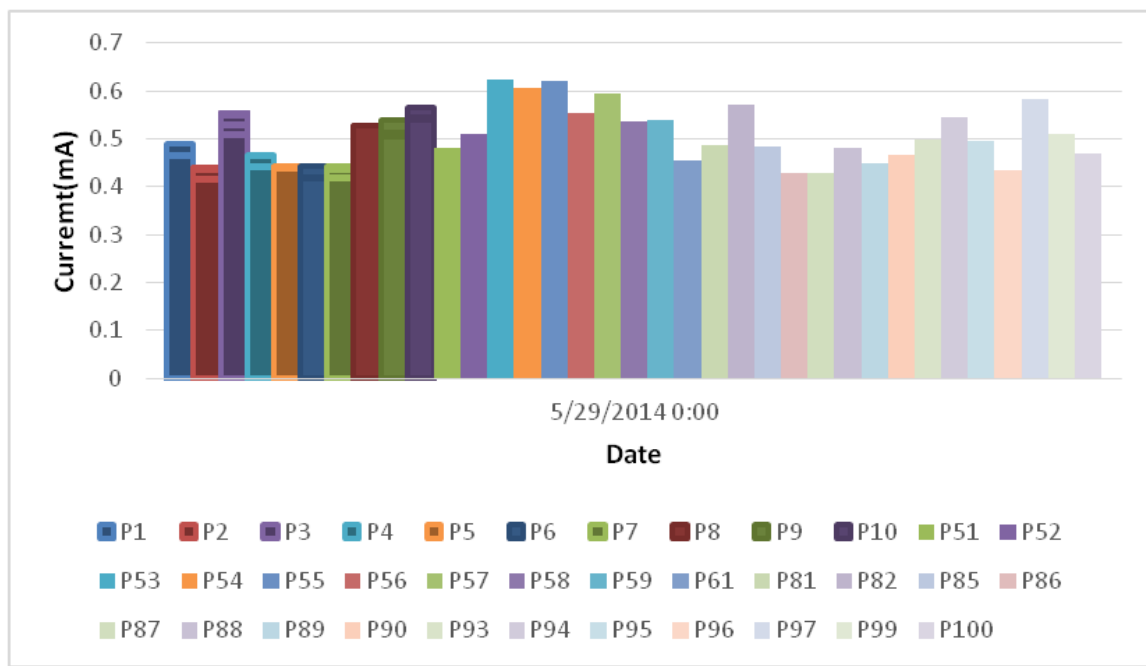


Figure 4-6: Current use by the nodes placed at beginning, center and end of the path for

5/29

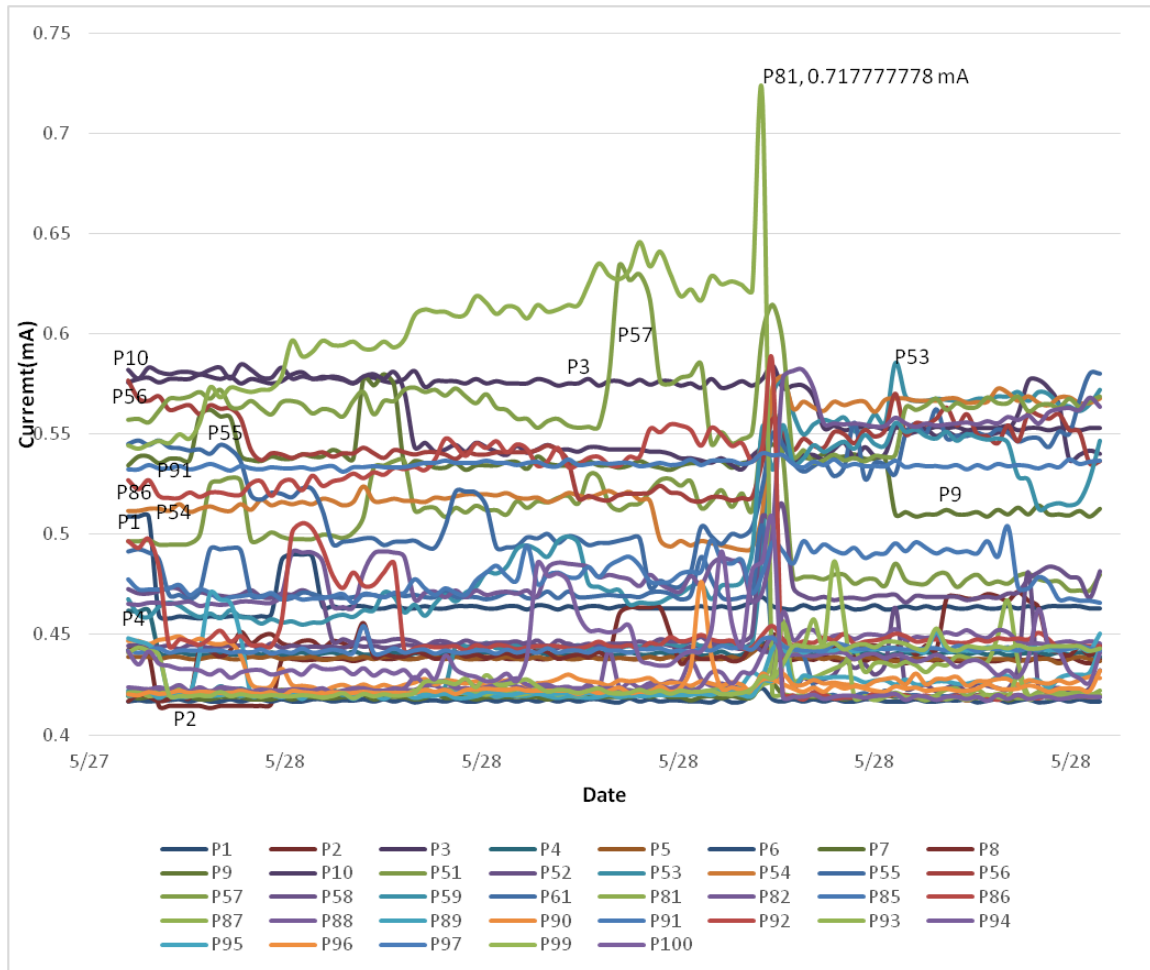


Figure 4–7: Trend of the current used by the nodes placed at beginning, center and end of the path for 05/28

It was observed that nodes closer to the gateway did not significantly use more power than the rest of the nodes. The nodes in the middle were the busiest. The nodes on the second track (nodes 91 – 100) used the least cumulative power.



<b>Note:</b>	This result may vary when the devices are mounted on actual rail cars.
--------------	--

#### 4.1.4 Error Analysis

Further analysis was performed to understand why the nodes closer to the gateway (P1 – P10) used relatively the same amount of power as the rest of the network as seen in Figure 4–4. In the sensors architecture, each node will try to have at least 4 neighbors (links). The neighbors periodically sent heartbeat packets to each other. An aggregated outcome of these packets is sent as a synchronous event to the gateway. The gateway then uses this information to compute the entire network health. The chart below is an hour snapshot of the number of links each node has and with the position the node was placed.

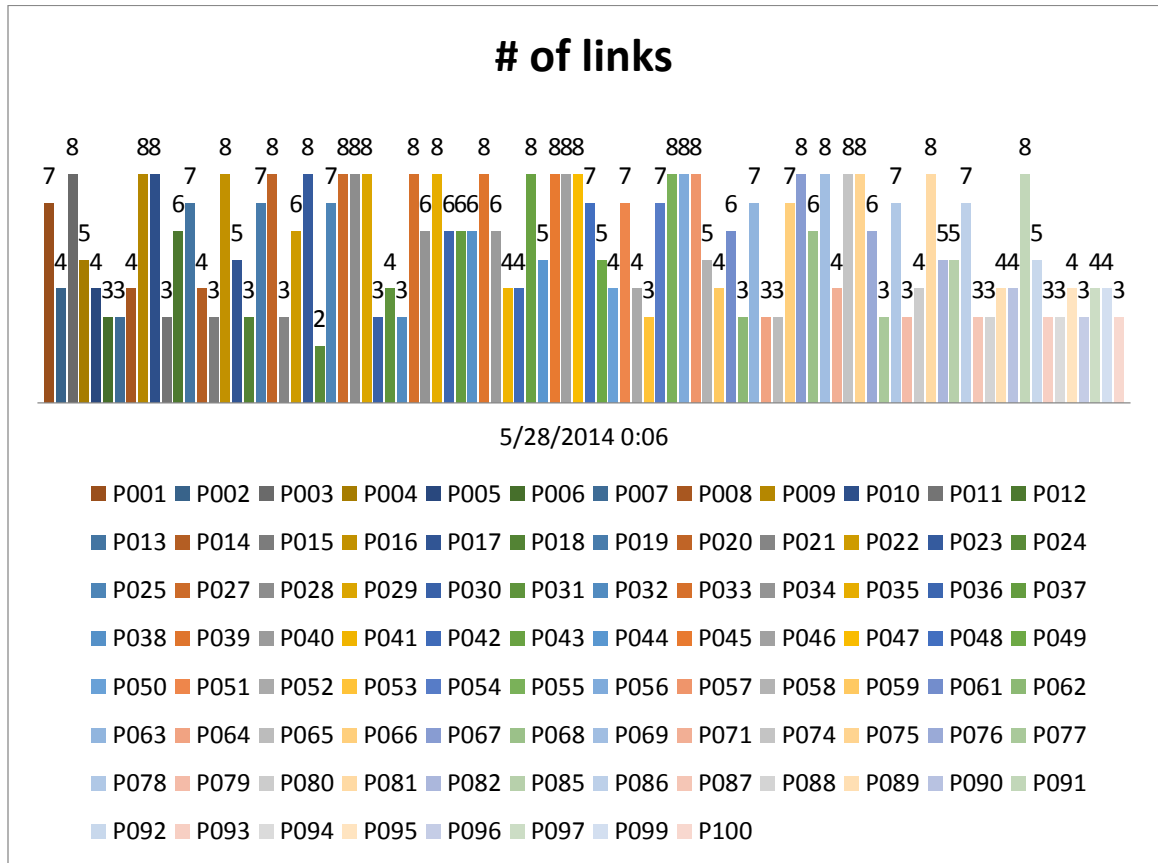


Figure 4–8: Motes Link count

There were 25 nodes with 8 links (including node placed on P033), only 6 of those were placed in the first 25 position (P001 – P025). Nodes with more links are expected to use more power since they have to send and receive packets to maintain those links. A weak RSSI of a link can result in increased retries. This occurred more in the nodes in the middle.

The total packets sent and received by each nodes are shown on **Figure 4–12**.



Figure 4–9: Sum of Total TX and RX (for 5/27)

Node 33 (P033) sent ~ 2000 more packets than the rest of the network as shown above in

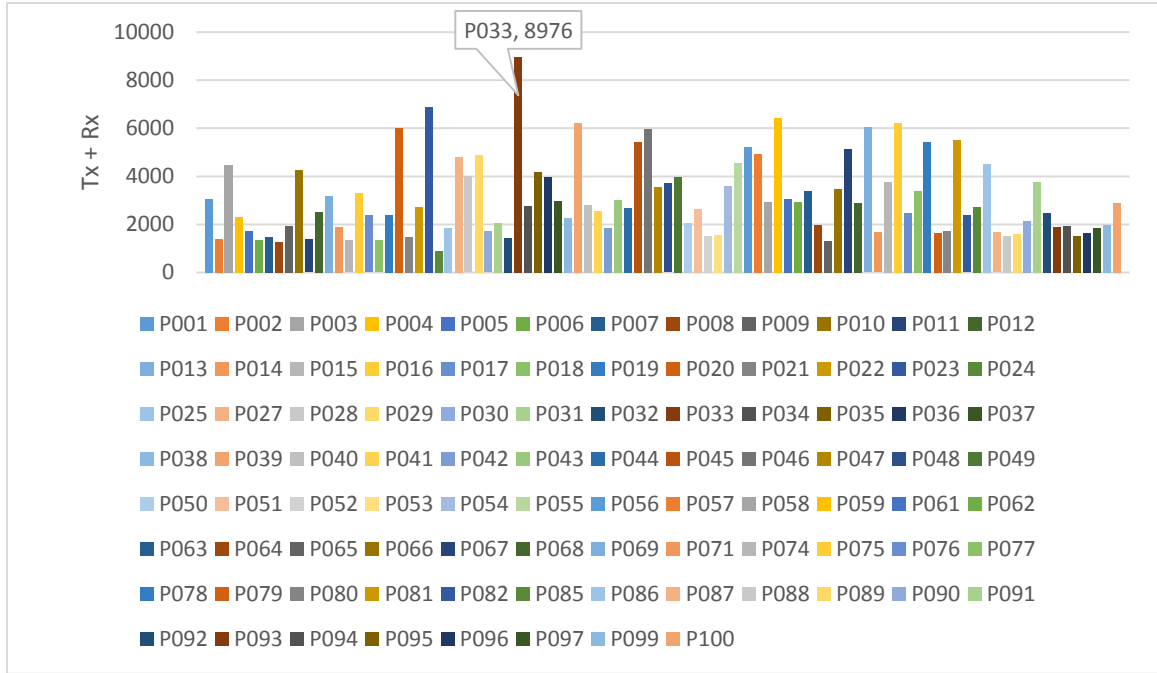


Figure 4–9: Sum of Total TX and RX (for 5/27)

Why did P033 send so much packet and who were those packets sent to?

Node 33 maintained direct links to 15 neighbors. Recall the distance constant is 25 yards.

So, the distance between each nodes can be quickly derived by the formula:

$$|(Node_n - Node_{n-i}) \times Distance\ constant| \quad (10)$$

Where the Distance constant = 25 yards.

The formula was used to generate the distance values in **Table 2** which shows the neighbor list with the distance and average RSSI. Node in position 0 (P000) is the gateway.

Table 2: Node 33 Neighbor List

Neighbor	Distance To Node 33 (Yards)	Distance To Node 33 (Miles)	Distance to Node 33 (Meters)	Average RSSI
<b>P000</b>	825	0.47	754.38	-92.00
<b>P016</b>	425	0.24	388.62	-93.00
<b>P019</b>	350	0.20	320.04	-94.00
<b>P022</b>	275	0.16	251.46	-92.60
<b>P027</b>	150	0.09	137.16	-85.83
<b>P029</b>	100	0.06	91.44	-81.00
<b>P035</b>	50	0.03	45.72	-65.17
<b>P036</b>	75	0.04	68.58	-70.67
<b>P041</b>	200	0.11	182.88	-88.50
<b>P042</b>	225	0.13	205.74	-78.50
<b>P043</b>	250	0.14	228.60	-84.70
<b>P044</b>	275	0.16	251.46	-90.17
<b>P045</b>	300	0.17	274.32	-82.33
<b>P046</b>	325	0.18	297.18	-90.17
<b>P062</b>	725	0.41	662.94	-93.50

**Figure 4–10** is an aggregation of the total traffic exchanged between Node 33 and neighboring nodes. The X-axis is the Neighbor position. The distance to the neighbors and average RSSI for the packets is listed in **Table 2**. Y-axis represents the sum of the receptions and the transmission for Node 33.

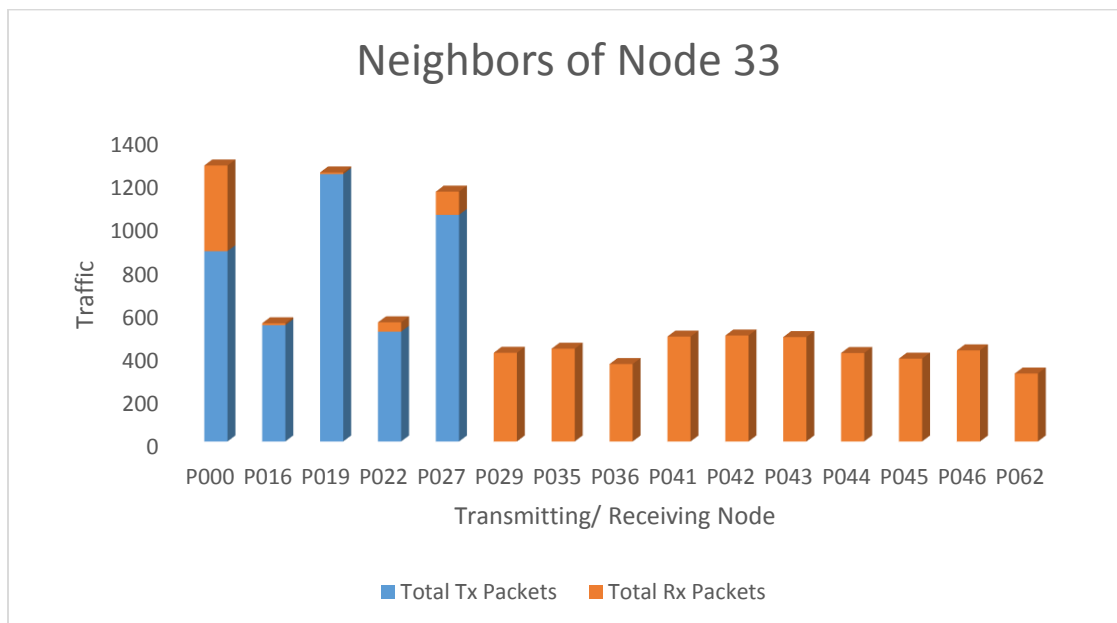


Figure 4–10: Transmissions and Receptions for Node 33

Node 33’s direct link to the gateway that was 825 yards away caused 40% of retried messages. Most of the traffic was attributed to this link and was sent at a very low average signal strength of -92dBm.

Another observation from **Figure 4–9** is that Node 33, located somewhere between P029 (100 yards to the right) and P035 (50 yards to the left), has a consistent pattern for its traffic. The upstream traffic (towards the gateway at P000) appears to be mostly transmissions with a few exception, while the downstream traffic (away from the gateway) are all receptions. This brings up the question – which traffic is more power intensive? Transmissions or receptions? Unfortunately, the data from the sensors doesn’t provide the granularity to trace what aspect of the system is using the most charge. That

notwithstanding, we will be able to formulate a theoretical conclusion that the charge usage should be directly proportional to the bytes.

Next, let's look at the total transmissions verses the failed transmissions. This will give an indication of how the power usage is influenced by the network stability. **Figure 4–11** is an illustration of this.

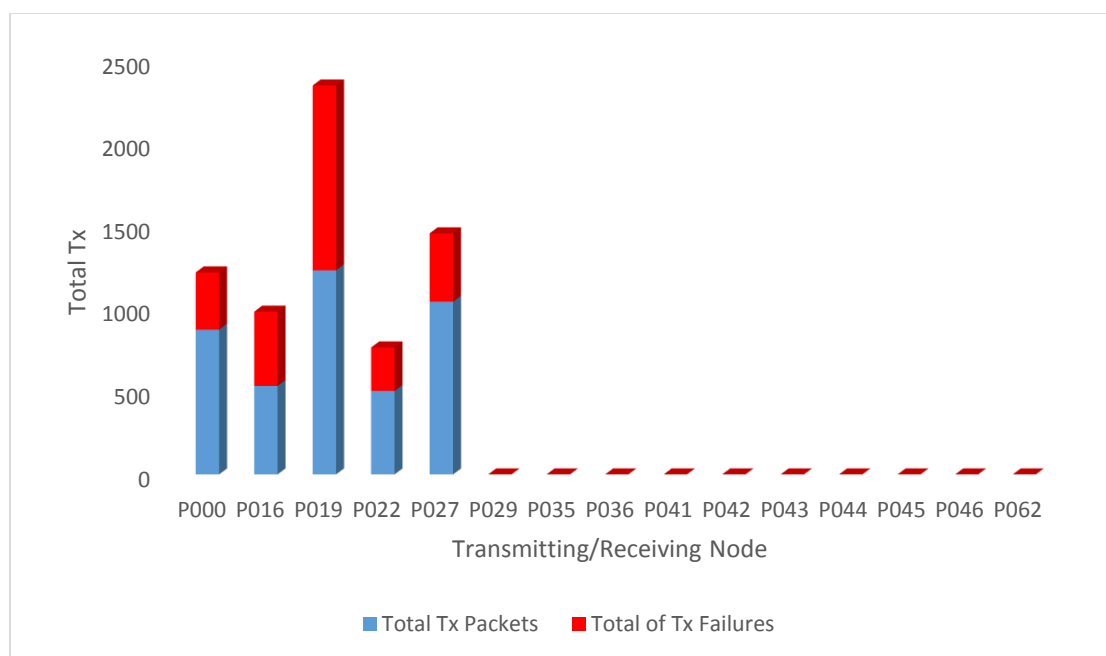


Figure 4–11: Failed Tx vs. Total Transmissions for Node 33

Node 33's neighbor on position 19 (P019) had the most retries. This node was physically closer to P033 than the gateway. Node 33 was 350 yards away from P019 and 825 yards from the gateway.

Why does P019 have over 4 times as much failed transmissions as the closer gateway?

The gateway had a much higher antenna placed at 16 feet. Referring back to **Table 2**, the average RSSI for links to P019 and P000 are -94dBm and -92dBm.

Total packets sent and received by each node for the second day of the experiment are shown on **Figure 4-12**.

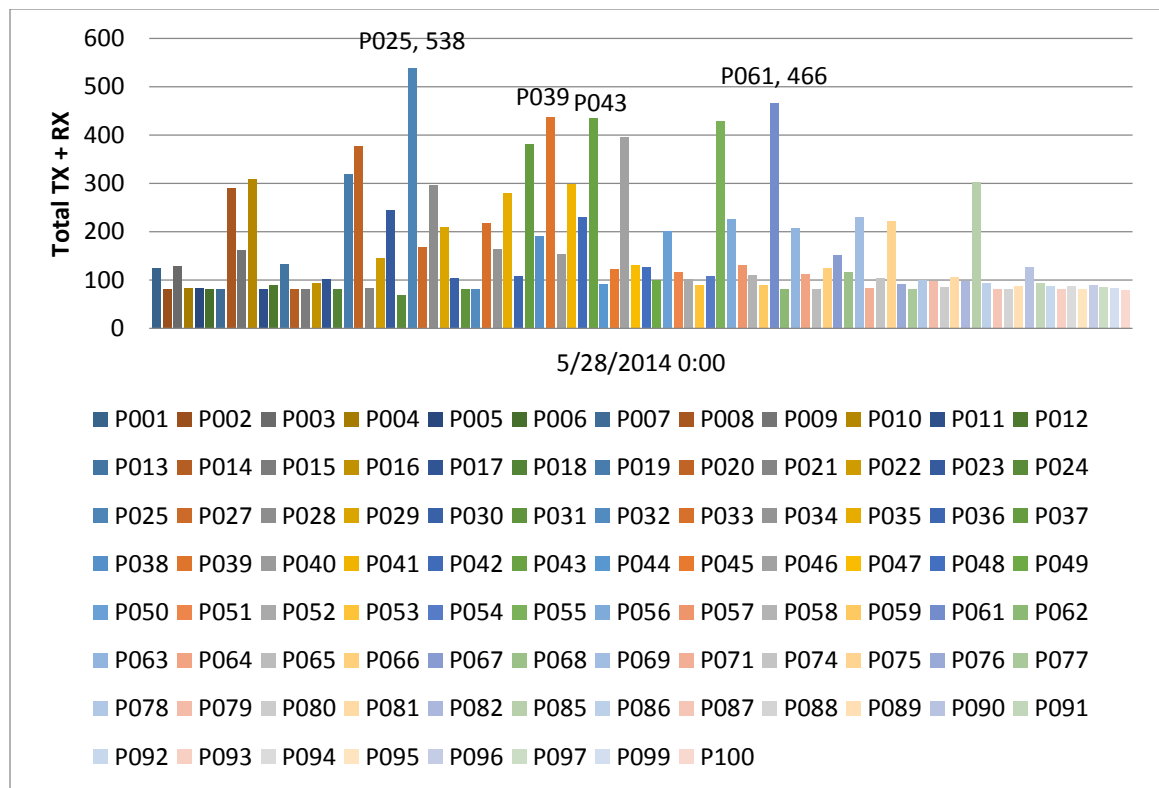


Figure 4-12: Sum of Total TX and RX (5/28)

There are different factors that lead to the even distribution of the power used by the network.



1. **Retries:** The network had an average stability of 68%. This means that 32% of the events sent in were retries. These retries account for the spikes on the **Figure 4–7**.
2. **Link counts:** The number of links is directly proportional to power use. More links indicate more TX and/or RX per node, which equates to more power per bits. Node placed at position 47 was observed trying to maintain a direct connection to the gateway. The link status is as follows:  
  
RSSI: -95 numTxPackets: 696, numTxFailures: 657, numRxPackets: 5.  
  
Almost 100% of the messages sent by this node failed. The cost of maintaining this link resulted in more power use.
3. **Sensor features:** In addition, parent nodes with multiple sensors are expected to use more power since these nodes will be receiving and reporting additional sensor events.

#### 4.1.5 Section summary

0.96mA was the maximum current drawn by the mote. This equated to 3.168mW of power. Referring back to Figure 3–1, mechanical sources would provide 100μW per cm<sup>3</sup>. This means that 31.68cm<sup>3</sup> of surface volume is needed to power the sensor. This is a theoretical value. In the next section, we will determine how much vibration is actually generated by the car.

## 4.2 How much vibration does the Railcar generate?

The Slam Stick [42] vibration data logger shown in **Figure 4–13** was used to record the vibration generated by different types of railcars that make up a train in four scenarios.



Figure 4–13: Slam Stick Data Logger Mount orientation

### 4.2.1 Experimental Setup

The Slam Stick data loggers were cable secured close to the bearing on four different types of railcars as shown in the following figures. The railcars were part of a train comprised of 20+ cars. The experiment was performed at the hump yard. The train was traveling approximately 1.9 mph to the hump. At the hump, the freight cars were uncoupled and allowed to free fall at a maximum rate of 20mph to the end of the hump.

The data logger was retrieved from the railcars at the end of hump and the experiment was repeated. The vector sum of the acceleration for all axes was computed using the following formula:

$$\sqrt{X^2 + Y^2 + Z^2} \quad (11)$$



Figure 4–14: Railcar 1 (Flat car)



Figure 4–15: Vibration Data logger Mount location on Car 1



Figure 4–16: Railcar 2 (loaded Covered Hopper Car)





Figure 4–17: Vibration Data logger Mount Location on Car 2



Figure 4–18: Railcar 3 (Empty coal car)



Figure 4–19: Vibration Data logger Mount Location on Car 3



Figure 4–20: Railcar 4 (Loaded Tank car)



Figure 4–21: Vibration Data logger Mount location for Car 4

#### 4.2.2 Experimental Procedure

The following four scenarios were evaluated using the different railcars shown in **Figure 4-11 to 4-18**.

**Scenario 1 – Cars loaded and stationery:** The purpose of this case study is to record the amount of vibration generated when the cars on the train are loaded but not in motion.

This is a common scenario that happens during the process of combining the cars to form the train.

**Scenario 2 – Loaded moving cars:** This is the typical scenario when the customer delivers the cars to the railroad for shipping and the trip from the sender to the receiver. The sensors availability will be critical during this time.

**Scenario 3 – Empty stationery car:** This case study examined the vibration generated when the cars were empty and not moving. This scenario is expected during inbound when commodities have been delivered to the customers. The mote sensors are expected to be operational during this time for car ordering, inventory tracking, exception reporting...etc., which implies that the energy harvester circuit should provide power during this scenario.

Note: a train can simultaneously be in scenario 1 and 2 state, comprising of both loaded and empty railcars.

**Scenario 4 – Empty moving railcars:** There will be several cases when cars are empty. As noted earlier, the railcars can have both loaded and empty cars. This scenario examines the vibration while the train is in motion.

The railcars designated as “Loaded” in the figures above were used to gather data for scenarios 1 and 2, and the railcars designated as “Empty” were used for Scenario 3 and 4.



### 4.2.3 Analysis of Data from Loaded Car

**Figure 4–22** shows the time domain view of vibration recorded for scenario 1 and 2. The train was moving in the Y axis direction. Refer to **Figure 4–13: Slam Stick Data Logger Mount orientation**.

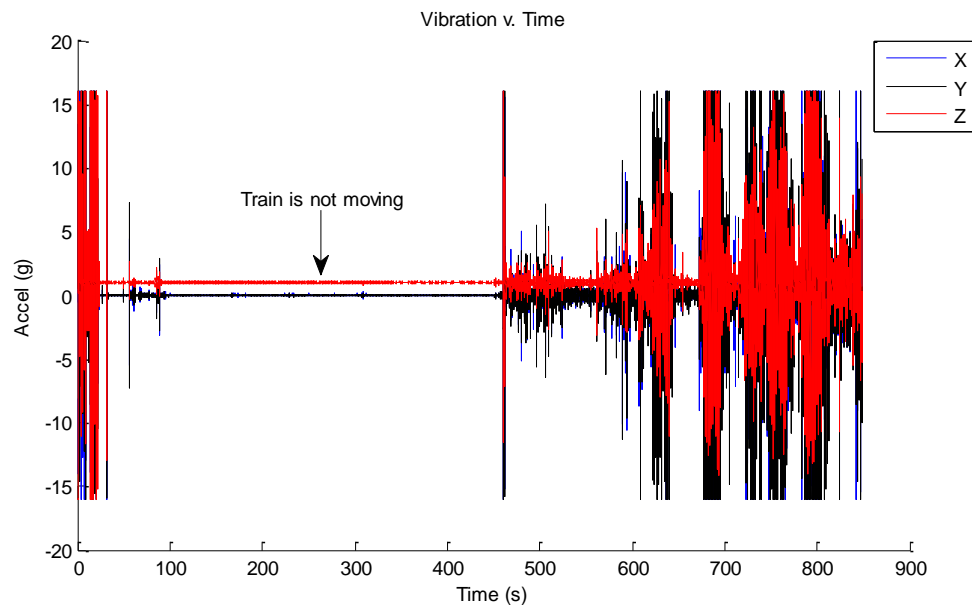


Figure 4–22: Time Domain (Loaded Railcar)

The amplitude of acceleration observed for the loaded train exceed the maximum capacity of the data logger which is  $\pm 16g$ . The data was gathered at a sample rate of 3200.00Hz. The combined duration of the recording was 872.32 seconds. **Figure 4–22** is a graphical representation of the total 2791421 data points per axis.

For a loaded train that was not moving, there was very little noticeable vibration.

#### 4.2.3.1 Determining the Resonance Frequency

To determine the natural frequency of the railcar, the data was represented in the frequency domain using the DFT/ FFT algorithm. The frequency representation is immensely useful in tuning the natural frequency of the harvester to match the vibrating body. This will yield an optimal power. To accomplish this, a discrete Fast Fourier Transform (FFT) was applied using the following function:

$$X(k) = \sum_{j=1}^N x(j) \omega_N^{(j-1)(k-1)} \quad (12)$$

Where  $\omega_N = e^{(-2\pi i)/N}$

This was computed using MATLAB. The resulting output for all axes is as follows:

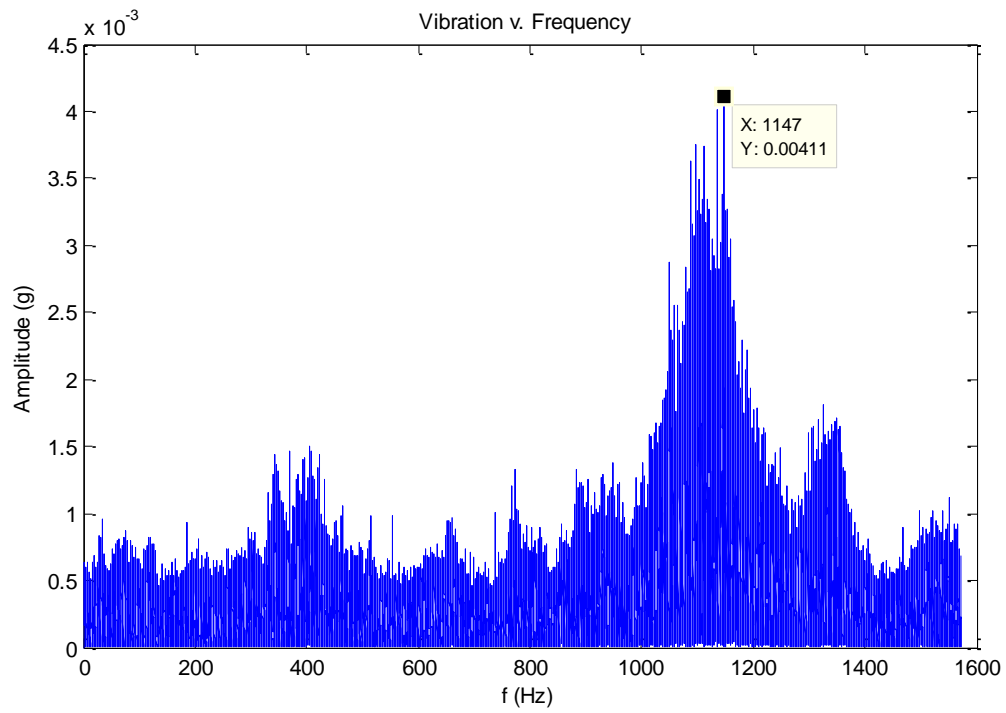


Figure 4–23: X – Axis Frequency

The resonance frequency for the X – axis is ~1.1 kHz shown in the figure above.

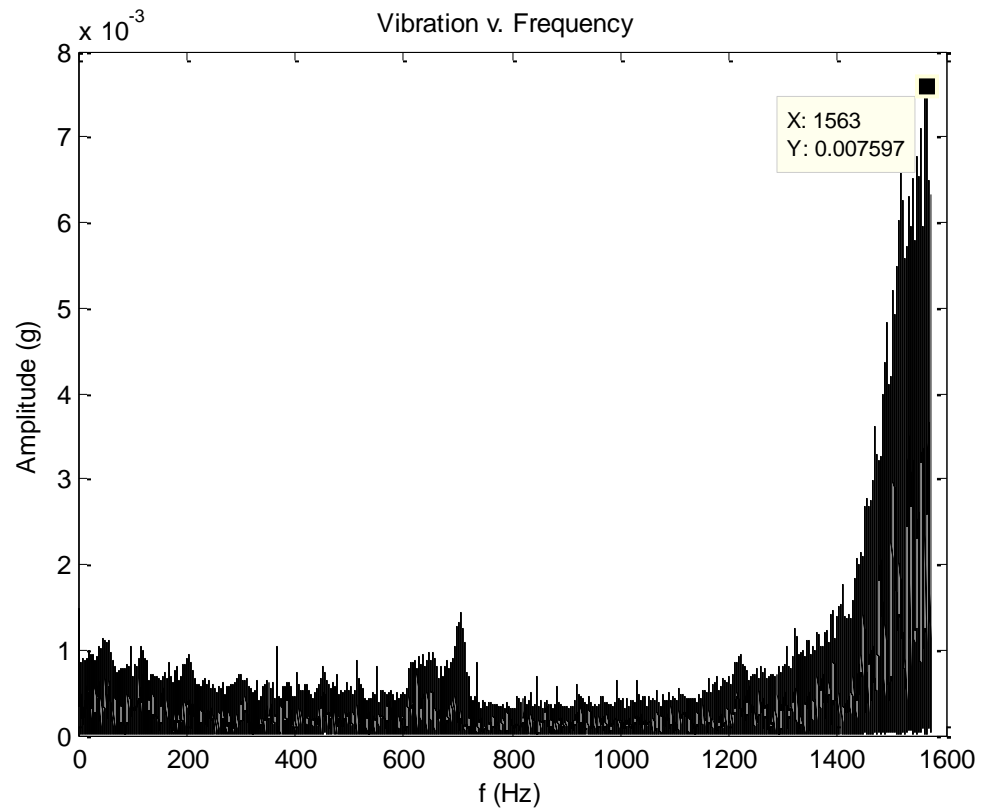


Figure 4–24: Y – Axis Frequency

The Y-axis shows a higher resonance frequency as expected because the train's movement was on this axis as illustrated in Figure 4–25. The frequency exceeds 1.6 kHz.

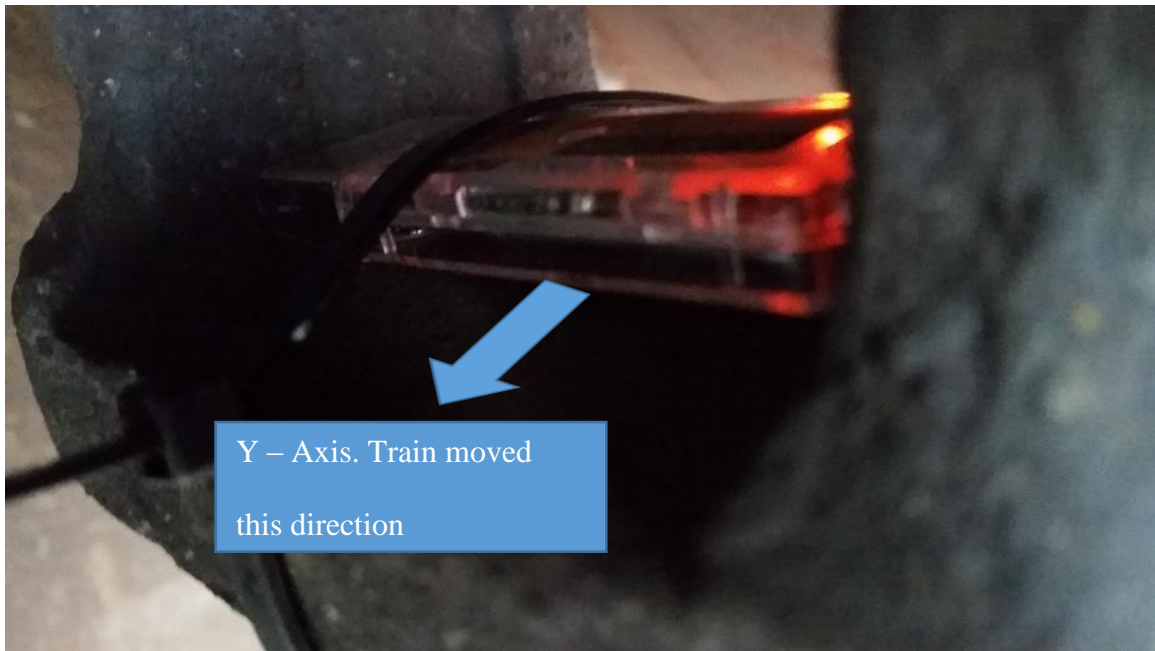


Figure 4–25: Vibration Data Logger mount location for Loaded Car

For the Z – axis in Figure 4–26, the resonance frequency was half the Y – axis. The value is 0.7 kHz.

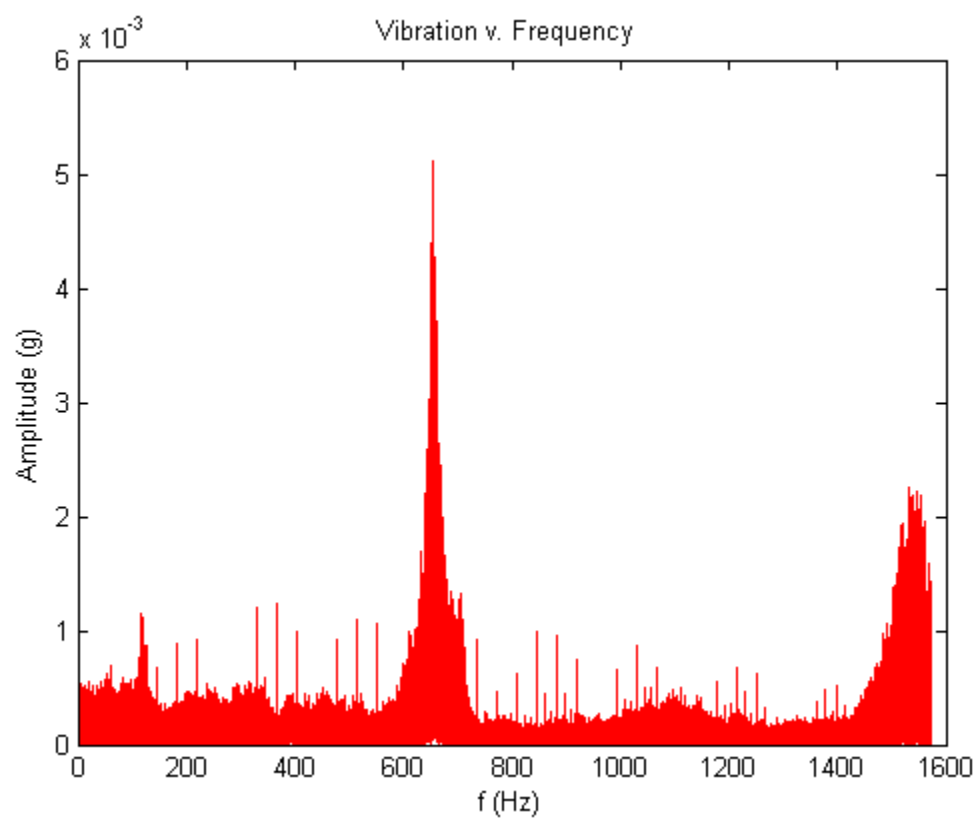


Figure 4–26: Z – Axis Frequency

The Time and Frequency domain representations were combined in a 2D plot to get a better view of where most of the displacement occurred as shown in the following figure.

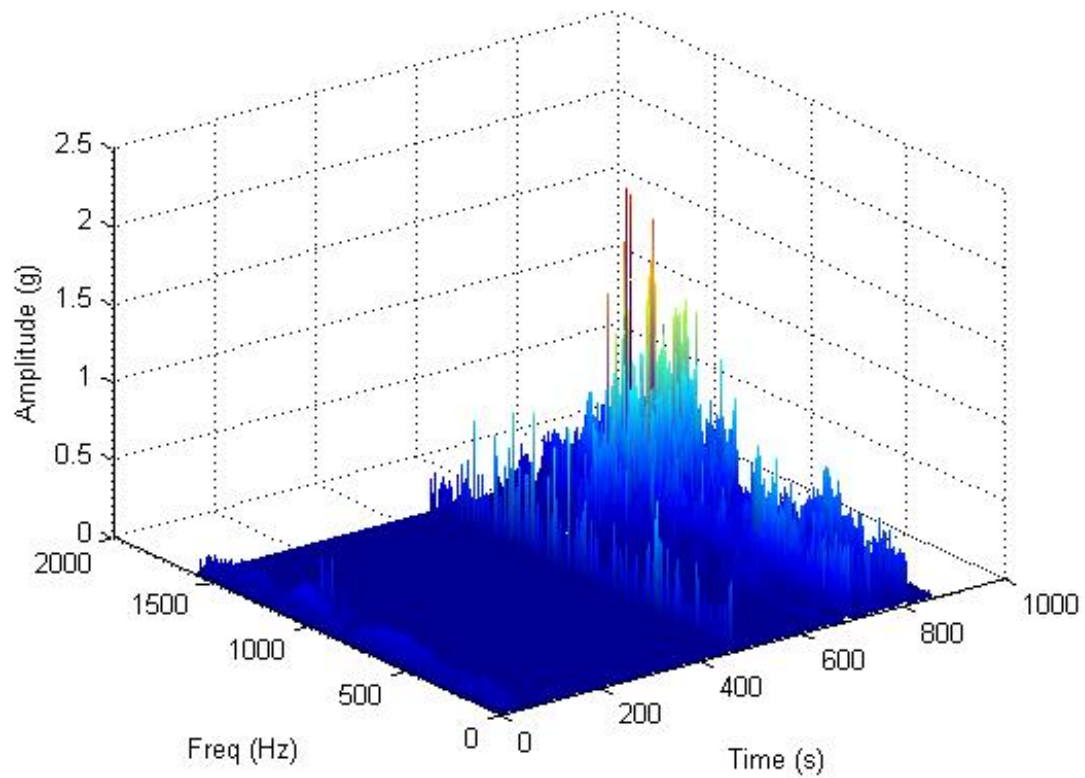


Figure 4–27: X Channel Frequency (2-D)

The flat area shown on the graph occurred when the train was stationary.

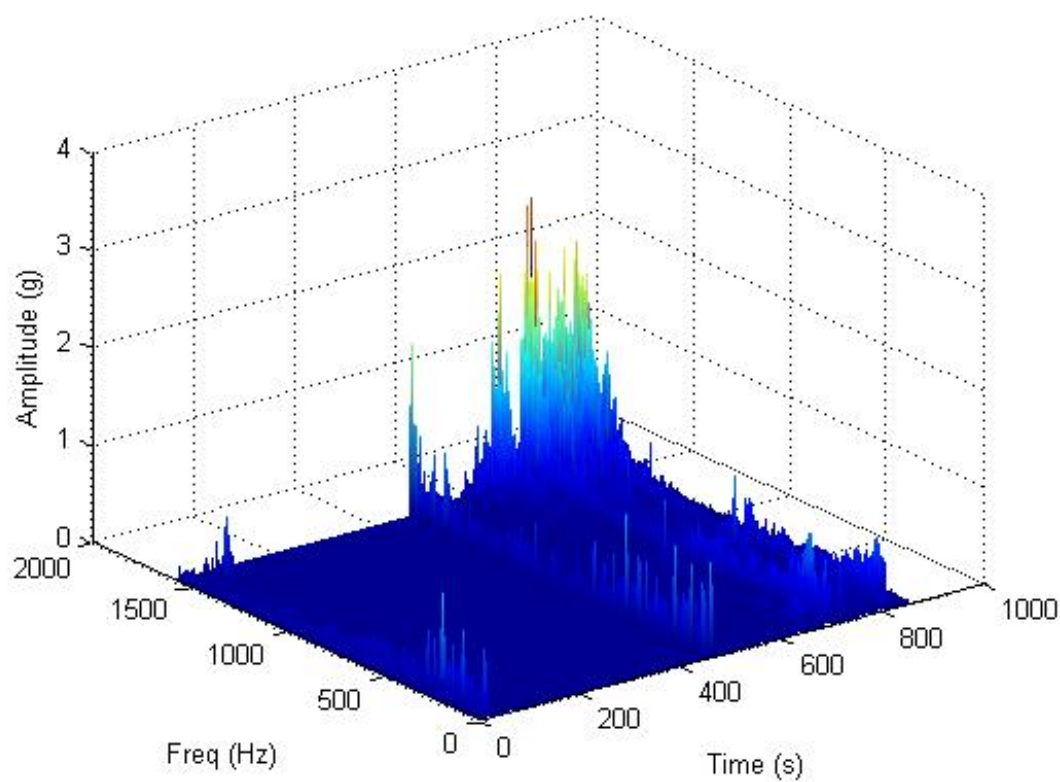


Figure 4–28: Y Channel Frequency (2-D)

The same 1-D plot seen in Figure 4–24, the Y –axis showed the highest resonant frequency.



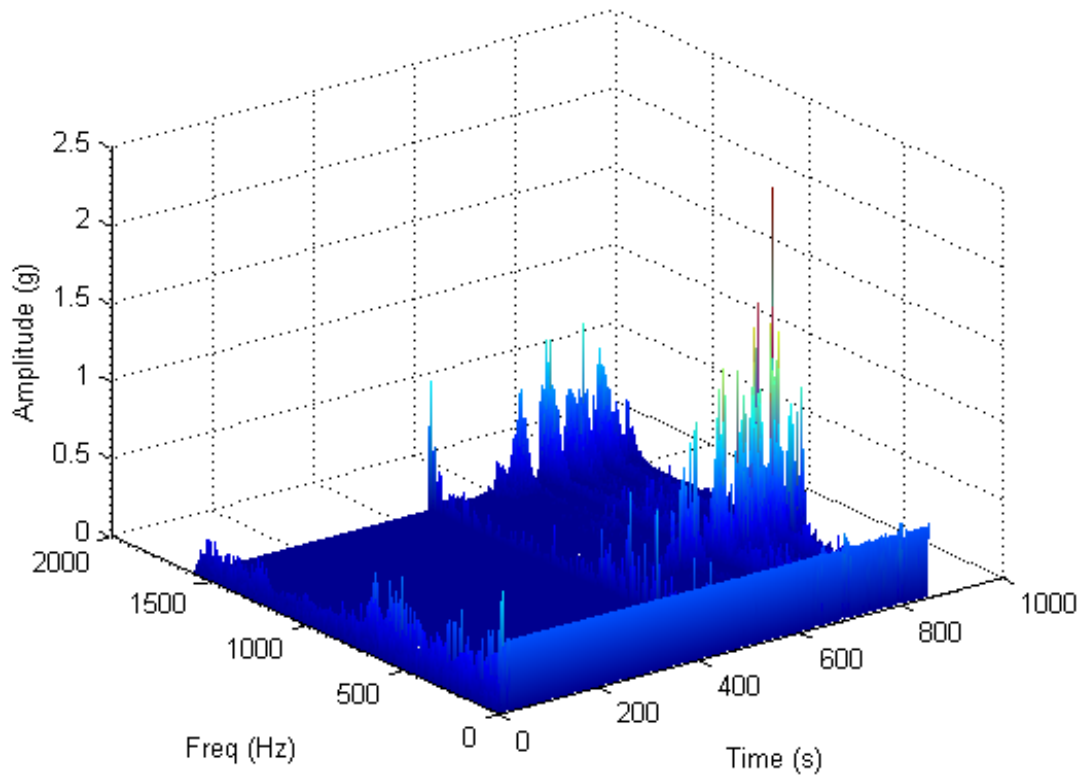


Figure 4–29: Z Channel Frequency (2-D)

#### 4.2.4 Analysis of Data from Empty car

The empty car experiment was problematic. The railcar vibrates at a very high rate that the sensors were not able to handle the high vibration. The experiment was repeated three times. The following figures show the vibration occurring during the creation of the train. The vibration was recorded at a sample rate of 3200.00Hz. The high amplitudes were the

result of impact when the cars coupled. The plot is in a time domain. Recording time: 27852.68 seconds. Total of 696317 data points per axis.

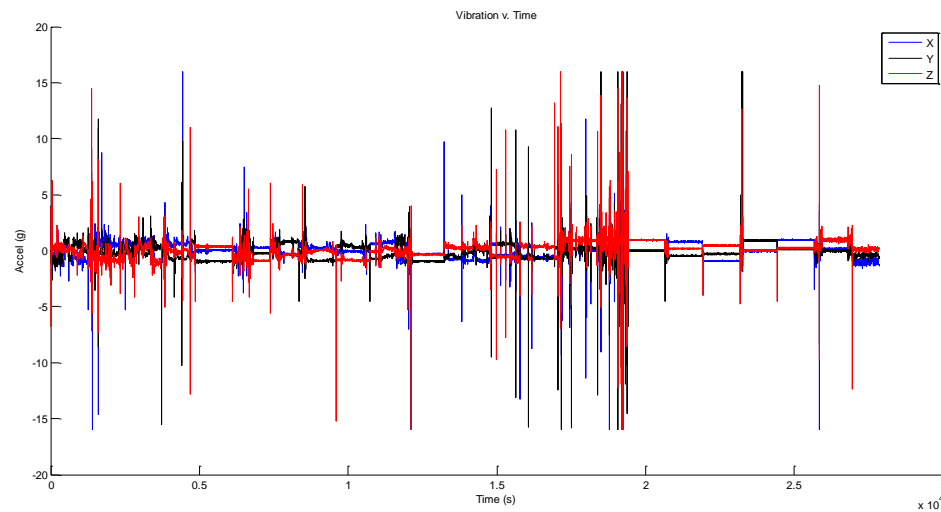


Figure 4–30: Time Domain

Stats	X - axis	Y-axis	Z-axis
Min	-16.00g	-16.00g	-16.00g
Max	15.99g	-0.12g	0.09g
Average	-0.00g	-0.12g	0.09g
StdDev	0.60g	0.61g	0.62g
vector sum	0.15g		

Table 4–3: Statistics of data from Empty car (Experiment 1)

---

Note: The data logger maximum threshold is  $\pm 16g$ . The plot above clipped at acceleration beyond the threshold.

---

#### 4.2.4.1 Determining the Resonance frequency

After the maximum displacement was determined, the next step was to determine the resonance frequency of the cars, which was used to tune the natural frequency of the harvester to maximize power generated. The frequency was determined by performing a Fourier transform of the Time domain data.

##### 4.2.4.1.1 Experiment 1

The graph below is the 2-D plot for the Y- axis. The resonance frequency appears to be at zero.

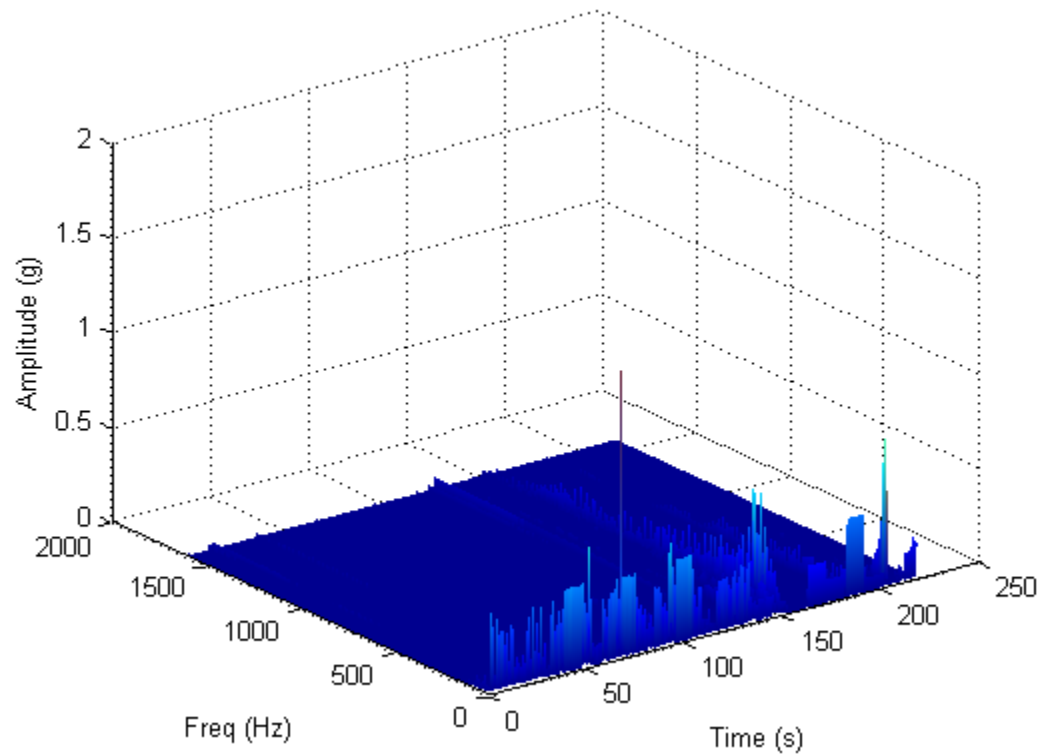


Figure 4–31: Y Channel Frequency (2-D Experiment Attempt 1)

#### 4.2.4.1.2 Experiment 2

The second experiment showed a higher vector sum but the frequency was still not as expected. This is shown in **Figure 4–32**:

Sample rate: 3117.43Hz. Recording time: 7.61 seconds. Total 23719 data points per axis.

Stats	X - axis	Y-axis	Z-axis
Min	-9.36g	-16.00g	-6.95g
Max	7.11g	0.16g	0.90g
Average	0.05g	0.16g	0.90g
StdDev	0.24g	0.40g	0.36g
Vector sum	0.91g		

Table 4–4: Statistics of data from Empty car (Experiment 2)

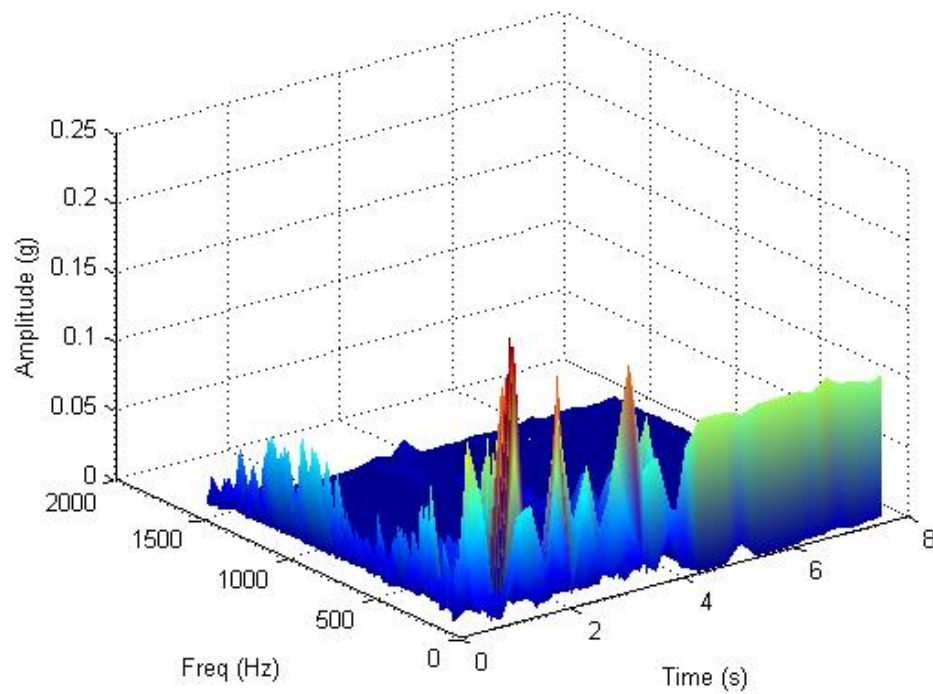


Figure 4–32: Y Channel Frequency (2-D Experiment Attempt 2)

A second attempt at experiment 2 showed frequency that was lower than 500 Hz for the Y – axis. The empty car was expected to have a much higher vibration than the loaded.

#### 4.2.4.1.3 Experiment 3

The phrase “*3rd time is a charm*” didn’t quite pan out. All three sensors were mounted on railcar. The resulting graphs are as follows:

Stats	X - axis	Y-axis	Z-axis
Min	-16.00g	-16.00g	-16.00g
Max	13.79g	-0.18g	-0.36g
Average	-0.04g	-0.18g	-0.36g
StdDev	0.53g	0.80g	1.06g
vector sum	0.40g		

Table 4–5: Statistics of data from Empty car (Experiment 3)

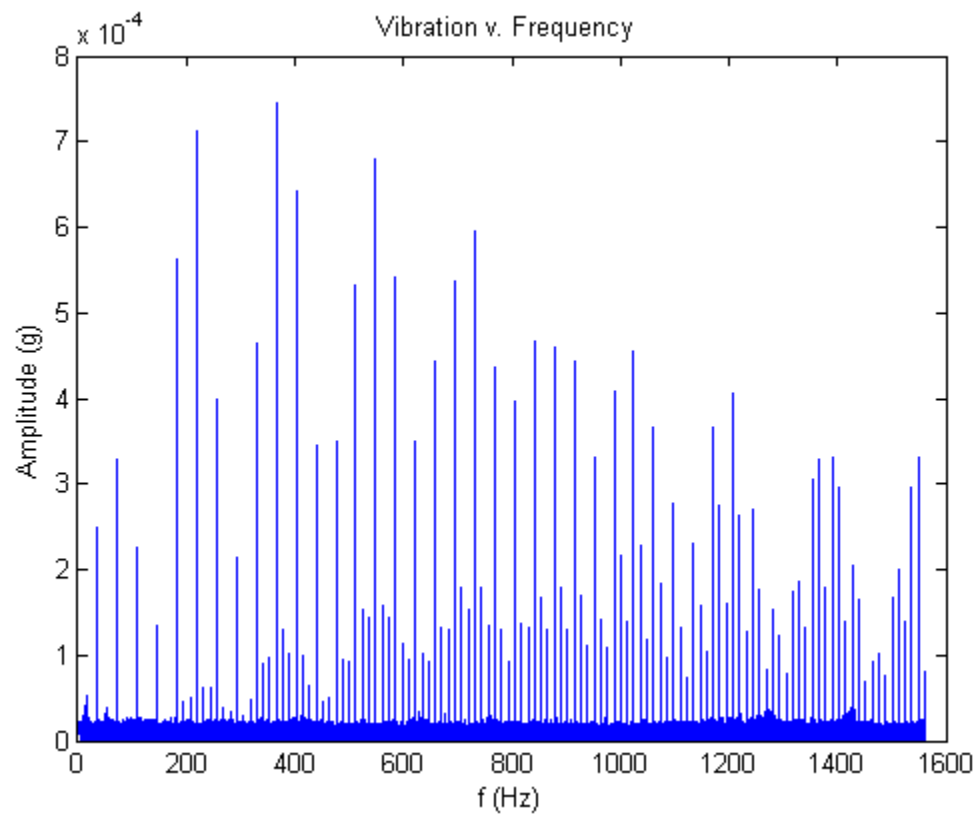


Figure 4–33: X – Axis Frequency

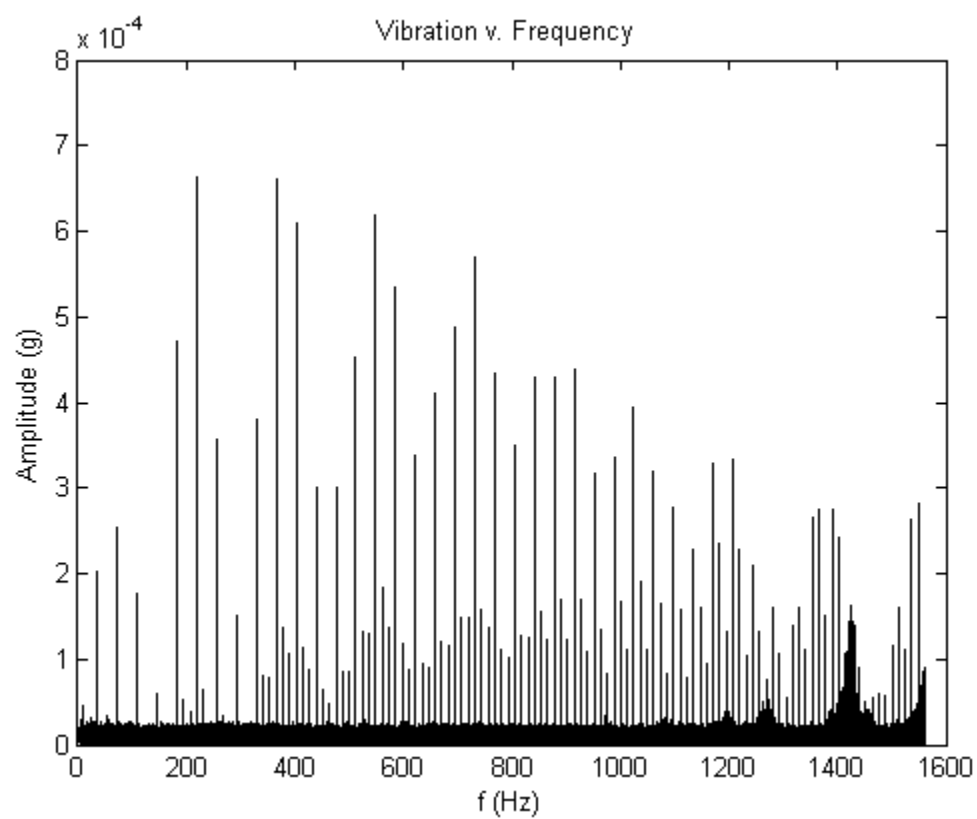


Figure 4–34: Y – Axis Frequency

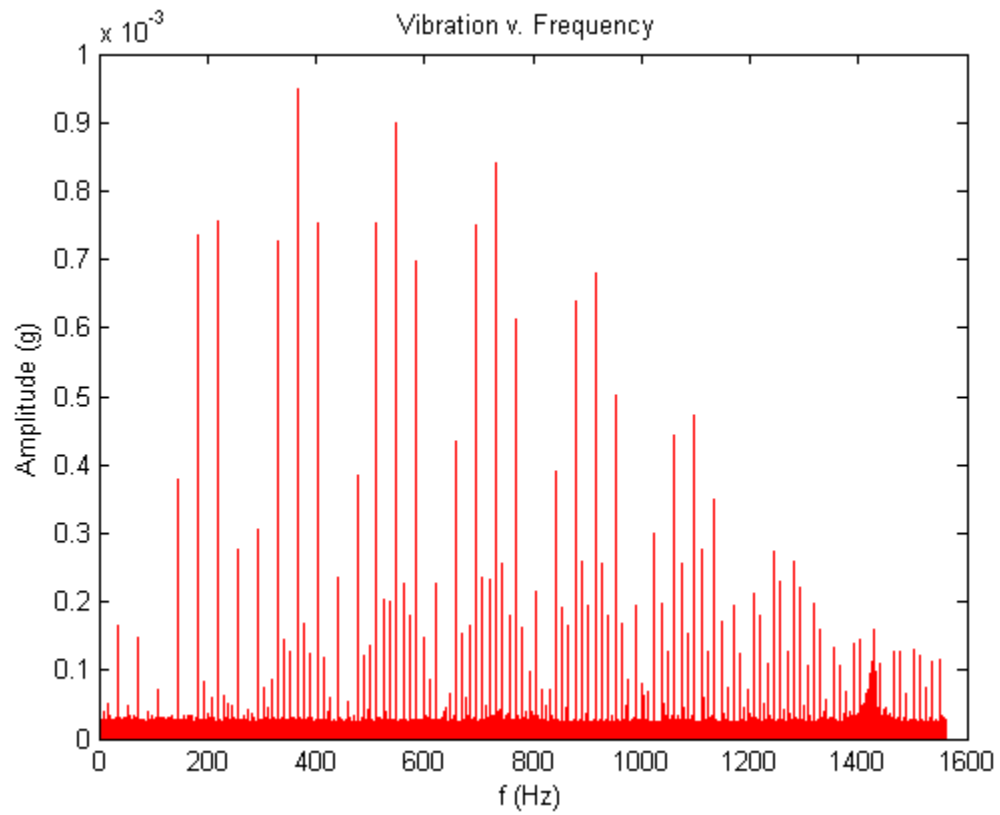


Figure 4–35: Z – Axis Frequency

Neither of the plots in Figure 4–33 to Figure 4–35 show the resonance frequency.



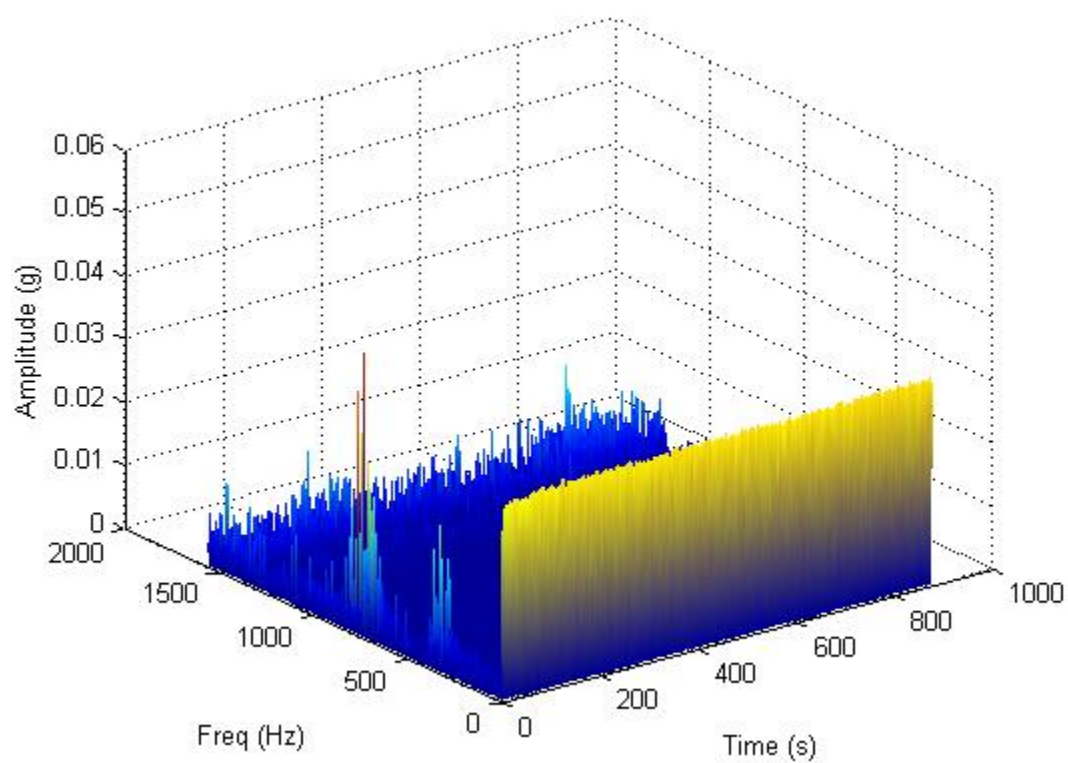


Figure 4–36: X Channel Frequency (2-D Experiment Attempt 3)

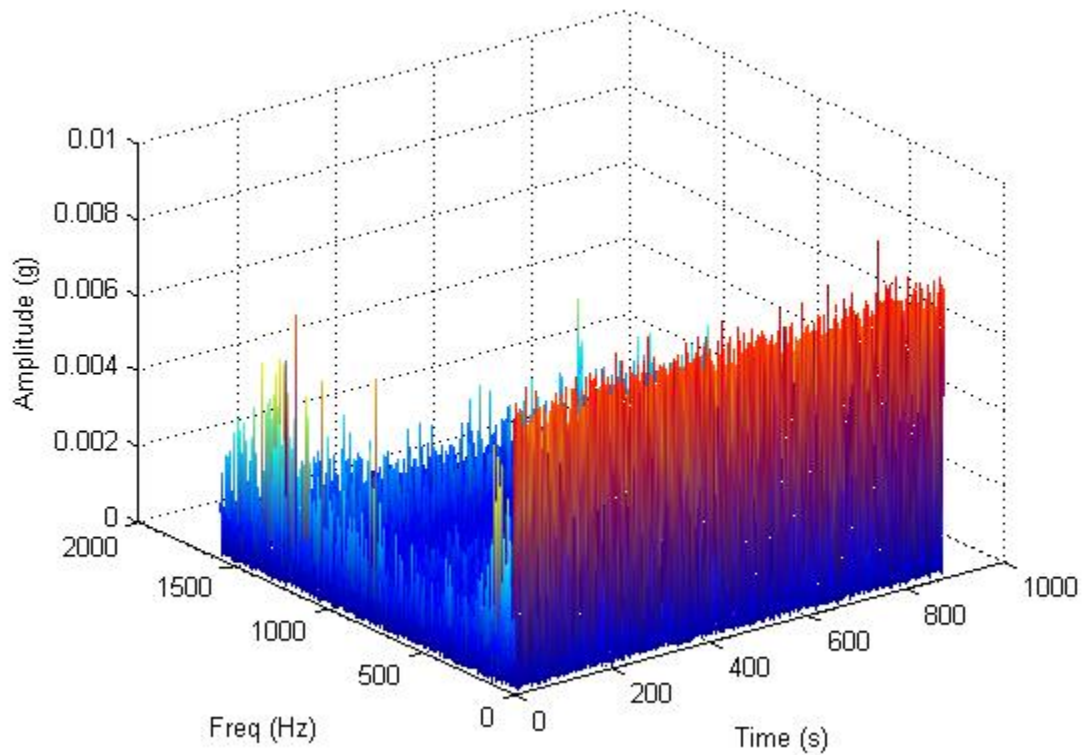


Figure 4–37: Y Channel Frequency (2-D Experiment Attempt 3)

**Figure 4–37** confirms that vibration data logger [39] was unable to handle the high frequencies when the railcar is empty. The data retrieved were transient noise.

An accelerometer [43] with higher resolution of  $\pm 200g$  was used to determine the maximum vibration of the railcar when moving. This is shown in **Figure 4–38**:

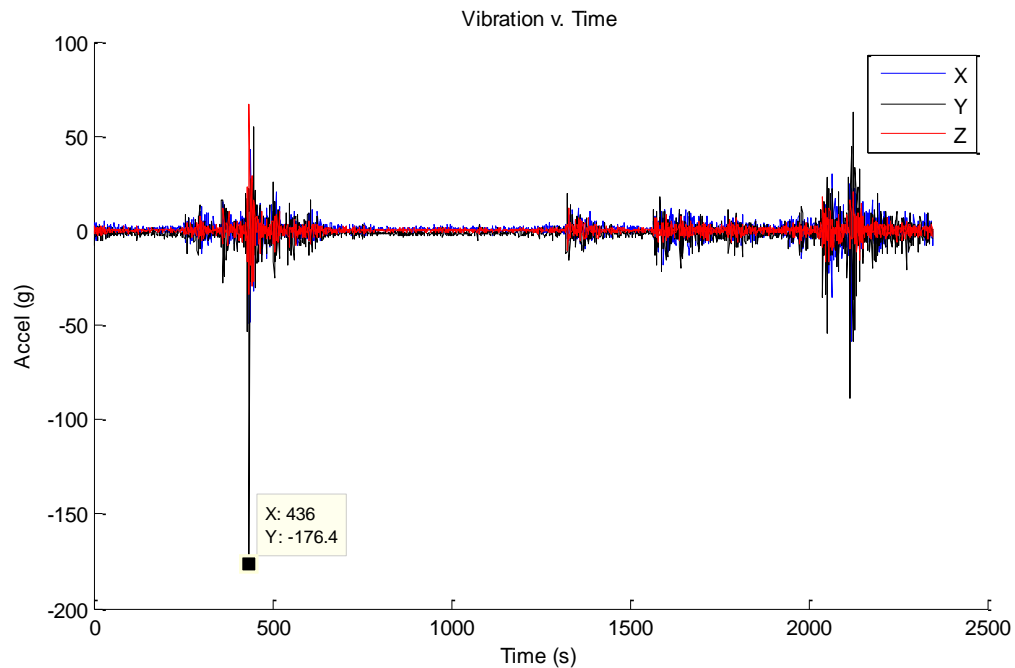


Figure 4–38: Maximum vibration of railcar

In this scenario, the train was allowed to travel faster at a rate lower than 50mph. The maximum instantaneous vibration recorded was close to  $\pm 200g$ , which is the capacity of the accelerometer.

### 4.3 Section Summary

Four different types of railcars were used for the experiment. The railcars investigated were flat, covered hopper, coal and tank cars. The stochastic-like data collected from these railcars in empty and loaded scenarios, revealed there was enough vibration to

power a sensor. The vibration data confirmed the hypothesis that the train has a high resonance frequency. The maximum amplitude seen in the time domain was -176g. The resonance frequency for the loaded railcar ranged from 700 Hz to over 1.6 kHz.

Determining the amplitude for the empty car posed a challenge when using the initial data logger.

To achieve the maximum output power, the natural frequency of the harvester must be tuned to match the vibrating body. A tungsten tip mass was used for the tuning. The frequency was tuned by first placing the harvester in a cantilever position and connecting the output lead to a load that can be monitored with a voltmeter or an oscilloscope. The tip mass was adjusted by sliding it slowly until the optimal power was achieved.

#### 4.3.1 Converting the Vibration to Power

We now know how much vibration is available but what does it equate to in power? The vibration-to-power conversion depends on the type of material the harvester is made of, Young's modulus of the material, the tip mass placed on the harvester, and so on.

However, a theoretical power can be estimated by using Williams-Yates model [44, 45, 46]:

$$P_{max}^4 = \frac{mY^2\omega_n^3}{4\zeta} \quad (13)$$

Where  $m$  is the seismic mass used to tune the harvester,  $Y$  is the amplitude of the vibration given by  $y(t) = Y \cos(\omega t)$ .  $\zeta$  is the damping ratio.  $\omega_n$  is the resonant frequency.

Using the data from Figure 4–23 let's determine an estimate of the power from it:

$$\omega_n = 1147 \text{ Hz};$$

$$Y = 0.00411 \text{ g (note: } 1 \text{ g} = 9.8 \text{ m/s}^2) = 0.040278 \text{ m/s}^2;$$

Seismic mass = 1 gram.

Let's assume that the system is tuned, meaning the electrical damping coefficient ( $b_e$ ) is equal to the mechanical damping coefficients ( $b_m$ ), and it is critically damped meaning  $\zeta = 1$ . Putting the values in the equation we get the following:

---

<sup>4</sup> Some sources like [41] have a slightly different formula where the denominator is  $16\zeta$  rather than  $4\zeta$ .

$$P_{max} = \frac{1 \times 1147^2 \times 0.040278^3}{4 \times 1}$$

$P_{max} = 21.5\text{W}$  or  $5\text{W}$  if using [46].

With the proper impedance matching, this is plenty to sustain the sensor's power need of  $3.168\text{mW}$ .

## Chapter 5: Conclusion

### 5.1 Summary

This thesis examined the study of existing and emerging Energy Harvesting technologies for use in freight car sensors. Specifically, the pros and cons of energy harvesting technologies such as photovoltaic, electrodynamics, thermoelectric or piezoelectric were presented. Energy harvesting is no longer a myth but a feasible method of powering devices using energy harvested from the environment. Vibration energy sources are recommended for the freight car environment.

The first step was to determine the power requirement from the data collected from 100 sensor nodes arranged in a linear topology. The physical layer of the sensors conforms to IEEE 802.15.4 standard. Maximum current draw observed was 0.96mA, equating to a power of 3.168mW.

The next step was to determine how much vibration was generated by the railcar in the following four scenarios:

1. When the freight car is loaded but the train is not moving.
  - a. In this scenario, acceleration seen was less than 1g ( $9.8\text{m/s}^2$ ). Shown in

**Figure 4-11.**

2. When the freight car is loaded and the train is moving.

a. This yielded acceleration that exceeded the  $\pm 16g$  threshold of the sensor.

Scenario 3 and 4 were similar to 1 and 2 with the freight car empty. The resonance frequency was different for each axis. It ranged from  $\sim 1.1$  kHz, 1.6 kHz and 800 Hz for X, Y and Z – axis respectively. The highest frequency was on the Y –axis because the train's movement was in the Y-axis direction.

The vibration data was converted to power using Williams-Yates model. Maximum power was estimated to be 21.5W or 5W in some definition. This is more than enough power to sustain the sensors.

Most of the piezoelectric harvesters surveyed at the time this thesis was written did not readily support the higher frequencies. Development effort are in progress.

Lithium-ion batteries are one of the best battery technologies when considering how long a charge can last compared to other elements. The limitations are cost and safety concerns because it is known to potentially cause fire. This limitation can be fixed by using tougher coating materials that are non-flammable.

Supercapacitors have a lot of potential considering they address some of the major shortcomings found in batteries; like charge time and environmental toxins. Energy density is one of the limitations of this technology. Full charge with the same surface area as the battery discharges quicker on a supercapacitor. Supercapacitors can be used in lieu of a battery for optimal performance.



## Chapter 6: Bibliography

- [1] M. Weiser, "The Computer for the 21st Century," *Scientific American*, pp. 94-104, 1991.
- [2] D. Saha and A. Mukherjee, "Pervasive computing: A paradigm for the 21st century," *IEEE Computer*, pp. 25-31, 2003.
- [3] "Smarter Railroads," [Online]. Available: [http://www.ibm.com/smarterplanet/us/en/rail\\_transportation/ideas/](http://www.ibm.com/smarterplanet/us/en/rail_transportation/ideas/). [Accessed 10 April 2015].
- [4] R. H. Weber and R. Weber, *Internet of Things*, Springer, 2010.
- [5] H. Sundmaeker, P. Guillemin, P. Friess and S. Woelfflé, *Vision and challenges for realising the Internet of Things*, 2010.
- [6] K. Ashton, "That 'internet of things' thing," *RFiD Journal*, vol. 22, no. 7, pp. 97-114, 2009.
- [7] "Positive Train Control (PTC)," US Department of Transportation Federal Railroad Administration, 14 May 2012. [Online]. Available: <http://www.fra.dot.gov/Page/P0621>. [Accessed 20 March 2015].
- [8] G. Bibel, *Train Wreck: The Forensics of Rail Disasters*, JHU Press, 2012.
- [9] Association of American Railroads , "Railroads: Moving America Safely," May 2015. [Online]. Available: <https://www.aar.org/BackgroundPapers/Railroads%20Moving%20America%20Safely.pdf>. [Accessed 20 June 2015].

- [10] C. Murphy, "Union Pacific Delivers Internet Of Things Reality Check," *InformationWeek*, pp. 1-4, 3 August 2012.
- [11] L. Smith and I. Lipner, "Free Pool of IPv4 Address Space Depleted," 3 February 2011. [Online]. Available: <https://www.nro.net/news/ipv4-free-pool-depleted>. [Accessed 30 March 2015].
- [12] S. Bradner and A. Mankin, "The Recommendation for the IP Next Generation Protocol," RFC 1752, January 1995. [Online]. Available: <http://tools.ietf.org/html/rfc1752>. [Accessed 30 March 2015].
- [13] "IPv6," Google, 6 June 2012. [Online]. Available: <https://www.google.com/intl/en/ipv6/statistics.html>. [Accessed 24 May 2015].
- [14] D. M. Dobkin, *The RF in RFID: UHF RFID in Practice*, Waltham: Newnes, 2012.
- [15] "Nest Thermostat," Nest, [Online]. Available: <https://nest.com/thermostat/life-with-nest-thermostat/>. [Accessed 15 March 2015].
- [16] "Internet of Everything," Cisco, [Online]. Available: <https://youtu.be/Kt5VulFqBm4>. [Accessed 02 12 2014].
- [17] L. Wroblewski, "Quotes from Objectified," 19 March 2009. [Online]. Available: <http://www.lukew.com/ff/entry.asp?788>. [Accessed 10 March 2015].
- [18] "March 1880: The Curie Brothers Discover Piezoelectricity," American Physical Society, [Online]. Available: <http://www.aps.org/publications/apsnews/201403/physicshistory.cfm>. [Accessed 31 January 2015].
- [19] Association of American Railroads , "High-Tech Advances Improve Railroad," 2014 July. [Online]. Available: <https://www.aar.org/BackgroundPapers/High%20Tech%20Advances%20Improve%20Railroad%20Safety.pdf>. [Accessed 20 June 2015].

- [20] Association of American Railroads , "POSITIVE TRAIN CONTROL," May 2015. [Online]. Available: <https://www.aar.org/policy/positive-train-control>. [Accessed 23 June 2015].
- [21] "Class I Railroad Statistics," 15 July 2014. [Online]. Available: <https://www.aar.org/Documents/Railroad-Statistics.pdf>. [Accessed 1 May 2015].
- [22] M. Chambers, "United States Department of Transportation," [Online]. Available: [http://www.rita.dot.gov/bts/sites/rita.dot.gov.bts/files/publications/national\\_transpo\\_ration\\_statistics/html/table\\_01\\_11.html](http://www.rita.dot.gov/bts/sites/rita.dot.gov.bts/files/publications/national_transpo_ration_statistics/html/table_01_11.html). [Accessed 5 May 2015].
- [23] M. Brain, "How Motes Work," *Howstuffworks*, p. 4, 2004.
- [24] F. Stodolsky, "Railroad and Locomotive Technology Roadmap," 01 December 2002. [Online]. Available: <http://www.transportation.anl.gov/pdfs/RR/616.PDF>. [Accessed 15 April 2015].
- [25] G. A. Hart, S. D. Moss, D. J. Nagle, G. Jung, A. Wilson, C. Ung, W. K. Chiu and G. Crew, "Vibration Energy Harvesting for Aircraft, Trains and Boats," in *Acoustics*, Victor Harbor, 2013.
- [26] C. Ung, S. D. Moss, L. A. Vandewater, S. C. Galea, W. K. Chiu and G. Crew, "Energy harvesting from heavy haul railcar vibrations," in *Intelligent Sensors, Sensor Networks and Information Processing, 2013 IEEE Eighth International Conference on*, IEEE, 2013, pp. 95--98.
- [27] C. A. Nelson, S. R. Platt, D. Albrecht, V. Kamarajugadda and M. Fateh, "Power harvesting for railroad track health monitoring using piezoelectric and inductive devices," *Proceedings of the SPIE*, vol. 6928, 2008.
- [28] A. Pourghodrat, "Energy harvesting systems design for railroad safety," Master Thesis, University of Nebraska-Lincoln, 2011.
- [29] T. Lin, J. Wang and L. Zuo, "Energy Harvesting from Rail Track for Transportation Safety and Monitoring," New York, 2014.

- [30] Wikipedia, "Energy harvesting," 23 May 2015. [Online]. Available: [http://en.wikipedia.org/w/index.php?title=Energy\\_harvesting&oldid=663679882](http://en.wikipedia.org/w/index.php?title=Energy_harvesting&oldid=663679882). [Accessed 23 May 2015].
- [31] J. Walker, R. Resnick and D. Halliday, Fundamentals of Physics 10th Edition, John Wiley & Sons, Inc, 2012.
- [32] Dictionary.com, "Energy," The American Heritage® Science Dictionary. Source location: Houghton Mifflin Company, [Online]. Available: <http://dictionary.reference.com/browse/energy?s=t>. [Accessed 23 May 2015].
- [33] Dictionary.com, "harvesting," Collins English Dictionary - Complete & Unabridged 10th Edition, [Online]. Available: <http://dictionary.reference.com/browse/harvesting>. [Accessed 23 May 2015].
- [34] H. A. Haus and J. R. Melcher, Electromagnetic fields and energy, Prentice Hall, 1989.
- [35] S. Boisseau, G. Despesse and B. Ahmed Seddik, Electrostatic Conversion for Vibration Energy Harvesting, Small-Scale Energy Harvesting, Intech, 2012.
- [36] "Energy Harvesting Systems: A Block Diagram," 16 July 2010. [Online]. Available: <http://www.holistic.ecs.soton.ac.uk/res/eh-system.php>. [Accessed 23 March 2015].
- [37] M. Rouse, "photovoltaic cell (PV Cell)," September 2005. [Online]. Available: <http://whatis.techtarget.com/definition/photovoltaic-cell-PV-Cell>. [Accessed March 2015].
- [38] "Supercapacitors," in *IDTechEx Energy Harvesting and Storage USA 2014*, Santa Clara, 2014.
- [39] "Mide.com," [Online]. Available: [http://www.mide.com/pdfs/Vulture\\_Datasheet\\_001.pdf](http://www.mide.com/pdfs/Vulture_Datasheet_001.pdf). [Accessed 2 Feb 2015].

- [40] M. M. Doeff, "Battery Cathodes," in *Batteries for Sustainability Selected Entries from the Encyclopedia of Sustainability Science and Technology*, New York, Springer-Verlag, 2013, pp. 5-49.
- [41] A. Martin, "Hunter Valley Lines," [Online]. Available: <http://www.huntervalleylines.com/content/binary/Hunter%20Valley%20Lines%20-%20Interline%20Carrier%20Rail%20Equipment%20Descriptions.pdf>. [Accessed 21 March 2015].
- [42] "Vibration Data Logger," [Online]. Available: [http://www.mide.com/pdfs/slamstick\\_datasheet.pdf](http://www.mide.com/pdfs/slamstick_datasheet.pdf).
- [43] "Data Sheet ADXL375," [Online]. Available: <http://www.analog.com/media/en/technical-documentation/data-sheets/ADXL375.PDF>. [Accessed 12 February 2015].
- [44] C. B. & Y. R. B. Williams, "Analysis of a micro-electric generator for microsystems," *Sensors and Actuators A-physical*, vol. 52, pp. 8-11, 1996.
- [45] D. J. I. Shashank Priya, *Energy Harvesting Technologies*, Springer Science & Business Media, 2008.
- [46] S. Boisseau, T. R. G Despesse, E. Defay and A. Sylvestre, "Cantilever-based electret energy harvesters," IOP Publishing Ltd , France, 2011.
- [47] M. Leopold, "Sensor Network Motes:: Portability & Performance," København: Department of Computer Science, University of Copenhagen., 2008.
- [48] B. Gholamzadeh and H. Nabovati, "Concepts for Designing Low Power Wireless Sensor Network," *World Academy of Science, Engineering and Technology* 45, 2008.
- [49] P. D. Mitcheson, E. M. Yeatman, G. K. Rao, A. S. Holmes and T. C. Green, "Energy Harvesting From Human and Machine Motion for Wireless Electronic Devices," in *Proceedings of the IEEE*, 2008, pp. 1457-1486.

- [50] Y. Zhang, W. Han, D. Li, P. Zhang and S. Cui, "Power vs. Spectrum 2-D Sensing in Energy Harvesting Cognitive Radio Networks," *arXiv preprint arXiv:1502.04099*, 2015.
- [51] E. Gelenbe, "Synchronising Energy Harvesting and Data Packets in a Wireless Sensor," *Energies*, vol. 8, no. 1, pp. 356-369, 2015.
- [52] S. Boisseau, G. Despesse and A. Sylvestre, "Optimization of an electret-based energy harvester," *Smart Materials and Structures*, vol. 19, no. 7, p. 075015, 2010.
- [53] C. S. R. Murthy and B. S. Manoj, *Ad Hoc Wireless Networks Architectures and Protocols*, New Jersey: Pearson Education, Inc, 2004.
- [54] D. Maurath and Y. Manoli, "Energy Supply as the Basic Challenge," in *CMOS Circuits for Electromagnetic Vibration Transducers: Interfaces for ...*, Springer, 2015, pp. 4-21.
- [55] A. Miller, "BrainyQuote.com," Xplore Inc, 2015. [Online]. Available: <http://www.brainyquote.com/quotes/quotes/a/arthurmill162582.html>. [Accessed 23 May 2015].
- [56] C. S. Lewis, "BrainyQuote.com," Xplore Inc, 2015. [Online]. Available: <http://www.brainyquote.com/quotes/quotes/c/cslewis121182.html>. [Accessed 23 May 2015].
- [57] R. S., *Energy Scavenging for Wireless Sensor Networks with Special Focus on Vibrations*, Springer, 2003.

## Appendix A: Source Code

```

function ss_view(filename, varargin)

% Read a 3 channel x 16-bit data file from the MIDE Slam Stick V1
% (digital USB stick) and display it as g's. If no other arguments are
% input, all plots will be displayed with the full data range.

% referenced from [39]

nSlicesPerSecond = 4;

close all;

% Contents of BW_RATE[3..0] is used as an index into this table to determine the
% nominal sample rate.
% Note that the exact sample rate is determined by the number of samples vs.
% nTimerTicks, so this value
% should only be used as a fallback in case nTimerTicks is not set, e.g. abnormally
% terminated recording.
frequency_table = [-1 -1 -1 -1 -1 -1 6.25 12.5 25 50 100 200 400 800 1600 3200]; %
% Legal values of BW_RATE[3 .. 0] are 0x06 ~ 0x0F.


filesize = fread(hFile,1,'uint32'); % Not used or needed to display recorded data

samplerate_reg = fread(hFile,1,'uint8'); % Sample rate, encoded as contents of
ADXL345's BW_RATE register.

fread(hFile,1,'uint8'); % skip 1 byte

nTimerTicks = fread(hFile,1,'uint32');

fread(hFile,1,'uint16'); % skip 2 bytes

```

```

fread(hFile,3,'uint16'); % skip 6 bytes - reserved for timestamp data

datalist_interleaved=fread(hFile, inf, 'int16');

fclose(hFile); % done slurping

nPts=length(datalist_interleaved)/3; % # points per channel. For recording lengths
determined by sectors, last data triad may be incomplete.

% Nominal sampling rate is 3.2KHz for each channel, but this clock is
% generated by the accelerometer itself and is not terribly accurate. Here,
% determine the exact sampling rate using the ticks elapsed on a known-good
% crystal oscillator.

% This field and the # bytes written are updated only at the end of a recording.
% If the field is invalid for any reason (recording abnormally terminated
% or xtal failure), we're forced to rely on the inaccurate ADXL internal
% timebase, and frequency results will be off by up to a few percent(!).

fNominal = 3200;
%fNominal = frequency_table(bitand(samplerate_reg , 15) + 1);

if (nTimerTicks == 0)
    fActual = fNominal;
    disp('WARNING: Recording timer invalid (xtal oscillator failed?), using less accurate
nominal samplerate (+/- several percent).');
%end
else
    if (nTimerTicks == 4294967295) % 0xFFFFFFFF
        fActual = fNominal;
        disp('WARNING: Recording timer not set (recording ended prematurely?), using
less accurate nominal samplerate (+/- several percent).');
    else
        fActual = ceil(nPts)/(nTimerTicks / 32768);
    end
end

% If for any reason oscillator is 'dead' but floating, could still produce a non-zero count.
Check if timer is grossly out of expected range...

```



```

if (fNominal > 0)
    if ((fActual/fNominal < 0.9) || (fActual/fNominal > 1.1))
        fActual = fNominal;
        disp('WARNING: Recording timer out of range (+/-10%) using less accurate nominal
samplerate (+/- several percent).');
    end
end

nPts = floor(nPts);

tActual = 1 / fActual; % create us a variable for the actual period too

recording_time_disp = nPts * tActual;

datalist=zeros(nPts,4); % time vector + 3 axes

% Split the x,y,z samples into their own columns
datalistx=datalist_interleaved([1:3:length(datalist_interleaved)]);
datalisty=datalist_interleaved([2:3:length(datalist_interleaved)]);
datalistz=datalist_interleaved([3:3:length(datalist_interleaved)]);

%length(datalistx)
%length(datalisty)
%length(datalistz)

datalist(:,2)=datalistx(1:nPts);
datalist(:,3)=datalisty(1:nPts);
datalist(:,4)=datalistz(1:nPts);

% create the time vector in the 1st column
datalist(:,1)=(0:1:nPts-1)' ./ fActual; % nPts-length array scaled by 1/ 3.2kHz

%           1      2      3      4
% datalist now contains [timevec, xdata, ydata, zdata]

% normalize to Gs. Note data is actually 13-bit, padded to
% 16 and left-justified for storage to the Flash memory.
% Full-scale is +/-16G.

datalist(:,[2 3 4])=(datalist(:,[2 3 4]) * (16/32768)); % rescale

```

% We know col[0] is time and the rest are Gs, so now we have all the data we need.

% get number of columns so we know how many plots to make...  
[rows,cols]=size(datalist);

% Generate some basic stats about our signal.

%Orientation (means / vector sum)

```
sum_x = mean(datalist(:,2));
min_x = min(datalist(:,2));
max_x = max(datalist(:,2));
std_x = std(datalist(:,2));
sum_y = mean(datalist(:,3));
min_y = min(datalist(:,3));
max_y = mean(datalist(:,3));
std_y = std(datalist(:,3));
sum_z = mean(datalist(:,4));
min_z = min(datalist(:,4));
max_z = mean(datalist(:,4));
std_z = std(datalist(:,4));
vector_sum = sqrt(sum_x^2 + sum_y^2 + sum_z^2);
```

% Display basic information about this recording.

```
disp(['Sample rate: ' num2str(fActual, '%.2f') 'Hz. Recording time: '
num2str(recording_time_disp, '%.2f') ' seconds. Total ' num2str(nPts) ' data points per
axis.' ]);
fprintf(sprintf('\nMin values: x= %.2fg y= %.2fg z= %.2fg', min_x, min_y, min_z));
fprintf(sprintf('\nMax values: x= %.2fg y= %.2fg z= %.2fg', max_x, max_y, max_z));
fprintf(sprintf('\nAverage values: x= %.2fg y= %.2fg z= %.2fg vector_sum= %.2fg',
sum_x, sum_y, sum_z, vector_sum));
fprintf(sprintf('\nStdev values: x= %.2fg y= %.2fg z= %.2fg', std_x, std_y, std_z));
```

```
figure(1);
hold on;
```

% first col is time, which should obviously not be plotted against itself.  
% plot each of the remaining cols against time.

```

% Also, want to plot each one in a different color, preferring
% easily-readable ones until we run out and have to start using light
% yellow, hot pink etc. :-(

colorlist=['b', 'k', 'r', 'g', 'm', 'c', 'y'];

for i=[2:cols]
    %disp(datalist(:,1))

    plot(datalist(:,1),datalist(:,i), colorlist(mod(i-1,length(colorlist)+1)));
end

title('Vibration v. Time');
set(gcf(), 'Name', 'Time Domain'); % this sets the window titlebar
legend('X', 'Y', 'Z');

xlabel('Time (s)');
ylabel('Accel (g)');

%print( '-dpng', 'csvplot')

%%
%Now lets do that whole FFT thing...

% Hamming window:  $w(n) = 0.53836 - .46164 \cdot \cos(2 \cdot \pi \cdot n / N - 1)$ 

window=[1:length(datalist(:,1))];

windowy = (0.53836 - .46164*cos((2*pi*window(:)) ./ (length(window)-1)));

%%% debug: to show the window itself, uncomment the below %%%
%figure(90);
%plot(window,windowy);

% Generate a correctly normalized frequency vector to display with the FFT results
%
% get the elapsed time of the data set. The recording time should be
% available from above, but recalculating it here from the current data
% simplifies things if user script modifications have removed data between
% then and now. MATLAB stores data in double precision, but if this script

```

```

% is ever used to plot a recording imported from e.g. CSV, the below will compute
% more accurate timesteps than the limited decimal precision of the CSV
% time vector.
recordTime=datalist(length(datalist(:,1)),1) - datalist(1,1); % last minus first time (the
data set we get may not necessarily start at zero)
recordTime=recordTime+(recordTime/length(datalist(:,1))); % result will exclude
the time elapsed by the first sample, so add 1 sample worth

%fStep = 1/(recordTime/length(datalist(:,1))) % get the step value in Hz between the
FFT frequency bins

% These variables are not used subsequently; they are only for display
% purposes
nPts=length(datalist(:,1));
samplerate=nPts/recordTime;

x=(0:length(datalist(:,2))-1);
x = x .* (1/recordTime); % normalize frequency according to sample rate and nPts

% HACK: keep the plotting loop below while adding the correct motion axis
% label. Remember, the first col is the time (freq) vector, which will not be plotted
axes_list = ('XYZ ');

% print the FFT for each column in its own figure
for i=(2:cols)
    yfft=fft(datalist(:,i) .* windowy(:)); % window
    %length(yfft)
    % yfft=fft(datalist(:,i)); % no window
    % realify and scale from per-f-bin to per Hz
    % yabs=(yfft.*conj(yfft)) / (samplerate / length(yfft));
    yabs=abs(yfft) / (0.5*length(yfft));
    yabs(1) = yabs(1)/2;
    yabs(1)=0; % Get rid of DC component
    yabs(2)=0; % Get rid of DC component
    yabs(3)=0; % Get rid of DC component
    figure(i+cols); % figures [1 .. cols] will be taken up by time-domain column data

    plot(x([1:length(yfft)/2]),yabs([1:length(yfft)/2]), colorlist(mod(i-
1,length(colorlist)+1))); % colored to match time-domain figure. "length/2" to throw
away the aliases.

```

```

title('Vibration v. Frequency ');
xlabel('f (Hz)');
ylabel('Amplitude (g)');
set(gcf(), 'Name', strcat([axes_list(i), ' Frequency (1-D)']));

end

%% Now split column of interest into slices, window and fft()
%% them individually, and display the result in 3d...

% NOTE: DO NOT WANT "fft2()" here; the slices are not related to each other
% in anyway (except being from the same data capture), we just carved them
% up arbitrarily and smooshed them into the same matrix.
% In other words, blah(1,0) and blah(0,1) are not both neighbors to
% blah(0,0) in real life.

for i=[2:cols]

    yfft=datalist(:,i);
    nPointsPerSlice=floor(fActual / nSlicesPerSecond);

    % for very short recordings or stupid values of nSlicesPerSecond,
    % nPointsPerSlice may end up being outside a legal range for the actual
    % data series. In this case, warn and pick a sane value. Sliced data may
    % not render usefully, but avoid throwing a runtime error.
    if(nPointsPerSlice == 0 || nPointsPerSlice > nPts)
        disp('nPointsPerSlice cannot be achieved; slicing adjusted. ');
        nPointsPerSlice = nPts/4;
    end

    %nPointsPerSlice

    % Now try to slice/reshape the column vector to (x columns of nPointsPerSlice points
    each)
    % in such a way that it reshapes cleanly. We'll throw away up to 1 slice of data, but we
    % avoid reshape barfing up an error here.

    yfft=reshape(yfft([1:floor(length(yfft)/nPointsPerSlice)*nPointsPerSlice]),nPointsPerSlice,[],[]);

```

```

[fftrows,fftcols]=size(yfft);

% create the lone X vector to scale these all against...

x=[0:fftrows-1];
%fftrows
recordSliceTime=datalist(fftrows,1) - datalist(1,1); % again, accurately get the elapsed
time of each slice
recordSliceTime=recordSliceTime+(recordSliceTime/fftrows); % ...

x = x .* (1/recordSliceTime); % normalize frequency according to sample rate and
nPts

fSlice = max(x); % = x(fftrows) % display the maximum frequency bin in each FFT
slice

% Same windowing story as before... just precalculate it once and apply to
% each slice. Hamming window:  $w(n) = 0.53836 - .46164 \cdot \cos(2\pi n/N - 1)$ 

window=[1:fftrows];
windowy = (0.53836 - .46164*cos((2*pi*window(:)) ./ (length(window)-1)));

%%% debug %%%

%figure(11);
%plot(window,windowy);

yabs=yfft; % pre-allocate yabs with same size as yfft

for j=[1:fftcols]
    % yfft(:,j)=fft(yfft(:,j) );           % not windowed
    yfft(:,j)=fft(yfft(:,j) .* windowy(:)); % windowed
    % yabs(:,j)=yfft(:,j).*conj(yfft(:,j)) / length(yfft(:,j));
    yabs(:,j)=abs(yfft(:,j)) / (0.5*length(yfft(:,j)));
    yabs(1,j)=0; % Get rid of DC component
    % yabs(2,j)=0; % Get rid of DC component
    % yabs(3,j)=0; % Get rid of DC component
end

```

```

figure(12+i);

% Constrain the plot to show only the data range of interest. For unadorned
% FFT-ables, we want only frequencies up to half the sampling rate (Nyquist
% frequency).
% For accelerometers, only want data up to its own specified cutoff frequency.

% Create reasonable default values for 'points of interest'. This is
% the section of the plot we will actually show.
nPointsOfInterest=nPointsPerSlice /2;
startPointOfInterest=1;
endPointOfInterest=nPointsOfInterest;

% but if overridden by command line, use those instead.
% NB: Sample rate and slice length in seconds are now variable; scale
% user's inputs in Hz to actual slice width in f-bins...
if (nargin >= 3 && isnumeric(varargin{1}) && isnumeric(varargin{2}))
    if(isnumeric(varargin{1}))
        startPointOfInterest = floor(varargin{1} * (fftrows / fSlice)); % cell array! % Fix
the indexing to sane 0-based...
    end
    if(isnumeric(varargin{2}))
        endPointOfInterest = floor(varargin{2} * (fftrows / fSlice)); % cell array!
    end

end
if (nargin > 3 && isnumeric(varargin{3}))
    % Ceiling the data so the little stuff can be seen in the plot
    yabs(:)= (yabs(:) .* (yabs(:)<varargin{3})) + (yabs(:)>varargin{3})*varargin{3}; %
rewrite to ceiling if value>ceiling.
end

% if user entered invalid frequency values, constrain them to a range the plot actually
contains
if(startPointOfInterest < 0)
    startPointOfInterest = 0;
end
if(endPointOfInterest > length(x)/2)
    endPointOfInterest = length(x)/2; % do not show user aliased data
end

```

```

    % finally, actually make the plot!
    surf([1:fftcols] /
nSlicesPerSecond,x([startPointOfInterest+1:endPointOfInterest+1]),yabs([startPointOfInt
erest+1:endPointOfInterest+1],:));

    xlabel('Time (s)');
    ylabel('Freq (Hz)');
    zlabel('Amplitude (g)');
    set(gcf(), 'Name', strcat([axes_list(i), ' Frequency (2-D)']));
    shading interp
end

```



## Appendix B: Vulture Datasheet

### **Piezoelectric Energy Harvesters**



## PIEZOELECTRIC ENERGY HARVESTERS

### FEATURES

- Enables Vibration Energy Harvesting
- Robust Piezo Packaging
- Pre-Attached Electrical Lead Wires and Connector
- Hermetically Sealed for Use in Harsh Environments
- Low Profile
- Available in Different Sizes to Match to Application
- Directly Integrate with COTS Products Such As The Linear LTC3588 and Thin Film Batteries

### APPLICATIONS

- Industrial Health Monitoring Network Sensors
- Condition Based Maintenance Sensors
- Wireless HVAC Sensors
- Mobile Asset Tracking
- Tire Pressure Sensors
- Oil and Gas Sensors
- All Air, Land and Sea Vehicle Sensors
- Battery and Hard Wired Power Replacement

### DESCRIPTION

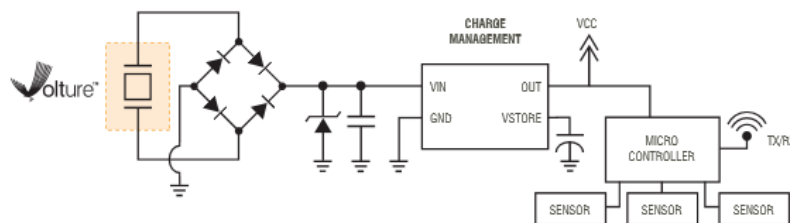
Vulture™ vibration energy harvesters convert otherwise wasted energy from mechanical vibrations into useable electrical energy. The Vulture™ accomplishes this by utilizing normally brittle piezoelectric materials. The Midé Vulture™ energy harvester is unique amongst other piezo based energy harvesters because it incorporates Midé's patented piezoelectric transducer packaging technology.

Through a proprietary manufacturing process, the Vulture™ packages piezoelectric materials in a protective skin with pre-attached electrical leads, producing a robust component with no soldered wires. The Vulture's™ protective skin also provides electrical insulation and defense against humidity and harsh contaminants.

The Vulture™ is available in six standard sizes. Custom sizes are available and a cost effective alternative.

If a custom size is required please contact Midé Technology Corporation by emailing: [vulture@mide.com](mailto:vulture@mide.com).

### TYPICAL APPLICATION



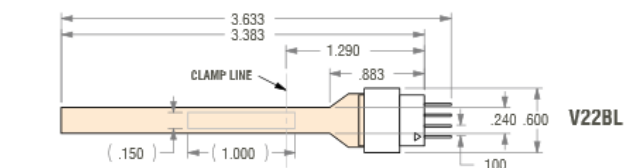
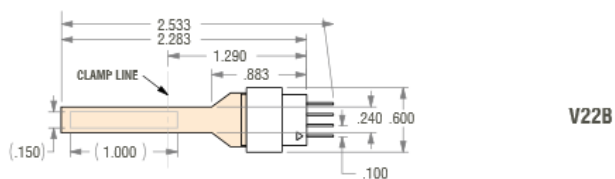
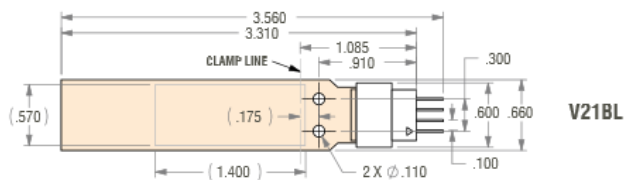
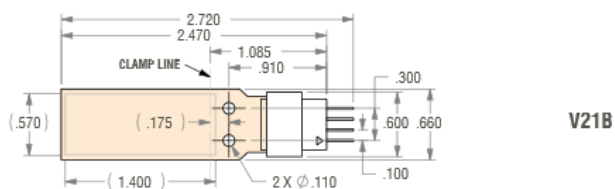
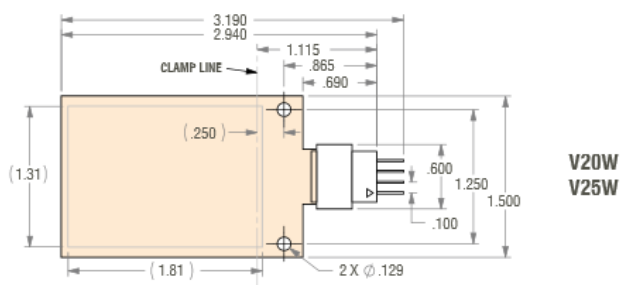


## PRODUCT DIMENSIONS

### NOTE:

1. All dimensions are in inches
2. Connector thickness = 0.100"

Product	Typical Thickness (in)
V20W	0.034
V25W	0.024
V21B	0.031
V21BL	0.031
V22B	0.031
V22BL	0.031



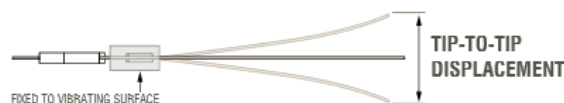


## ABSOLUTE MAXIMUM RATINGS

Operating Temperature Range	-40 to 90 C
Operating Temperature Range (Without Connector)	-40 to 150 C
Storage Temperature Range	-60 to 90 C
Storage Temperature Range (Without Connector)	-60 to 150 C
Lead Temperatures (Soldering, 10 sec)	300 C
Piezo Strain, max	800 micro-strain*
Maximum Voltage Output	Product and Vibration Dependent**
Maximum Current Output	Product and Vibration Dependent**
**See Performance Curves For Typical Values	
*Related to max. tip deflection, see Deflection Limits	

## DEFLECTION LIMITS

Energy Harvester Product Number	Max. Tip-to-Tip Displacement (in)
V20W	0.10
V25W	0.15
V21B	0.06
V21BL	0.18
V22B	0.03
V22BL	0.12



## ELECTRICAL CHARACTERISTICS

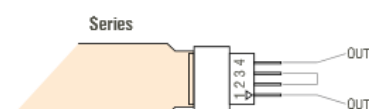
Product	Single Wafer Series Capacitance (nF), measured at 100 Hz	Single Wafer Series Resistance (Ohm), measured at 100 Hz	Single Wafer Series Capacitance (nF), measured at 120 Hz	Single Wafer Series Resistance (Ohm), measured at 120 Hz
V20W	69	390	69	340
V25W	130	210	130	175
V21B	26	950	26	770
V21BL	26	950	26	770
V22B	9	2400	9	2000
V22BL	9	2400	9	2000



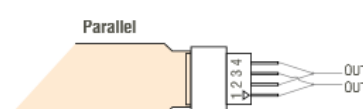
## PIN FUNCTIONS

**P1, P2:** Piezo wafer 1 output

**P3, P4:** Piezo wafer 2 output



**Series**  
Compared to Single Wafer Value  
Double Voltage  
Same Current  
Capacitance: Half the Single-Wafer Value

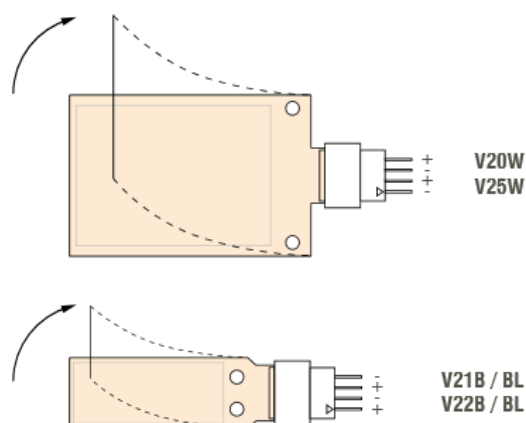


**Parallel**  
Compared to Single Wafer Value  
Same Voltage  
Doubled Current  
Capacitance: 2x the single-wafer value

Each Vulture contains two electrically isolated piezo wafers, which may be used independently or bridged for increased voltage (series configuration) or current output (parallel configuration). Series connection will double the open-circuit voltage compared to a single wafer, and the effective capacitance will be 1/2 the single-wafer capacitance listed in the "Electrical Characteristic Table (Pg. 3)". Parallel connection will double the current compared to a single wafer, and the effective capacitance will be double the single-wafer value. For most applications, parallel connection is

recommended. Please refer to the connection diagram above. Regardless of series or parallel connection, the power generated by the Vulture™ Energy Harvester will be the same.

In typical energy harvesting usage, the raw output is an AC waveform as the Vulture deflects in both directions. For sensing or dual-use applications where it is desired to know the direction of deflection at any given time, please refer to the relationship between deflection and output polarity for each wafer diagram below.





## OPERATION

The Vulture™ vibration energy harvester is designed to extract useable electrical energy from waste mechanical vibrations. The best means to accomplish this is to mount the Vulture™ product in a cantilevered configuration on the vibration source and tune the natural frequency of the Vulture™ harvester to match that of the vibration source.

### Vibration Source Characterization

The first step in successful energy harvesting is to fully understand the vibration environment in which the Vulture™ will be operating. The most effective means to accomplish this is to measure the vibration using an accelerometer, capture the data, and perform an FFT (Fast Fourier Transform) on the data to extract the relevant frequency information.

Some applications will not require this step since their dominant frequencies are inherently known. An example of this would be a 120 Hz AC motor or a 60 Hz appliance. However, most applications will require some form of vibration characterization to be successful.

Midé offers a vibration characterization product and service, the VR001. The VR001 is a small device that can be easily installed into many different vibration environments. The device is completely stand alone and can be applied to hard to reach areas. Built in timer delays allow for capture of many different types of vibration environments. A simple USB interface with

provided software allows the user to easily characterize any vibration.

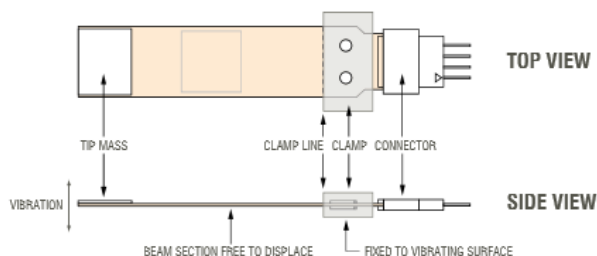
### Attaching And Clamping The Vulture™

For optimized energy harvesting from vibrations it is best to mount the Vulture™ products in a cantilevered configuration. This takes advantage of resonant beam harvesting. If the natural frequency of the Vulture™ is successfully tuned to that of the vibration source, the most energy will be harvested.

The first step in successful clamping is to ensure that both the base and clamp are constructed of rigid materials completely free of burrs and defects. Using a rigid material will minimize dissipation of energy through the clamp structure and avoiding burrs and defects will minimize the potential for stress concentrations on the Vulture™ which could lead to premature failure.

The clamp should completely extend beyond the piezo element within the Vulture product. The suggested clamp line shown in the product dimensions section of this document ensures that the clamp is clamping on the piezo element.

For long term installation, the fasteners used to secure the clamp should be properly torqued and should be reinforced either using lock washers or some kind of locking adhesive. This will ensure a proper long term clamp that will not loosen over time.



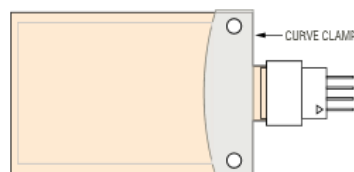


## OPERATION

Straight clamps are the simplest and often most cost effective clamps. However, curved clamps, as shown in the diagram below, have shown the capability to slightly increase performance of the Vulture. Straight clamps are sufficient for the majority of applications.

### Tuning The Vulture™

To ensure the most efficient harvesting, it is essential to tune the Vulture's™ natural frequency to match that of the vibrating source. Tuning is performed by adding a tuning mass to the end of the cantilevered Vulture™



until the natural frequency of the piezo beam is the same as the vibration source. The larger the tuning mass the lower the natural frequency of the Vulture™.

For non permanent installations or for active tuning it is best to use bee's wax or some other form of non-permanent attachment for the tuning mass to the Vulture. Bee's wax allows the mass to be moved along the beam, toward and away from the clamp, for tuning.

There are multiple means of tuning the Vulture™ depending on the equipment available to the user. If only the vibration source that will ultimately be harvested from is available to the user, it is recommended that the Vulture™ be properly mounted and clamped to the vibration source. The output of the Vulture should then be attached to an oscilloscope for monitoring. The output can be either the raw output of the Vulture™ (directly on two of the output pins) or through whatever electronics the user is using so long as the electronics allow for some measure of optimal

power output. The tuning mass can then be adjusted until the maximum power is achieved.

If the user has a shaker available, the tuning can be performed by driving the Vulture™ at the desired natural frequency and adjusting the mass until optimal power output is achieved. If connecting directly to the Vulture™ pins, optimal power output will be where the voltage output is maximized.

Another simple way to tune your Vulture™ product is to measure the frequency at which the device "rings out" when excited by an impulse mechanical load. The easiest way to perform this type of tuning is to properly mount and clamp the Vulture to a rigid structure. Next, attach at least one of the piezo's within the Vulture directly to an oscilloscope for monitoring (ex: connect to pins P1 and P2). Add the appropriate tip mass (See RELATION BETWEEN TIP MASS & NATURAL FREQUENCY section) to the end of the cantilevered Vulture, do not permanently adhere the tip mass yet. Bee's wax or tape is often the best material to use for non permanent tip mass installations. Apply an impulse mechanical load by very lightly "flicking" the end of the Vulture. This will cause the beam to "ring out". The frequency of the the decaying wave is the natural frequency that the Vulture is currently tuned to. To decrease this frequency move the mass farther away from the clamp point, to increase the frequency move the mass closer to the clamp point. If the natural frequency is not close to the desired frequency either a different tip mass or a different product may be required.

Once the tip mass is in the proper location for optimal energy harvesting it should be permanently adhered to the Vulture™. This ensures that the tip mass remains in place for the life of the Vulture™. It is recommended that a robust adhesive such as Loctite™ 404 be used for this permanent installation. Keep in mind that any added mass will impact the tuning of the system.



## POWER MEASUREMENTS

Piezoelectric material produces mechanical strain under the influence of an externally applied electrical field, and conversely produces electrical potential in response to applied mechanical strain. Products such as the Vulture™ piezo energy harvester are typically used in a cantilevered-beam configuration, in which the piezoelectric beam is clamped at one end and the other end allowed to oscillate freely in response to vibration normal to the flat surface of the beam, converting these vibrations to in-plane material strain. The beam dimensions and tip mass determine the resonant frequency of the beam, which is tuned to match the dominant vibrational frequency of its environment, mechanically amplifying this typically small vibration.

### Power Measurements

The power output capability of the Vulture™ products was measured in the following manner. In the cantilevered beam configuration above, the Vulture was mounted to a shaker capable of generating vibrations of varying frequency and amplitude. Tip masses (four for each product) were added to alter the natural frequency of the Vulture™ products. The vibration frequency being generated by the shaker was then matched to the frequency of the Vulture™ product to provide resonant and therefore optimized energy harvesting. Four different amplitudes were tested (0.25, 0.375, 0.5, and 1.00g) at each of these frequencies. The piezo's output was rectified and then placed across a purely capacitive load. The capacitor value was chosen using the following equation for average power, where C is the

capacitance in Farads, V is the piezo's open circuit voltage, and  $\Delta t$  is a reasonable time interval ( $\sim 10$  seconds), and solving for C:

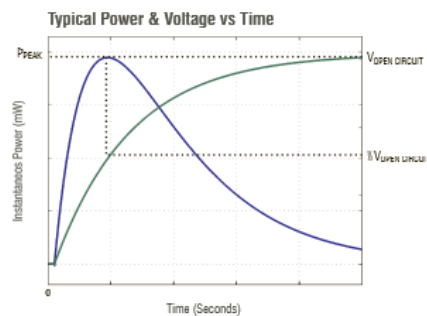
$$P_{AVG} = \frac{1}{2} C \cdot V^2 \cdot \Delta t$$

Yielding:

$$C = \frac{2 \cdot P_{AVG} \cdot \Delta t}{V^2}$$

The figure below shows the voltage (operating voltage) on the capacitor and instantaneous power into capacitor vs. time for a representative vibration level and frequency. The V25W product was used, demonstrating that the power increases until it peaks when the operating voltage is at about half its open circuit value. After that, it decreases.

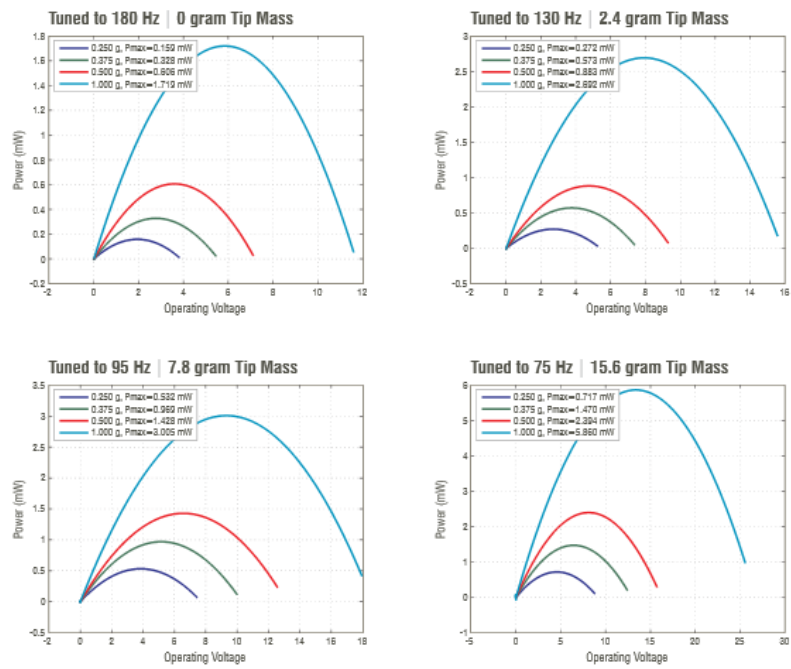
See Application Note: Load Isolation Example.



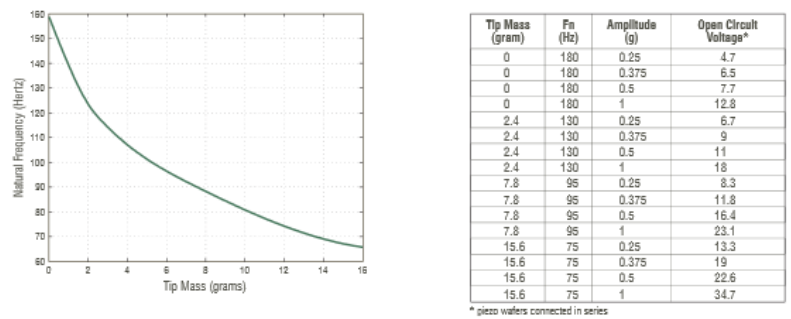




V20W TYPICAL PERFORMANCE POWER CHARACTERISTICS

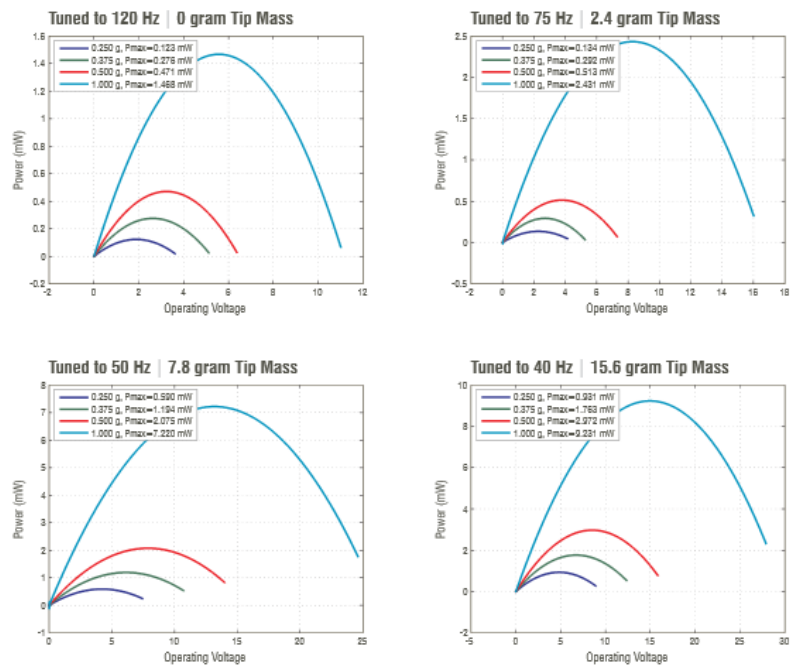


V20W RELATION BETWEEN TIP MASS & NATURAL FREQUENCY

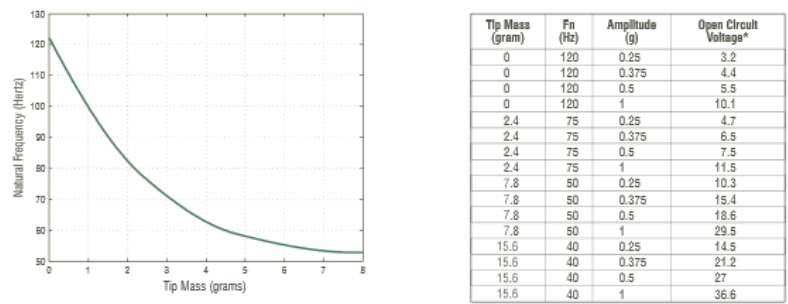




V25W TYPICAL PERFORMANCE POWER CHARACTERISTICS



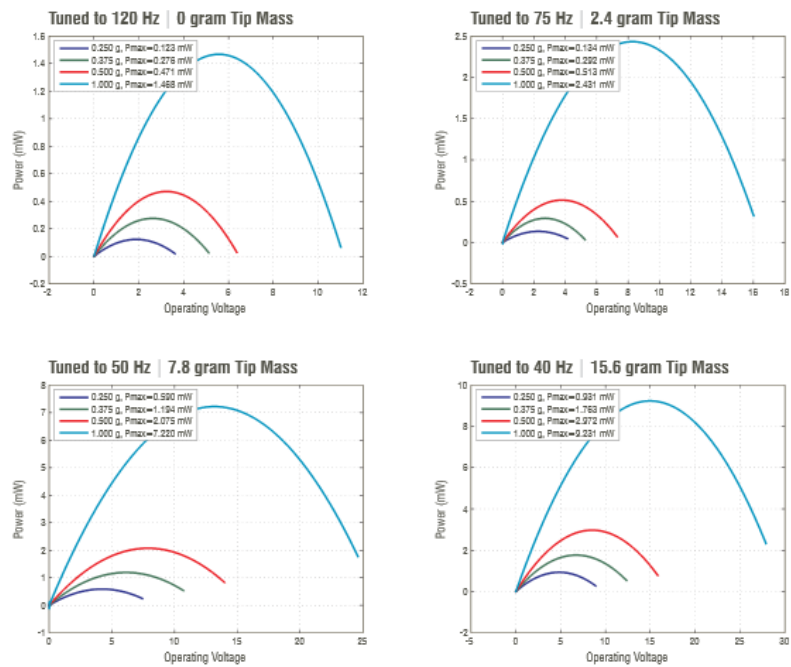
V25W RELATION BETWEEN TIP MASS & NATURAL FREQUENCY



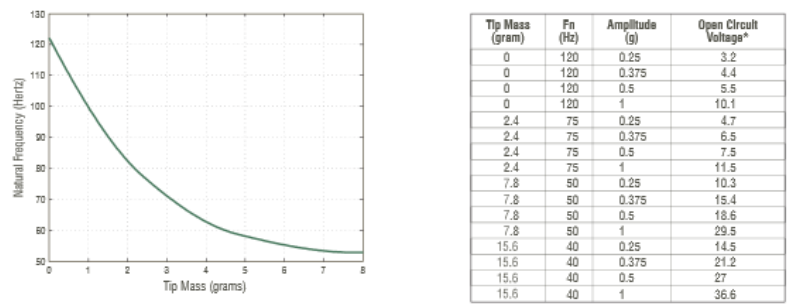
\* piezo wafers connected in series



V25W TYPICAL PERFORMANCE POWER CHARACTERISTICS



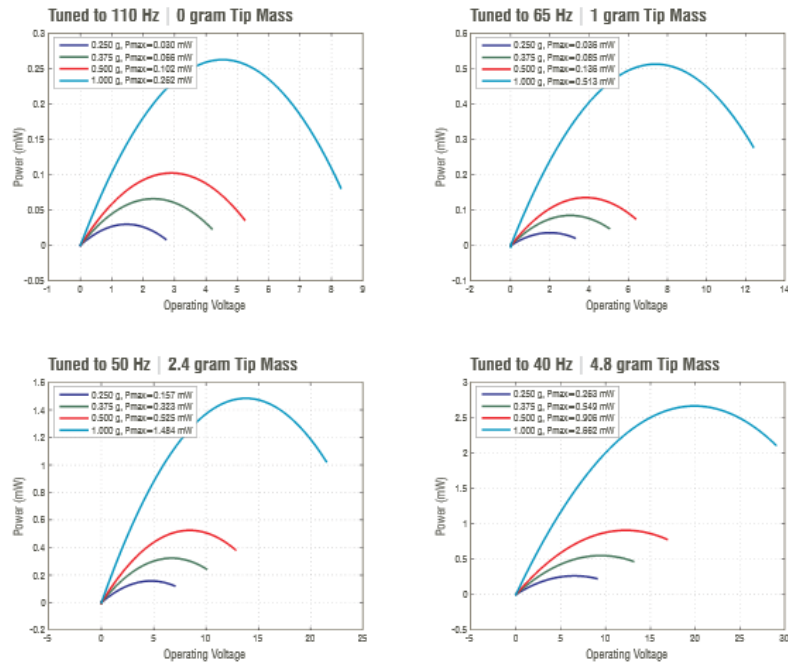
V25W RELATION BETWEEN TIP MASS & NATURAL FREQUENCY



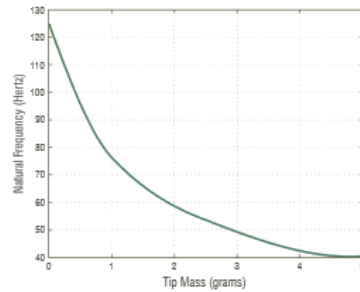
\* piezo wafers connected in series



## V21BL TYPICAL PERFORMANCE POWER CHARACTERISTICS



## V21BL RELATION BETWEEN TIP MASS & NATURAL FREQUENCY

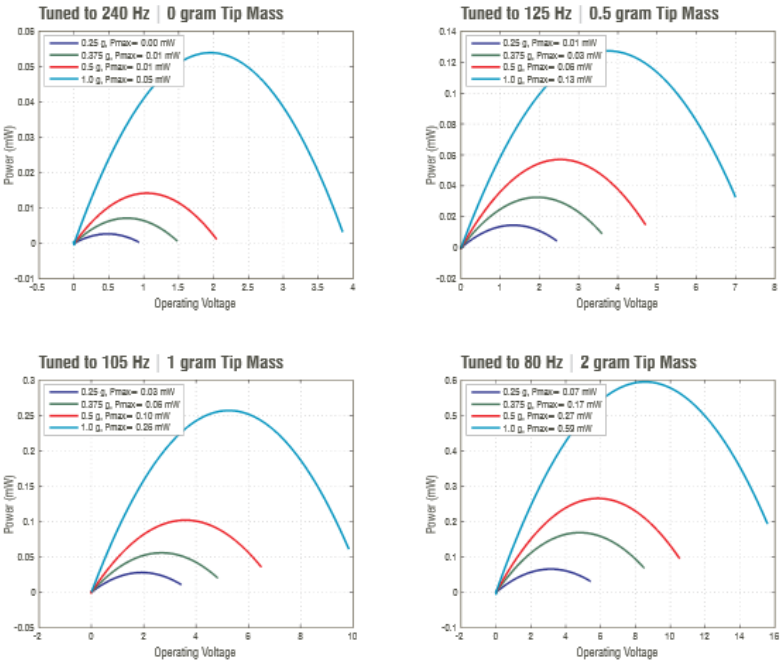


Tip Mass (gram)	F <sub>n</sub> (Hz)	Amplitude (g)	Open Circuit Voltage*
0	110	0.25	3.95
0	110	0.375	5.35
0	110	0.5	6.6
0	110	1	12.1
1	65	0.25	8
1	65	0.375	9.9
1	65	0.5	12.4
1	65	1	22.1
2.4	50	0.25	9.8
2.4	50	0.375	13.7
2.4	50	0.5	19.1
2.4	50	1	27.5
4.8	40	0.25	13.2
4.8	40	0.375	19.2
4.8	40	0.5	25.9
4.8	40	1	44.4

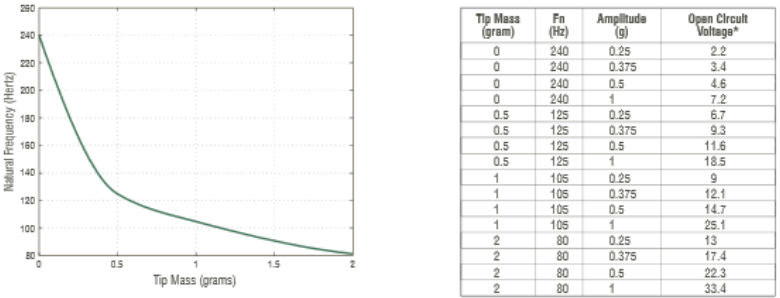
\* piezo wafers connected in series



V22B TYPICAL PERFORMANCE POWER CHARACTERISTICS

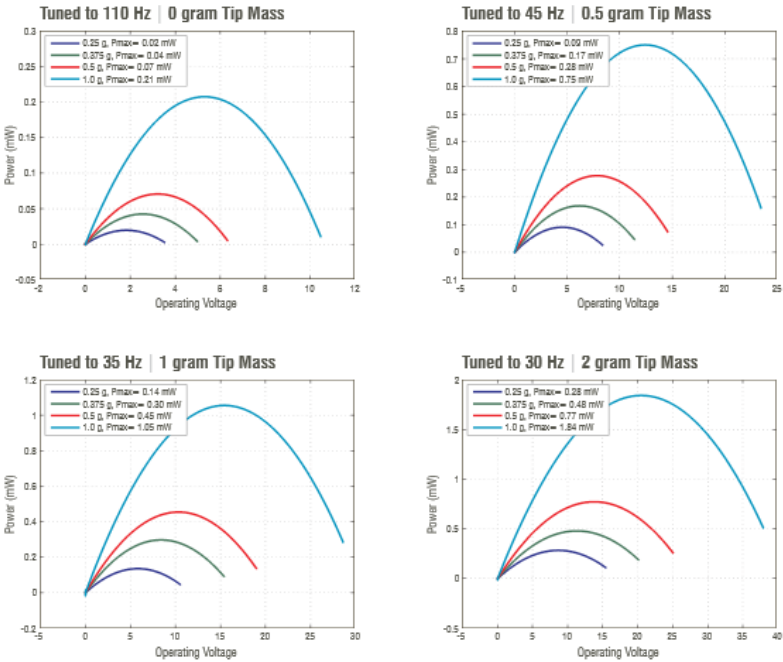


V22B RELATION BETWEEN TIP MASS & NATURAL FREQUENCY

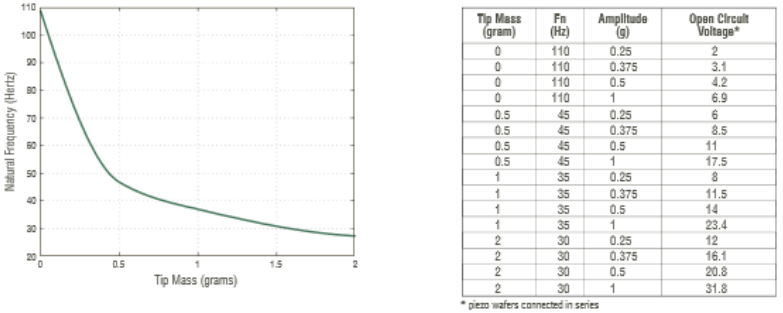




V22BL TYPICAL PERFORMANCE POWER CHARACTERISTICS



V22BL RELATION BETWEEN TIP MASS & NATURAL FREQUENCY



## Appendix C: Vibration Data Logger Specification

### **Shock Impact Vibration Data Logger**

## SLAM•STICK™

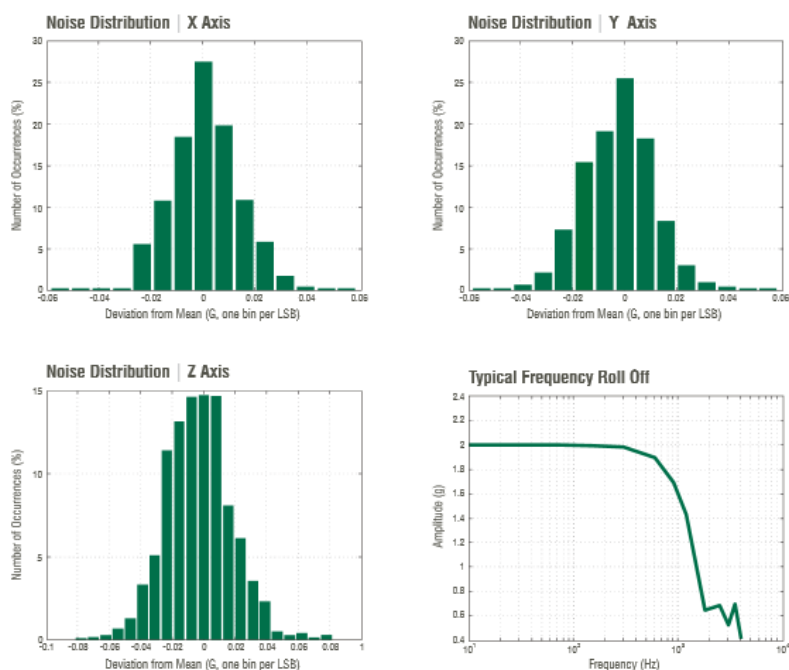
### SPECIFICATIONS

Accelerometer		LOG-0001
Range	±16 g	
Sampling Rate: Maximum   Minimum	3.2 kHz   100 Hz	
Amplitude Response Within ±5% Accuracy (X, Y)	0 to 300 Hz	
Amplitude Response Within ± 5% Accuracy (Z Axis)	0 to 500 Hz	
Transverse Sensitivity	< 10%	
Natural Frequency	> 6000 Hz	
Bandwidth	0 to 1000 Hz	
Noise Density	430µg/√Hz for Z Axis, 290µg/√Hz for X, Y Axis	
Resolution	13-bit (~3.9mg/LSB)	
Environmental		
Operating Temperature	-40°C to +80°C	
Accurate Temperature <sup>1</sup>	-20°C to +60°C	Accelerometer Accuracy is within ±5%
Storage Temperature	-30°C to +40°C	25°C is Recommended to Preserve Battery Life
Recharging Temperature	0°C to +45°C	
Humidity	0 to 95 %RH	Non-condensing
Shock Limit	>100 g	10,000g Raw Accelerometer Shock Rating
Physical		
Mass	16 grams	
Dimensions	0.34" x 0.91" x 2.71"	See Product Dimensions for Axis Direction
Case Material	Polycarbonate/ABS	
Miscellaneous		
Battery Life	>15 Minutes @ 3.2 kHz Sampling >90 Minutes @ 100 Hz Sampling	
Battery Lifetime	2 years	Battery needs to be charged at a minimum twice a year
Storage Capacity	16 MB (~ 8.4 million samples)	15 Minutes recording @ 3.2 kHz, or 7 hours @ 100 Hz
Analysis/Configuration Software Specifications		
Compatible Operating Systems	Windows	
Interface	USB	
Maximum # of Data Samples	>500 Million	Analysis of Data is Available during Import
Software-Main Features		
Statistics	FFT and spectrograms can be generated for every sensor channel. Absolute maximum, minimum, as well as sampling rate and range of each sensor channel is provided.	
Logger Configuration	Configure the sampling frequency, calendar wake, time delay, recording duration, and g-level triggers.	
Export Data	Ability to export all data in a CSV format for use with Excel, MATLAB, or other analysis software packages. FFT and Spectrogram can also be exported. The time range of exported data is user selectable.	
Part Number	Product Description	
LOG-0001	±16 g Acceleration, Data Logger. Included: Analysis Software.	



## SLAM•STICK™

### PERFORMANCE PLOTS



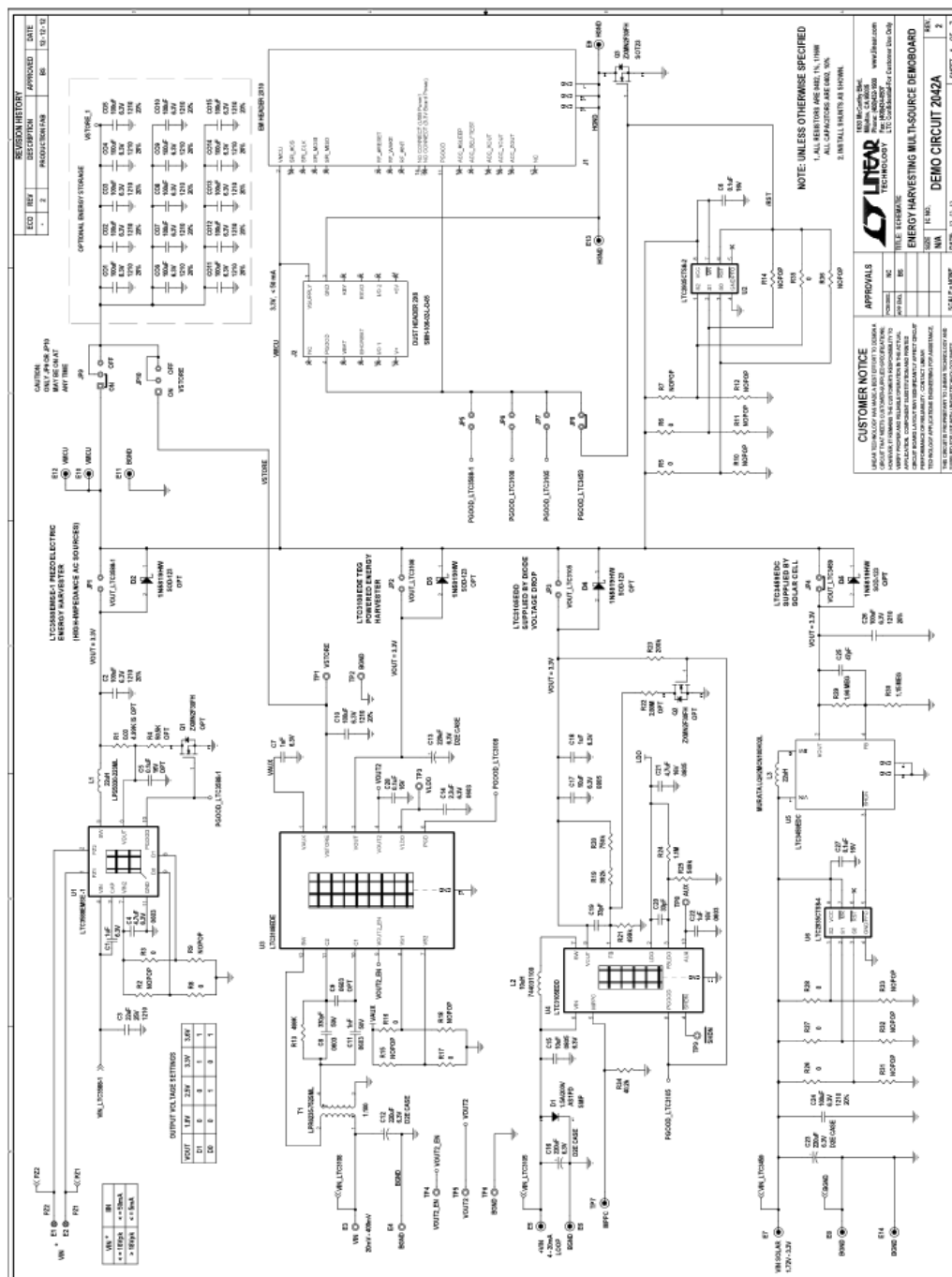
For the noise measurement, a sample Slam Stick recording was taken at room temperature with no vibrations present. The plots above represent the distribution of noise in the recorded data for each axis. This distribution is approximately Gaussian, with the majority of samples falling very close to the correct value and less frequent outliers falling further from the correct value. This distribution is typical of random noise present in any measurement.

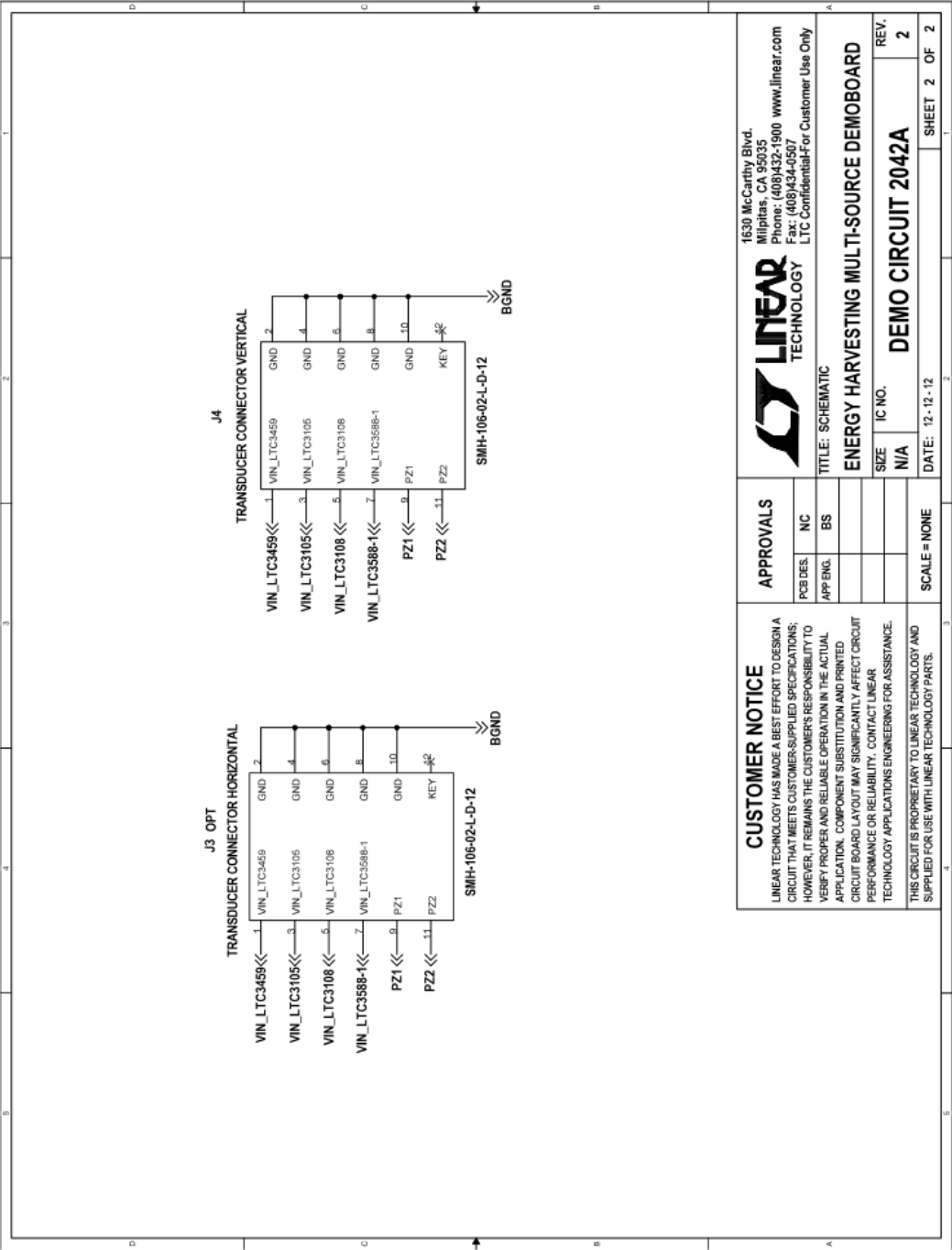
Frequency roll off data was taken by exciting the Slam Stick at a constant amplitude (1 gee in this case) over a range of frequencies from 10 Hz to 3200 Hz. The measured vibration amplitude from the Slam Stick was then plotted versus frequency. Note that the roll off is severe after ~500 Hz in the Z axis. This roll off occurs at ~300 Hz in the X and Y axes. Different devices performed differently after this frequency and amplitude data should not be trusted when above this frequency. Frequency data is not impacted by this roll-off.

## Appendix D: Electrical Circuit Schematic

### **Multi – Source Energy Harvester Circuit**

**Linear Technology part no. 2042A**





CUSTOMER NOTICE

LINEAR TECHNOLOGY HAS MADE A BEST EFFORT TO DESIGN A CIRCUIT THAT MEETS CUSTOMER-SUPPLIED SPECIFICATIONS; HOWEVER, IT REMAINS THE CUSTOMER'S RESPONSIBILITY TO VERIFY PROPER AND RELIABLE OPERATION IN THE ACTUAL APPLICATION. COMPONENT SUBSTITUTION AND PRINTED CIRCUIT BOARD LAYOUT MAY SIGNIFICANTLY AFFECT CIRCUIT PERFORMANCE OR RELIABILITY. CONTACT LINEAR TECHNOLOGY APPLICATIONS ENGINEERING FOR ASSISTANCE.

THIS CIRCUIT IS PROPRIETARY TO LINEAR TECHNOLOGY AND SUPPLIED FOR USE WITH LINEAR TECHNOLOGY PARTS.

APPROVALS

PCB DES.

NC

APP'ENG.

BS

DATE: 12-12-12

SCALE = NONE

1630 McCarthy Blvd.  
Milpitas, CA 95035  
Phone: (408)432-1900 [www.linear.com](http://www.linear.com)  
Fax: (408)434-4507  
LTC Confidential For Customer Use Only

LINEAR

TECHNOLOGY

TITLE: SCHEMATIC

ENERGY HARVESTING MULTI-SOURCE DEMOBOARD

SIZE N/A

IC NO.

REV. 2

DEMO CIRCUIT 2042A

SHEET 2 OF 2